From Cobble to Canyon: inferring the effects of discharge, climate and trophic interactions on primary productivity in a Northern California river, over reach to watershed to coastal ocean and annual to multi-decadal scales

by

John Blackburn Sculley

A dissertation submitted in partial satisfaction of the

requirements for the degree of

Doctor of Philosophy

in

Integrative Biology

in the

Graduate Division

of the

University of California, Berkeley

Committee in charge:

Professor Mary E. Power, Chair
Professor Anthony D. Barnosky
Professor Todd E. Dawson
Professor Inez Fung

Fall 2013

Abstract

From Cobble to Canyon: inferring the effects of discharge, climate and trophic interactions on primary productivity in a Northern California river, over reach to watershed to coastal ocean and annual to multi-decadal scales.

by

John Blackburn Sculley

Doctor of Philosophy in Integrative Biology

University of California, Berkeley

Professor Mary E. Power, Chair

Climate change along the California North Coast is expected to have significant impacts on primary production by riverine algae in coastal watersheds through increased precipitation intensity and duration (Snyder and Sloan 2005), and regional changes in fog frequency (Johnstone and Dawson 2010, Lebassi et al. 2009), potentially altering solar irradiance and extending higher flows and spates later into the summer low flow period when algae accrue. Changes in flow velocity and irradiance may alter relationships between primary producers and affect biomass accrual (Dodds 1991a, Stevenson 1983). Primary production in the Eel River has been established by isotopic studies to feed local aquatic and terrestrial food webs (Finlay et al. 2002) before being exported by winter high flows to the continental shelf and submarine canyons by the following summer (Drexler et al. 2006).

I examined the combined and separate effects of two different radiation levels and flow velocity ranges on the growth and interaction of algae that dominate mainstem primary producer guilds in the food web of a northwestern California river during the biologically active summer baseflow season: *Cladophora glomerata* (L.) Kutz, (the dominant benthic macroalga) and *Cocconeis placentula* (Her), *C. pediculus* (Ehrenb.) Kütz., and *Epithemia turgida* (Ehrenb.) Kütz. and *E. sorex* Kütz. (the dominant genera of epiphytic diatoms on *Cladophora* during the middle and later summer months, respectively). *Cladophora*-epiphyte assemblages attached to cobbles were collected from the South Fork Eel River (39°43'47"N, 123°38'34"W), and placed in in-stream channels that were gated and shaded to provide two velocity regimes (slow (0-9 cm/s) and faster (10-20 cm/s)) and two light treatments (shaded (peak irradiance 150 $\mu E \cdot m^{-2} \cdot s^{-1}$) and full sunlight (peak irradiance 1500 $\mu E \cdot m^{-2} \cdot s^{-1}$)). *Cladophora* filaments grew 68% longer under the higher light level (26.5 vs 15.8 cm in high vs low light), but did not differ under different water velocities. Epiphyte densities on *Cladophora* were 65% higher (6141 vs 3726 cells/mm^2 of host area) in slow velocity treatments. However, epiphyte biovolume was 67% higher (4.26

vs. 2.55 x 10^5 $\mu m^3/mm^2$) in faster velocity treatments. Total epiphyte biovolume per host filament increased 88% in higher light.

I identified and counted freshwater diatom frustules in datable annual layers (varves) from a sedimentary core recovered from the submarine Eel canyon, which receives up to 50% of discharged sediment from the nearby Eel River. These freshwater diatoms, mainly *Epithemia*, *Cocconeis*, and *Rhoicosphenia* spp., appear to provide an accurate paleo-productivity (bloom size) proxy of algae and algae-based food web dynamics over an 84 year period. With more than 47% of the variation in algal bloom height being captured by *Epithemia* spp. in offshore canyon cores, and more than 33% of the variation captured by total freshwater diatoms, I have discovered a useful proxy for algal biomass throughout the Eel River basin. I can thus extend temporal inferences about hydrologically mediated food web responses, e.g. the two-state algae bloom response to bankfull discharge regimes, back to 1918, and upscale these inferences to the entire 9540 km^2 watershed.

Using this proxy record of freshwater diatom frustules for basin-wide algal productivity, I discovered a strong and significant correlation between Rhopalodiaceae and total freshwater frustules and two satellite records of marine chlorophyll in the coastal ocean adjacent to the Eel mouth. Records of mean annual chlorophyll from the SeaWiFS sensor over the period 1997-2001 (the period where the core and satellite records overlap) and from the CZCS sensor over the entire mission period of 1978-1986 are positively correlated with Rhopalodiaceae and total freshwater frustules, accounting for between 62 and 72% of the variation in mean annual chlorophyll *a* in a ~2400 km^2 region of the continental shelf directly offshore of the Eel River mouth. I also found a significant and strongly positive correlation of mean annual marine chlorophyll with peak averaged modal *Cladophora* bloom height from upstream algal surveys during the period of overlap with the satellite record (1988-2011). River plumes have been posited as a possible source of nutrients for marine phytoplankton blooms off the California and Oregon coasts (Bruland *et al.* 2001, Wetz *et al.* 2006). These results imply a connection between riverine algae and the offshore marine ecosystem. While upwelling is clearly the major driver of marine phytoplankton blooms, my data support a role for freshwater-derived nutrients in winter/spring marine productivity.

Taken together, these results provide a more detailed picture of how environmental conditions can affect the biomass of hosts and epiphytes in riverine primary producer assemblages, and they enable the tracking of this biomass from production in river channels to burial in submarine canyons. Better knowledge of how environmental controls exert different effects on the relative growth and colonization rates of hosts and epiphytes will improve my understanding of how the energy flow and biogeochemical fluxes that they mediate may change with climate change. The ability to track primary production using the direct correlation between freshwater diatoms and bloom height allows us insight into algal food web dynamics far earlier than contemporary observations permit. These records have the potential to greatly increase the spatial and temporal scales of inferences linking food webs to environments, enhancing our understanding of how river webs may respond to future changes in climate, land cover, and other factors affecting riverine runoff and conditions, as well as their linkages to marine systems worldwide.

Dedication

Dedicated to my amazing wife, Terry Brooks Sculley, without whose love, encouragement, patience, brilliance, good humor and long hours of support none of this would be possible, and to my two fantastic daughters, Emma Margaret Elizabeth Sculley and Sophia Grace Elizabeth Sculley, whose curiosity and enthusiasm for creation continues to inspire me on a daily basis.

Table of Contents

List of Tables

List of Figures

Acknowledgements

I would like to offer heartfelt thanks to my committee chair, advisor and friend, Dr. Mary Power, for inspiring me to pursue a graduate program in biology, for helping me focus on a research problem that combined my interests in climate science and ecological interactions, and for encouraging me to keep going in the face of adversity.

I would also like to thank everyone on my committee: Dr. Mary Power, Dr. Tony Barnosky, Dr. Todd Dawson and Dr. Inez Fung for inspiring me with your amazing research, enabling me to define a research focus that was tractable and patiently helping me to develop the scientific tools needed to carry out this research.

Dr. Rex Lowe provided the inspiration to look for *Epithemia* in marine cores where no one had thought to find it. Dr. Charles Nittrouer and Dr. Tina Drexler graciously provided the STRATAFORM cores and insights needed to identify the best ones for analysis.

Dr. Chris McKay first inspired me to link life sciences to my interests in astrophysics and solar system exploration. Dr. Paula Furey provided invaluable help in algal identification. Dr. Scott Starratt provided help in developing diatom analysis protocols. Peter Steele, Maria Goodrich and Mike Limm provided hours of help setting up and maintaining the stream channels. Charlene Ng provided helpful assistance with the Eel basin algal surveys.

The University of California, Berkeley, and the Angelo Coast Range Reserve provided much needed equipment and facilities. The Environmental Protection Agency's Science To Achieve Results Fellowship provided invaluable funding and inspiration to tackle a research problem that has practical environmental applications.

I especially want to thank my grandparents, Oliver and Lorraine Grace, my parents, John Sculley and Ruth Grace Jervis, and my parents-in-law, Dr. Charles and Romona Brooks, for their love and support and for encouraging me to pursue my interests in science.

PREFACE

Primary production by riverine algae provides food and refuge to invertebrate and vertebrate grazers and fuels aquatic, riparian and upland terrestrial, and estuarine foodwebs with labile carbon and inorganic nutrients (Stevenson and Stoermer 1982, Dodds 1991a, Power et al. 2004). Filamentous green algae such as the macroalga *Cladphora glomerata* (L.) Kutz., and its epiphytes, can achieve high biomass production in temperate rivers worldwide (Whitton 1970, Dodds and Gudder 1992).

Subtle changes in summer irradiation or flow velocities can strongly influence how long *Cladophora* grows before getting smothered by its epiphytes (see Channels chapter below). If low flows and light lead to rapid *Cladophora* overgrowth and senescence early in the growing season, there will be less net productivity generated to feed consumers in the rivers, uplands, and coastal oceans. If high flows and light prolong *Cladophora* growth relative to its epiphytes, there will ultimately be more summer primary production of both host green algae and epiphytes. Changes in climatic conditions may have dramatic effects on the interactions and biomass of primary producers. Therefore, environmental tolerances for specific producer taxa will have to be accounted for in projections of aquatic food web responses to climate change, if we are to accurately predict the fate of riverine productivity and its impacts on connected ecosystems.

Freshwater diatom frustules recovered from deep marine canyon cores accurately track basin-wide algal primary production and algae-based food web dynamics going back nearly a century (see Cores chapter below). These results suggest that we can use *Epithemia* and other freshwater epiphytic diatoms to extend temporal inferences about hydrologically mediated food web responses, e.g. the two-state algae bloom response to bankfull discharge regimes, across the entire 84 year time period of the recovered sedimentary record, and across the entire 9540 km^2 spatial extent of the Eel River watershed. Further, these data provide a sufficiently long time series of river productivity to compare with marine plankton blooms directly offshore.

Here I describe results connecting local changes in irradiance and flow velocity to the interactions and accrual of the dominant primary producers in the Eel River watershed, and to basinwide responses of algal biomass to discharge. I examine the linkages of Eel River nutrients, in particular, those associated with riverine algal proliferation and export, with winter marine phytoplankton blooms over the nearby continental shelf, using diatom counts from marine canyon cores and satellite data.

The objectives of this study were to assess how environmental conditions can affect the biomass of hosts and epiphytes in riverine primary producer assemblages, to track this biomass from production in river channels to burial in submarine canyons, and to infer how climatic conditions over annual to multi-decadal scales influence the production and fate of these algal nutrients as they are delivered to connected ecosystems. Descriptions of this research and its results are thus organized around the following questions:

How does algal biomass in the Eel River basin respond to changes in flow velocity and insolation on daily, seasonal and annual scales?

How persistent is the two-state food web and productivity regime temporally over centennial scales? How has this regime functioned in the past? What is its spatial extent in the watershed?

How has algal biomass in the Eel River basin responded to multi-year and multi-decadal patterns of change in discharge and climate over the past century? How should these patterns change in the future as global climate change affects multi-year and multi-decadal patterns in climate (ENSO, PDO), and climate extremes (heat waves, floods and droughts)?

How might these changes affect delivery of nutrients to the California Current marine system?

BACKGROUND

Freshwater diatoms in oceans, lakes and rivers

Marine and freshwater sediments are extremely useful paleoarchives of proxy data, including diatoms, radiolarians, foraminifera, isotopic markers and other direct and indirect correlates of climatic and biological conditions in the past. Diatoms have commonly been used to provide information on nutrients, pH, temperature, salinity, and other parameters in lakes, rivers and oceans. The diatom *Chaetoceros* is an important genus of marine diatom commonly associated with upwelling zones (Gil et al. 2007). Freshwater diatoms in annually varved sediments have frequently been used to reconstruct the environmental history of lakes (Smol et al. 2001 and references therein). Round et al. (2007) review prior ecological and morphological studies using diatoms.

Diatom studies in rivers have more commonly been used as indicators of contemporary conditions, but diatom stratigraphy has been studied in river deltas, where lower water velocities and the presence of off-channel bodies of water ("backwaters") permit deposition and accumulation of sediments containing diatom frustules. A recent study in the Murray River of Australia (Gell et al. 2002) recovered abundant diatoms recording seasonal changes in the pelagic and benthic fauna of the Murray-Darling floodplains. The US Geological Survey has conducted preliminary studies of sediments in the Columbia River delta (Oregon, USA) where *Epithemia* spp. (Figure 1) and other freshwater diatom frustules recorded historical changes in algal communities and contaminants (Petersen et al. 2003). Estuarine core sediments were aged using ^{210}Pb and ^{137}Cs with two cores dating back to the 1850's. Algal pigments, organics and stable isotopes were also examined providing a time series of changes in algal communities (including diatoms) from 1853 to 2000. Unfortunately, this preliminary study was never fully developed due to the death of the PI shortly after its publication.

Freshwater diatoms in marine sediments

Despite extensive studies of continental shelf sediments, including those in areas of high discharge from major rivers, I know of few previous studies of freshwater diatoms in marine sediments. The reasons for this range from the difficulty of getting significant numbers of freshwater frustules amidst the typically very high concentrations of marine diatom frustules, difficulty dating sediments in rapidly accumulating regions (Gil *et al.* 2007), frequent bioturbation of marine sediments by benthic infauna, to frequent turbidity flows and overturned layers in submarine river canyons (Drexler *et al.* 2006). One recent study from the Tagus River of Portugal using marine box cores attempted to compare the instrumental records of river discharge and offshore upwelling intensity with proxy records of freshwater diatoms and phytoliths from the river and upwelling-associated marine diatoms (Gil et al. 2007). Due to rapid sediment accumulation, bioturbation was moderate, and relatively intact sequences of 75 – 100 years were collected. Despite some problems with silica dissolution (a common problem for diatom studies, particularly in low-silica lakes (Smol *et al.* 2001)), the authors found that major upwelling events and major discharge events recorded in the instrumental record were also captured in the

proxy record. Based on this verification, freshwater diatom proxies were recommended for use in extending the timescales of palaeoenvironmental studies far beyond the range of instrumental data (Gil et al. 2007).

The Eel River

In comparison with the Columbia and Tagus Rivers, the Eel River basin presents additional challenges and opportunities for application of diatoms to efforts to reconstruct environmental history. The Eel has few depositional environments. It is a steep, canyon-bound, mountainous river that is incising into its bed for much of its length (Lisle 1990, Seidl and Dietrich 1992), from its headwaters high in the Coast Range to its mouth near Fernbridge, CA (Figure 2a). It transports a relatively thin veneer of gravel and cobbles over a bedrock bed (Seidl and Dietrich 1992).

The steep topography, intense winter storms and relatively erodible terrain of the Eel basin combine to create the highest recorded average sediment yield per watershed area of any river in the coterminous United States, and among the highest worldwide (Brown and Ritter 1971, Lisle 1990, Milliman and Farnsworth 2008). Much of the 9540 km^2 Eel River watershed is mountainous and sparsely settled. Forestry has been the principal land-use, with dairy and small-scale agriculture near the estuary.

The Eel has a short, high energy delta with tidal influences over its last few kilometers and only a few isolated depositional settings along its northern margin (Figure 2b) (Sommerfield et al. 2007, Goni 2011). In test cores here, I found sediment accumulations of a decade or less, with high bioturbation and low freshwater frustule concentrations (Sculley, unpublished data). The only lentic environment of any size in the Eel basin is Lake Pillsbury (39.41°N, 122.96°W), near the headwaters of the Middle Fork. This reservoir presumably has sediment accumulations in a sub-aqueous alluvial fan at the reservoir head, but the surface slope, depth and episodic sediment inflows make it unlikely that a stable, long-term record could be extracted from this locality (Sculley, personal observation).

As a short, steep river (Sommerfield et al. 2007), even the lower reaches of the main stem Eel River have substrates coarse and stable enough to support macroalgal growth for nearly its entire length. In monthly surveys conducted from the headwaters down to the river mouth, I found that while the algal communities are markedly similar throughout the watershed, they appear to be exported from sites where attached filaments originated fairly quickly, within months of growth. Even at Fernbridge (40.62°N, 124.21°W), about 11 km from the mouth, the riverbed is gravel and small cobbles, and deposition is limited to a small (ca. 10 km^2) estuarine zone (Figure 2b).

Continental shelf and Shelf sediments

In part because it lacks dams, the Eel delivers the largest total sediment load of any river to the California coast (Andrews and Antweilier 2012). Extensive studies have been made of the sediment dynamics off the mouth of the Eel, due to these high rates of

delivery (Lisle 1990, Sommerfield and Nittrouer 1999, Mullenbach and Nittrouer 2000, Farnsworth and Milliman 2003, Sommerfield et al. 2007). Offshore of the Eel River mouth is a ~20 km wide section of the California continental shelf ranging from 25-200 meters in depth (Drexler et al. 2006) that captures and stores Eel River sediment as it flows out to sea. Sediment deposition occurs year-round but peaks during winter storms, and especially during flood events, when the average shelf sediment accumulation rate of 4 mm/yr can be exceeded by tenfold or more (Leithold 1989). Bioturbation is very high in shelf sediments, mainly by marine polychaete worms that make their burrows in the top few meters of sediment (Sommerfield and Nittrouer 1999) and can erase physical strata. High wind events (also known as "dry storms") can resuspend the top few centimeters or more of sediment and transport suspended material to other parts of the shelf (Sommerfield et al. 2007). These challenges typically limit the resolution of shelf sediment studies to decades, making them unsuited for studying interannual patterns.

Eel submarine canyon

Incised into the continental shelf opposite the Eel River mouth is a submarine canyon formed during the low sea stands of glacial maxima (Leithold et al. 2005, Drexler *et al.* 2006, Mullenbach *et al.* 2004). During these periods, the Eel flowed across and cut into the continental shelf as it emptied into an ocean as much as 100 m lower and 20 km west of the present shoreline (Figure 3). The canyon itself extends as close as 10 km from the present Eel mouth, beginning at the 60 m isobath. The Eel canyon has four main entrances known as Larry, Moe, Shemp and Curly (Drexler et al. 2006) (sic)).

Sediment budget studies, using isotopic tracers and fixed ocean-floor monitors in the canyon entrances, confirm that the submarine Eel canyon receives up to 50% of the Eel River's sediment flux (Leithold 1989, Leithold and Hope 1999, Puig et al. 2003, Mullenbach and Nittrouer 2006) at rates high enough to limit bioturbation (Drexler et al. 2006). ^{7}Be, ^{137}Cs and ^{210}Pb isotopic analyses confirm rapid (sub-annual) delivery of sediment from the river mouth to the canyon (Sommerfield and Nittrouer 1999). Analyses of cores from canyon walls and floors (of which the deepest parts are called thalwegs) show that sediment has been accumulating in the Eel canyon without significant loss to turbidity flows (underwater avalanches) down-canyon since 1906, when a magnitude 8 earthquake triggered massive turbidity flows out to the deep ocean. Sediment accumulation is expected to continue until the next temblor of sufficient magnitude (in excess of magnitude 7.5) triggers new turbidity flows (Mullenbach et al. 2004, Drexler et al. 2006, Mullenbach and Nittrouer 2006).

Surveys show that the northern entrances, Larry and Moe, receive most of the sediment from the Eel River, typically as gravity flows (sediment-water flows influenced by gravity alone) through the canyon thalwegs, and nepheloid layers (suspended sediment flows just above the bottom). Flows here are rich in fine sand, and sediment accumulation rates are high enough to suppress bioturbation, except in canyon walls (Drexler et al. 2006). Consequently, physical structure preservation (defined as the predominance of physical stratification) is quite high (75-95%) while sediment

accumulation rates (SARs) are poorly constrained ($r^2 < 0.50$) (Figure 4). Steady state SARs are defined as having a logarithmic decrease in ^{210}Pb activity with depth in the core. A linear regression of ^{210}Pb activity with depth was used to generate an r^2 for each core, with values over $r^2 = 0.50$ considered statistically significant. For these cores sediment accumulation rates were calculated using the advection-diffusion equation (Nittrouer et al. 1984) with the impact of biological mixing considered minimal because of the predominance of physical strata.

The southern entrances, Shemp and Curly, receive most of their sediment as suspended fine-grained nepheloid layers and hemipelagic sediment clouds (deposited too rapidly to chemically react with seawater), which accumulate on the bottom in nearly steady-state fashion (Drexler et al. 2006, Mullenbach et al. 2004). Consequently, physical structure preservation here is generally lower (<75%), because sedimentation rates are generally too low to suppress bioturbation, while sediment accumulation rates are better constrained ($r^2 > 0.50$) because they are steady-state.

During the STRATAFORM project, an extensive marine sedimentary coring project was conducted directly offshore of the Eel River mouth by the US Geological Survey, the University of Washington and the Office of Naval Research, (Nittrouer 1999). Nittrouer and Drexler (2006) collected 87 push cores from the Eel canyon using an ROV in August 2001 (Figure 4).

The ROV collected cores from several locations, including a number along the canyon thalweg between a tripod and mooring mounted in the head of the Larry arm. Additional studies have characterized the sediment influx past the tripod station and down canyon, and measured storm and discharge driven pulses of sediment regularly entering the canyon (Puig et al. 2003). Core profiles going back to 1906 found no evidence of rip-up clasts or other turbidite flows. The record for higher resolution canyon cores extends back up to 95 years for thalweg sediments. Longer, 8m cores have been archived from the shelf and provide lower resolution records dating back 2000 years.

Climate Phenomena of Interest

Projected climatic change over the next few decades includes both greenhouse-gas driven global and regional warming and precipitation changes as well as even less well-understood alterations in the intensity and frequency of natural cycles such as the El Niño Southern Oscillation (ENSO) (Snyder and Sloan 2005). Aquatic communities are projected to experience dramatic changes in key environmental factors affecting all species from primary producers to top predators.

One of the climate cycles with the greatest potential impact on the aquatic communities along the west coast of North America is ENSO. ENSO involves feedbacks between the tropical Pacific pool of warm surface waters and prevailing trade winds, and has global impacts driven by alterations in the Pacific jet stream, the Aleutian Low and the California High pressure systems (Cane 1992). At the Angelo Coast Range Reserve,

which sits near 40 degrees latitude, the effects of El Niños and La Niñas are quite variable and depend on another more recently described climatic system, the Pacific Decadal Oscillation (Milliman and Farnsworth 2008).

The Pacific Decadal Oscillation (PDO), also known as El Viejo, was first detected in fisheries records from the Eastern Pacific. A 20 to 40 year shift in salmon and other commercial catches appears to coincide with sea and land surface temperatures as well as river discharges in Alaska and the lower Pacific Northwest, including California, Oregon, Washington and British Columbia (Mantua et al. 1997, Hayward 1997, Minobe 1997). Warm/positive states increase river discharges and salmon abundances in Alaska, and reduce them in the lower Pacific Northwest, with the opposite occurring in Cold/negative states. Salmon appear to be responding to bottom-up effects of SSTs on marine phytoplankton and zooplankton. A regime shift in 1977 from colder conditions to warmer conditions (Baumgartner et al. 1992) is now reversed by the 2002 shift back to the colder state (Figure 5).

Along the west coast of North America, the influence of warm ENSO events (El Niños) on river discharge decreases north of 32°N, and the influence of cold events (La Niñas) increases (Cayan and Webb 1992, Andrews et al. 2004). The latitudinal gradient in PDO influence is equally marked: north of 30°N the influence of warm phase PDO on annual discharge disappears, and La Niñas are wetter during cold PDO phases north of 40°N (Figure 6, (Tootle and Piechota 2006)).

The final climate cycle affecting Pacific coast aquatic communities is the Arctic Oscillation, which directly modulates the Aleutian Low pressure system intensity and plays a role in opening and closing the "storm-door" on the North American west coast (Duffy et al. 2005, 2006).

All three climate cycles interact to create a complex pattern of discharge regimes on the Eel and other west coast rivers (Tables 1-3). For the entire Eel River basin, the PDO appears to "set the stage" for discharge regimes, with additional effects on fog, temperature and sediment transport. When the PDO, ENSO and the Arctic Oscillation are in phase (all positive or negative), the potential exists for megafloods such as the great floods of 1955 and 1964, as well as more generally enhanced peak flows and sediment transport. Reflecting this, peak sediment loads on the Eel occurred during La Niñas, during the cold PDO from 1945–1977, and during El Niños, during the warm PDO from 1977–2002 (Andrews and Antweiler 2012). Fog production is suppressed, while insolation and water temperatures are enhanced, during the warm phases of ENSO and PDO, while the reverse is true during cold phases. Areas that are strongly affected by ENSO and PDO are predicted to experience even stronger effects as global climate change amplifies natural climate cycles (IPCC 2012).

Changes in means and variances of a suite of global climate parameters are projected to lead to an increase in extreme meteorological events, including heat waves, floods and droughts (Meehl et al. 2001). For the west coast of North America, an increase in frequency of extreme heat and extreme precipitation events is forecast, as well as an

increase in multi-year droughts and flood events (Rosenzweig et al. 2000). Extreme events, being currently rare, are particularly difficult to predict, as there are few available data with which to make assessments regarding changes in their intensity or frequency. Global trends in precipitation are less reliably forecast than trends in temperature, due to the fine-scaled complexity of cloud and water vapor physics (IPCC 2012). Thus forecasts of extended droughts and/or floods are typically assigned low confidence in climate change predictions.

As changes in greenhouse gas forcing lead to increased frequencies and intensities of ENSO and PDO events (Meehl et al. 2001, IPCC 2012), large regions of the globe may experience prolonged anomalous periods, such as the 1990-1995 El Niño or the two "double" La Niñas – 1998/99, and 1999/2000 (Rosenzweig et al. 2000, Meehl et al. 2001). Sequential extremes, such as prolonged droughts followed by heavy rains, can decouple strongly interacting species, such as predator/prey, pollinators or mutualists, with cascading long-term effects on communities (Rosenzweig et al. 2000, Walther 2010). Biodiversity impacts of extreme events are likely to differ from those of common gradual climate change, leading to especially stressful conditions for species with low dispersal ability (Parmesan 2006, Walther 2010).

Johnstone and Dawson (2010) identified a 33% decline in summer fog frequency off the northern California coast since 1901 related to increased sea surface warming along the coast as well as the prolonged warm PDO of 1977-2002. The recent shift to cold PDO conditions has led to increased fog frequency (LeBassi et al. 2009) and most models of regional climate change project increased northerly winds, upwelling and fog frequency in the northern California Current System (CCS) (Diffenbaugh et al. 2004, Snyder and Sloane 2005, Duffey et al. 2006). However, these models project decreases in fog frequency in the southern limb of the CCS, which is supported by observations in southern California (Roberts et al. 2002).

Ecological Phenomena of Interest

A 24-year record of surveys has identified a two-state food web regime (Figure 7) driven by peak winter flows interacting with food web controls on algae (Power et al. 2008 and unpublished data). An armored grazer, *Dicosmoecus gilvipes*, can suppress algal growth in drought years, but is crushed or exported by high winter floods. The resulting shifts in peak filament lengths for the dominant macroalga *Cladophora glomerata* are reflected in shifts of its dominant epiphytes, including the diatom genus *Epithemia*.

These contrasting states shift with the magnitude of the previous winter floods, which in turn govern food web controls on algae (Power et al. 2008). *Cladophora glomerata* initiates growth vegetatively on boulder and bedrock substrates from basal cells that survive winter flood scour. Bed scouring floods obliterate large armored or sessile invertebrate grazers, which are not otherwise controlled by local predators. Following floods, blooms reach peak biomass in late spring or summer; by mid July,

Cladophora filaments can attain several meters in length, then decline due to grazing, sloughing and senescence caused by epiphyte overgrowth, temperature stress, nutrient limitation and self-shading (Power et al. 2008). In contrast, during flood-free drought years, *C. glomerata* biomass is severely grazed and never proliferates above lengths of a few cm (Power et al. 2008).

Epiphytes heavily colonize *Cladophora* beginning in late spring, as lower flows, warmer temperatures and increasing colonizable area provide favorable conditions for settlement. One diatom genus, *Epithemia*, (and two species: (*Epithemia turgida* (Ehrenb.) Kütz. Bréb. and *E. sorex* Kütz.) dominate the epiphyte assemblage that covers *Cladophora* (Figure 8) by mid- to late-summer (Power et al. 2009). Both long and short filaments become heavily epiphytized; individual *C. glomerata* cells can host over 50 epiphytic diatoms, and total epiphyte biovolume often exceeds that of *C. glomerata* (Burkholder and Wetzel 1990, Dodds 1991a, Peterson and Grimm 1992, Marks and Power 2001). As filament length (measured as peak averaged modal bloom height) increases, so does colonizable area. Research on epiphyte/host relations for these taxa has shown that epiphytes generally saturate available colonizable area (Bergey et al. 1995, Marks and Power 2001), with maximum biovolumes in moderate (10-20 cm s^{-1}) current velocities and high light conditions (see Channels chapter below).

Algal filaments and attached epiphytes are scoured away during winter floods at the return of the rainy season. Isotopic tracer studies show that most of the sediment load exported by the Eel River offshore is emplaced on the continental shelf and in the submarine Eel canyon within months (Sommerfield and Nittrouer 1999, Drexler et al. 2006). Thus the larger bloom sizes are reflected as higher epiphyte counts in emplaced sediments in the submarine canyon cores, depending on whether or not there is retention of frustules prior to burial in the canyon (see Table 4).

The maximum (instantaneous, operationally 15-minute) peak discharge will determine whether bed-mobilizing floods scour algae and grazers that potentially limit them. Over longer time scales, higher average annual discharges may reduce algal accrual by export, or by creating light-limiting turbidity. On the other hand, higher discharge during periods of stable or slowly declining baseflow will enhance nutrient fluxes and waste removal that, during the biologically active summer, can be very significant factors limiting macroalgal bloom size. Fog production and inland extent can affect insolation on algal blooms as well as water temperatures, both of which have been shown to influence algal growth (Dodds 1991a, 1991b, Smol et al. 2001).

Effects of flow velocity and radiation on interactions of a dominant alga and its epiphytes during summer baseflow in a Northern California river

SUMMARY

Climate change along the California North Coast is expected to increase precipitation intensity and duration via more convective storms, (Snyder and Sloan 2005), potentially extending higher flows and spates later into the summer low flow period when algae accrue. Climate change is also expected to decrease fog, although studies differ over the magnitude(s) and location(s) of change. Changes in flow and radiation during the active summer growing season would affect primary production by riverine algae. I examined the combined and separate effects of two different radiation levels and flow velocity ranges on the growth and interaction of algae that dominate mainstem primary producer guilds in the food web of a northwestern California river during the biologically active summer baseflow season: *Cladophora glomerata* (L.) Kutz, (the dominant benthic macroalga) and *Cocconeis placentula* (Her), *C. pediculus* (Ehrenb.) Kütz., and *Epithemia turgida* (Ehrenb.) Kütz. and *E. sorex* Kütz. (the dominant genera of epiphytic diatoms on *Cladophora* during the middle and later summer months, respectively). *Cladophora*-epiphyte assemblages attached to cobbles were collected from the South Fork Eel River (39°43'47"N, 123°38'34"W), and placed in in-stream channels that were gated and shaded to provide two velocity regimes (slow (0-9 cm/s) and faster (10-20 cm/s)) and two light treatments (shaded (peak irradiance 150 $\mu E \cdot m^{-2} \cdot s^{-1}$) and full sunlight (peak irradiance 1500 $\mu E \cdot m^{-2} \cdot s^{-1}$)). *Cladophora* filaments grew 68% longer under the higher light level (26.5 vs 15.8 cm in high vs low light), but did not differ under different water velocities. Epiphyte densities on *Cladophora* were 65% higher (6141 vs 3726 cells/mm^2 of host area) in slow velocity treatments. However, epiphyte biovolume was 67% higher (4.26 vs. 2.55 x 10^5 $\mu m^3/mm^2$) in faster velocity treatments. Total epiphyte biovolume per host filament increased 88% in higher light. Responses to light and water velocity differed among taxa, with *Epithemia* spp. and *Cocconeis* spp. increasing in higher velocities but other (mainly small and/or filamentous) epiphytes increasing in low velocities. *Cocconeis* spp. mean peak density was higher (from 1881 to 2772 cells/mm^2 of host area) in lower light conditions, possibly due to lower host growth rate (and more time for epiphyte colonization and local cell division).

Epiphytes can become dense enough to suppress the growth of their macroalgal host. If this happened early in the season, less total biomass of host-epiphyte assemblages would proliferate over the summer than if *Cladophora* grew longer, increasing surface area for later-colonizing epiphytes. Altered environmental conditions will generally exert different effects on the relative growth and colonization rates of hosts and epiphytes. Better knowledge of how environmental controls alter performances and interactions of both hosts and epiphytes in riverine primary producer assemblages will improve our understanding of how the energy flow and biogeochemical fluxes that they mediate may change with climate change.

INTRODUCTION

Global climate change is predicted to have dramatic impacts on rivers, including alteration of water and ground temperatures, precipitation, runoff and flow regimes, riparian corridors, oxygen saturation and other key ecological variables (Decamps 1993, IPCC 2007, Cayan et al. 2008, Stralberg et al. 2009, PRBO 2011). Projected impacts on

river food webs are complex, and include altered interactions among large predators such as salmon and steelhead (*Oncorhynchus* spp.), primary producers such as algae and macrophytes (Harrington *et al.* 1999, Power et al. 1996, McCarty 2001, Poff et al. 2002, Power et al. 2008), and invertebrates or other taxa at intermediate trophic positions (Gresens 2001, Power 1990b, Perkins et al. 2010, Woodward et al. 2010, Markovic 2013). Many of these interactions, particularly those involving primary producer taxa, are sensitive to variables like precipitation and discharge timing, fog and cloud cover, air and water temperature, for which predictions in current climate models remain uncertain (Cayan et al. 2008, Stralberg et al. 2009, Johnstone and Dawson 2010, PRBO 2011).

Cladophora glomerata is a dominant primary producer in temperate freshwaters around the globe (Whitton 1970, Dodds 1992). Filamentous green algae such as *Cladophora glomerata* are able to achieve high biomass production throughout temperate rivers on coarse, relatively immobile substrates. Their proliferations greatly increase surface area for growth of epiphytes, often dominated by diatoms and cyanobacteria. Together, hosts and epiphytes provide food and refuge to invertebrate and vertebrate grazers and fuel aquatic, riparian and upland terrestrial, and estuarine foodwebs with labile carbon and inorganic nutrients (Stevenson and Stoermer 1982, Dodds 1991a, Power et al. 2004). A dominant filamentous primary producer in the Eel River of northwestern California, this macroalga can reach lengths of up to 8 m (Power 1990). *Cladophora glomerata* and its epiphytes, including *Epithemia* and *Cocconeis* spp., are sensitive to variations in light, temperature and nutrients (Dodds 1991a). Epiphytes are also influenced by the macroalgal host performance and standing biomass (Dodds 1991b). I studied responses by host *Cladophora* and its dominant epiphytes to altered water velocity and light conditions that may arise in the region over the coming decades. Climate change is predicted to alter fog density and duration, water temperature, and flow velocity in rivers along the California Coast, with significant differences between northern and southern regions (LeBassi et al. 2009, Diffenbaugh 2004, Snyder and Sloane 2005, Duffey et al. 2006, Johnstone and Dawson 2010). Flow velocities during the summer baseflow period of high algal production will change with precipitation, and also with water impoundment or extraction from channels.

BACKGROUND

Site Description

I studied *Cladophora* and its epiphytes in experimental channels in the upper South Fork Eel River in the Angelo Coast Range Reserve in northern coastal California. The Angelo Coast Range Reserve (39°43’45’’N, 123°38’40’’W, ACRR; http://angelo.berkeley.edu), is a protected research reserve in the University of California Natural Reserve System in Mendocino County, California. The Angelo Reserve contains diverse aquatic and terrestrial habitats, including mixed conifer-deciduous forests and a 5 km reach of the South Fork of the Eel River, as well as several perennial and ephemeral tributaries. With elevations ranging from 378-1290 m, the Angelo Reserve is shielded from maritime fog by Elkhorn Ridge, a high region of the California Coast Range.

Consequently, it experiences more temperature extremes, drier summers, and more insolation than might be expected for a site only 15 km east of the Pacific Ocean.

Tectonic uplift and incision by the Eel River and its tributaries have generated the steep topography. Forested banks, with slopes up to 50 percent, limit light in north-south river reaches unless a tributary or other topographic low extends to the east or west of the reach. East-west reaches in general are more productive due to higher incident solar radiation (Bode et al. 2013). The main SFE channel is canyon-bound, and contains little woody debris. Floodplain terraces elevated 6-30 m above the channel bed create the only level land in an otherwise rugged terrain of narrow ridges and steep valleys. Underlying most of the reserve are marine sediments: greywacke sandstones and mudstones of the Franciscan Complex (Lisle 1990). In the channels, relatively immobile bedrock and boulders are surrounded, and bypassed during floods, by more mobile cobbles, pebbles and gravels (Seidl and Dietrich 1992, Finlay et al. 2002, Power et al. 2004).

Timing of key Physical Factors

The Mediterranean climate of the Eel River basin delivers most precipitation between October and April, followed by warm, dry summers. Average annual precipitation is moderate to high, ranging from 70 cm in the south to over 100 cm in its northern reaches. Most precipitation falls as rain during winter storms, with least 65 percent reaching the Eel River as runoff (Lisle 1990). Summer fog is possible during the peak ocean upwelling season of May to August, but is rarely a significant factor in reducing insolation or temperatures, as it is on the nearby coast. Within the Angelo Reserve, the South Fork of the Eel River has a mean gradient of 0.005 and drains areas ranging from 114 – 153 km^2 (Power et al. 2008). Winter storms lead to bed scouring floods and smaller spates, followed by a long period of stable, low summer baseflow. Peak discharge recorded in the past century range from a high flow of 566 m^3/s in December 1955 to a low flow of 0.013 m^3/s in August 1977.

Phenology of key algal taxa

Seasonal changes in flow, light, temperature and nitrogen availability affect growth rates and drive successional changes in *Cladophora* and its epiphytes. *Cladophora glomerata* (L.) (Kütz.) initiates growth vegetatively on boulder and bedrock substrates from basal cells that survive winter flood scour. Following floods, blooms reach peak biomass in late spring or summer; by mid July, *Cladophora* filaments can attain several meters in length, then decline due to grazing, sloughing and senescence (Power et al. 2008). In contrast, during flood-free drought years, *C. glomerata* biomass is severely grazed during the onset of its growth in late spring and rarely exceeds lengths of more than 10-15 cm (Power et al. 2008). Both long and short filaments become heavily epiphytized and total epiphyte biovolume often exceeds that of *C. glomerata* (Burkholder and Wetzel 1990, Dodds 1991a, Peterson and Grimm 1992, Marks and Power 2001). Over the summer months, proliferations of *Cladophora glomerata* change from green, to yellow, then rusty red colors, due to their increasing encrustation by epiphytic diatoms (Power et al. 2009). During early-middle epiphyte succession (June-early July), epiphytes are dominated by monolayers of tightly adhering, low profile taxa like

Cocconeis placentula (Her). and *Cocconeis pediculus* (Kütz.). Stalked diatoms such as *Rhoicosphenia* Grunow and *Gomphonema* Ehrenb. spp. are also common during these mid-successional stages.

As river discharge ebbs and producer biomass accumulates, increasingly limiting nitrogen favors diatoms in the nitrogen-fixing family Rhopalodiaceae, which includes *Epithemia*, over other epiphytes (Fairchild and Lowe 1984, Bahls and Weber 1988, Peterson and Grimm 1992, Marks and Power 2001). *Cladophora* epiphyte layers become many cells deep, darkening assemblages to a deep rusty red (Power et al. 2009). *Epithemia turgida* (Ehrenb.) Kütz. and *Epithemia sorex* Kütz, have cyanobacterial endosymbionts that are capable of nitrogen-fixation (Floener and Bothe 1980). Non-endosymbiotic cyanobacteria (e.g. *Rivularia spp., Anabaena sp.*, *Heteroleibleinia* (Geitler) and *Chamaesiphon* Braun *et* Grunow spp.) are also common epiphytes of *Cladophora* during this later successional stage.

Effects of light and flow velocity

Benthic algal accrual is typically modeled as increasing but saturating with irradiance (Hill 1996). Benthic algae rarely experience photoinhibition or even photosaturation, but are more typically light-limited (Dodds 1991a), unless they have proliferated to float at the water surface. Minimum irradiances of 35 to 104 $\mu E \cdot m^{-2} \cdot s^{-1}$ were required for positive net photosynthesis in *Cladophora* in studies from the Great Lakes region (Graham et al 1982, Tomlinson et al. 2010). The maximum dry weight production of *Cladophora glomerat*a has been estimated to occur at light intensities ranging from 125 $\mu E \cdot m^{-2} \cdot s^{-1}$ in a Wisconsin study (Hoffman and Graham 1984) to 300–600 $\mu E \cdot m^{-2} \cdot s^{-1}$ in studies of Great Lakes algae (Graham et al. 1982), although more recent studies support the higher values (Tomlinson et al. 2010). Published saturation intensities for attached *Cladophora* are from 300–1125 $\mu E \cdot m^{-2} \cdot s^{-1}$ (Hill 1996, Tomlinson et al. 2010). Light affects accrual rates but not typically standing biomass if grazers are present (Stevenson *et al.* 1996, Dodds 1991b). Dense accumulations of epiphytes can also drastically reduce host photosynthesis (Stevenson and Stoermer 1982). Under high light regimes, however, the density of epiphytes per surface area of host alga might decrease if host growth could outpace epiphyte colonization and local growth.

Water velocity affects algal growth positively through nutrient and waste transport. Lotic green algae such as *Cladophora glomerata* typically rely on nutrients transported by flowing water to replace those used in photosynthetic and metabolic processes (Dodds 1991a). In still water, lack of nutrient supply and waste removal may severely inhibit metabolism and growth. Nutrient supply increases with stream velocity because higher velocities thin the viscous boundary layer between the filament or epiphyte surface and the water column, and also increase the large-scale flux of inorganic nutrients past that surface (Whitford and Schumacher 1961, 1964, Stevenson *et al.* 1996). Waste products must also be transported away from algal filaments to permit proper metabolic function (Stevenson et al. 1996). Above a certain threshold, however, flow can negatively affect accrual through sloughing and export (Hondzo and Wang 2002). When drag exceeds algal tensile strength, algal filaments and epiphytes detach and are exported. At higher flows, *Cladophora* filaments have reduced branching angle and frequency (Dodds 1991a,

Marks and Power 2001). Experiments with *Cladophora* and epiphyte communities have shown that immigration of host and epiphyte cells is reduced as current velocities increase for most taxa, while export is increased (Bergey *et al.* 1995, Stevenson *et al.* 1996). However, taxon-specific traits may confer an increase in relative settlement of specific epiphytes (Stevenson and Peterson 1989).

Overall, the optimal water velocity that maximizes primary production or fitness would depend on algal taxon, condition, density, morphology, nutrient concentrations, and light intensity (Stevenson *et al.* 1996). For example, the positive effects of increased water velocities on growth are typically experienced by algae in high light conditions, as they are better able to use the increased nutrients. The largest green algal blooms are found at the 10-20 cm/s velocities typical of river runs (Stevenson *et al.* 1996). Experiments performed *in situ* have measured maximum per biomass photosynthetic rates for *Cladophora glomerata* at water velocities of 8 cm/s, known as the saturating current velocity (Dodds 1991a).

Expected Results

I attempted to predict the relative duration of active growth and lengths attained for *Cladophora* host filaments, and the relative densities (per area of host) of total epiphytes and of Rhopalodiacean epiphytes, based on prior knowledge of how gain and loss processes for each variable would be likely to respond to different levels of light and flow velocity. (Table 1). Irradiance ranges in shaded treatments were below the threshold for filamentous algae net growth (Tomlinson 2010, but see Hoffman and Graham 1984), but not for many diatoms, which have more efficient photosystems in low light (Hynes 1975, Dodds 1991 a, b, Stevenson 1996). Hill and Knight (1988) reported photoinhibition of diatom assemblages at the Angelo Coast Range Reserve at 200 $\mu E \cdot m^{-2} \cdot s^{-1}$ and abundant growth at irradiances as low as 18 $\mu E \cdot m^{-2} \cdot s^{-1}$. Other studies have documented light saturation for common diatoms at levels below 100 $\mu E \cdot m^{-2} \cdot s^{-1}$ (Hodoki and Obayashi 2005, Saunders 2009, Lange et al. 2011). Lower light would be expected to be more limiting for Rhopalodiaceae and diazotrophic free-living cyanobacteria than for non-fixing epiphytes, because nitrogen fixation imposes high energetic costs. Therefore, I expected non-fixing epiphytes to outperform both Rhopalodiaceae and their *Cladophora* host in lower light levels.

Slower flow treatments were below optimal velocities for macroalga blooms (Dodds 1991a) but in a range more favorable to diatom settlement (Round 1973, Peterson 1987, Stevenson 1983, Stevenson and Peterson 1989). Stevenson and Peterson found a ten-fold increase in immigration rates when current velocity was reduced from 30 to 10 cm/s. I therefore expected higher densities of epiphytes, for example, if they outperformed their host *Cladophora* in the slower flow treatments. Higher flow velocities will increase the supply of inorganic nutrients (and thus reduce the advantage of N-fixers), leading non-fixing epiphytes to outperform N-fixers in higher velocity treatments.

The combination of higher velocity and higher PAR was predicted to allow the host *Cladophora glomerata* to achieve larger size, outgrow its epiphytes and delay

senescence. Epiphyte growth once cells settled on hosts could also be highest in this treatment, but the reduced settlement, increased export (particularly of multi-story Rhopalodiaceae) and increased host area expected in higher flow velocities might reduce epiphyte density (numbers or biovolume per surface area of host). In addition, I predicted that reduced competitive advantage for *Epithemia* spp. for nitrogen under higher flows could lead to low-medium numbers for Rhopalodiaceae. Higher flows would also tend to limit the abundance of high-profile, stalked epiphytic taxa like *Gomphonema* and *Rhoicosphenia*. I predicted dominance by tightly adhering, low profile *Cocconeis* spp. under higher flow conditions.

Under lower velocities, reduced nutrient supply and waste clearance were predicted to lead to earlier host senescence. In addition, rates of epiphyte colonization, and densities of epiphytes per surface area of host were expected to increase, while delivery of dissolved nitrogen would decrease. Under the higher light regime and lower flow regimes, I predicted the highest densities of nitrogen-fixing epiphytic Rhopalodiaceae. Higher PAR and increased photosynthesis in unshaded treatments were expected to stimulate higher growth rates in both host and epiphytes, leading to increased nutrient demand, particularly of nitrogen, which might favor Rhopalodiaceaen N-fixers. Slower flow velocity could also make nitrogen flux more limiting.

The combination of lower light and flow levels was predicted to lead to the shortest *Cladophora* filament lengths and earliest senescence. Epiphyte densities on host cells were predicted to be high as they overgrow their senescent host, but total numbers of epiphytes on attached filaments were predicted to be lower due to lower host surface area.

METHODS

Experimental installation and design

Twenty in-stream channels were constructed with PVC planks (Home Depot, Emeryville, CA, Model # PVC6233-10), non-toxic aquarium silicone glue and connected side-by-side with aluminum brackets (Fig. 1). The channel array was tethered on fixed anchors and floated (with "wacky noodles" www.lifoam.com) above the bed in a 0.6-0.9 m deep pool in the South Fork Eel 50 m upstream of its confluence with Elder Creek (latitude 39°43'47" and longitude 123°38'34"). In floating channels, algae were protected from *Dicosmoecus gilivipes*, large limnephilid caddisfly grazers that when abundant, can rapidly remove *Cladophora*.

The foam floats were adjusted to maintain a constant water depth (12–15 cm) in the channels for the duration of the experiment. The site had relatively uniform light and flow conditions through the duration of the project (9 June to 4 August 2008).

I covered the bed of each channel with local in-stream gravel (~ 3 cm deep). The channels were protected from floating debris by drift diverters 5 m upstream from each channel entrance. I collected 80 ~10 cm-diameter cobbles with attached *Cladophora* from a nearby riffle and placed four in each channel (Figure 2). Light and flow

conditions where algae were collected were similar to those created in my channels. Algae was subsampled and documented to have clean *Cladophora* with few epiphytes. ~~C~~obbles were incubated for 10 days under ambient temperature, velocity and light conditions. Before the velocity and shade treatments were applied, each cobble was subsampled and filament lengths and epiphytes documented ("T_0" data).

To examine the separate and interactive effects of each factor on algae, I imposed two current velocities ("Slow" 0–9 cm/s and "Faster" 10–20 cm/s) and two light levels ("Dark" 150 $\mu E \cdot m^{-2} \cdot s^{-1}$daily maximum and "Light" 1500 $\mu E \cdot m^{-2} \cdot s^{-1}$ daily maximum) in a 2x2 factorial design, with five replicates of each treatment. To simulate predicted climatic changes I chose the "Shade" light treatment with a peak irradiance of 150 $\mu E \cdot m^{-2} \cdot s^{-1}$ (typical solar radiation levels on foggy days (Snyder et al. 2003)). Velocity regimes were chosen to bracket the critical velocity for optimal nutrient supply (8 cm/s; Dodds 1991a)

Water velocities were controlled by raising or lowering rectangular PVC gates installed at the head of each artificial stream-channel. Because ambient river water velocities dropped quite slowly over the weeks of my experiment, I could establish water velocity regimes of 0 – 9 cm/s and 10 – 20 cm/s and maintain them with daily gate adjustments. Water velocity was measured using a Marsh-McBirney Model 201D portable water flow meter (www.marshmcbirney.com).

Light intensity in each shaded channel was controlled using commercially available shadecloth (www.gemplers.com) rated for the desired light reduction of 90%. The shaded treatments had shadecloth cut to fit and held in place with metal fasteners. Ambient light intensity channels were left uncovered. Light levels measured with a radiometer (Li-Cor Li200X, www.licor.com) and had average daily maxima of (mean ± se) 146 ± 4.6 $\mu E \cdot m^{-2} \cdot s^{-1}$for shaded channels and 1512 ± 52 $\mu E \cdot m^{-2} \cdot s^{-1}$for unshaded channels.

Monitoring and Sampling

Following the ten-day incubation period, from 31 May to 9 June, I sampled each cobble to establish baseline conditions (T_0 = 9 June). I regularly monitored the channels for debris, grounding, water temperature and velocity and adjusted the entry gates as needed to maintain the velocity regimes. Actual velocities in the Faster flow treatments ranged from 10-20 cm/s, and from 0-9 cm/s in the Slow treatments, instead of the originally intended 0-5 cm/s and 10-15 cm/s. Every 15 days, cobbles in each replicate were sampled for attached algae and diatoms using forceps and scissors. Representative samples were selected from filament bases, mid-points and tips. Algae and epiphytes were transferred to a 1.5 ml Epitube and preserved in a 3% formalin solution for later microscopic analysis. I measured modal *Cladophora* filament lengths on cobbles in the field and observed grazers by standing quietly near channels randomly selected from each treatment for five minutes, noting conspicuous grazers and their activity. I continued sampling from 9 June until *Cladophora* blooms collapsed and senesced, which occurred on or around 4 August.

Over 400 samples were collected and three representative filaments from each cobble per channel were selected and analyzed with an Olympus BH dissecting

microscope at 400x. Equal numbers of cobbles were selected from upstream, middle and downstream positions within each channel in a stratified random pattern. I followed the protocol of Lowe (2011) for counting attached epiphytes: counting (at 440x magnification) all attached epiphytes in ten 440 μm-wide fields-of-view randomly selected along the sampled *Cladophora* filaments. Diatoms were identified to species where possible, otherwise to genus or family.

To assess grazing pressure in each channel, I collected healthy samples of *Cladophora glomerata* from a nearby boulder and divided them into 20 strands, weighed wet and damp (after blotting each strand between paper towels) on a ScoutPro 50g scale (precision to 0.001g). I attached them to ceramic tiles using rubber bands and placed a tile in the center of each channel. After two weeks, I collected each tile with care taken to catch all mobile grazers on the tile. Each algal sample was re-weighed (wet and damp-dry) and preserved in 20 ml scintillation vials filled with 10% buffered formalin along with all collected grazers for identification and counting.

Data Analysis

I grouped epiphyte counts into three categories at each of the five time periods: Total Rhopalodiaceae, including all *Epithemia* and *Rhopalodia* species, *Cocconeis* spp. including *C. placentula* and *C. pediculus*, and Total Epiphytes (all attached epiphytes visible on both sides of the filament using optical dissection (Lowe 2011)). Using Two-Way ANOVA with replication, I tested whether the means of each treatment group were significantly different from each other. For the grazer assessment, I used a Two-Way ANOVA to test for differences in the mean biomass of introduced, pre-weighed strands lost due to grazing, export and rot in each treatment group.

RESULTS

By day 30 in the experiment, *Cladophora* filaments in unshaded channels were longer (26.5±2.4 cm, mean±se) than in shaded channels (15.8±2.3 cm) and had reached their peak lengths over 5 days later (Table 2, Figs. 3 a,b,c). Mean filament widths in the Slow x Dark treatment were marginally higher, ($P = 0.06$), but filament widths overall were not significantly correlated with either treatment (see Table 7 for a summary of results for two-way ANOVAs). Water velocity did not significantly affect streamer length or width (Fig. 4a, 4b). Total *Cladophora* biovolume per filament increased marginally in unshaded channels ($P = 0.07$) and in slower velocity treatments ($P = 0.09$).

Peak total epiphyte densities were higher in slow channels than in fast channels (Table 3a, Fig. 5a,b). Peak total epiphyte biovolumes, however, were higher in fast channels than in slow (Table 3b, Fig. 5c,d). Rhopalodiaceae epiphytes, however, became more abundant per area of host cell in the faster flow treatments than in the slow treatments, and had significantly higher peak abundances and biovolumes (Table 4a,b, Figs. 6a,b,c,d).

Cocconeis spp. mean density in the faster treatments was higher versus the slow treatments and reached higher peak abundances and biovolumes (Table 5a,b, Figs. 7a,b,d,e). *Cocconeis* also reached those peak abundances nearly a week later in faster channels compared to slow (Fig. 7c).

Total epiphyte biovolume per host filament, defined as the mean epiphyte biovolume per µm host multiplied by the mean host filament length, increased 88% in unshaded treatments ($P = 0.025$). Among all epiphyte classes (Rhopalodiaceae, *Cocconeis* and Total Epiphytes), only *Cocconeis* had a significant response to light, with higher peak abundances in the shaded channels compared to unshaded channels (Figure 7, Table 5). The timings of peak Rhopalodiaceae and peak total epiphytes densities and biovolumes were not significantly related to light or water velocity ($P = 0.54$).

Relative maximum biovolume of Rhopalodiaceae was marginally higher in unshaded channels compared to shaded channels ($P = 0.07$), while the timing of peak relative maximum biovolume of *Cocconeis* was a week later in shaded channels compared with unshaded channels ($P < 0.05$).

Algal strands secured to tiles with rubber bands in the four different flow x light treatments showed no significant differences in biomass losses, expected from rotting, grazing, export or some combination of these ($P > 0.05$) (Table 6, Figure 8). I also observed similar numbers of various grazer taxa among treatments, suggesting that differences in bloom size were more likely due to treatment-related differences in accrual rather than loss processes.

DISCUSSION

Cladophora glomerata filaments grew longer in unshaded channels, as expected (Dodds 1991a&b, Hill et al. 1995, Stevenson et al. 1996), leading to an ~11 cm or 68% increase in peak lengths over shaded channels. *Cladophora* filaments in the unshaded ("Light") treatments also reached their maximum lengths more than 5 days later than those in the shaded ("Dark") treatments, indicating a longer period of net growth.

The lack of a significant response of filament lengths to water velocity could indicate that other velocity-related factors offset or limited growth, or that my relatively modest velocity increase for "faster" flow treatments was not fast enough to cause a response. Bergey et al. (1995) reported no significant difference in *Cladophora* filament lengths between their slow (1.5 cm/s) and medium (16–27 cm/s) treatments, a larger velocity difference than my two treatments.

The offsetting effects of nutrient/waste transport and hydrodynamic drag provide an alternate explanation. While increasing water velocity should increase nutrient supply and waste removal, the associated increase in drag might also export algal filaments (Stevenson 1983, Bergey *et al.* 1995, Dodds 1991a). I do not think flows in my faster treatment were likely to have detached filaments, however.

I should note that the ambient channels were left uncovered while the shaded channels were covered with shade cloth, and this may have resulted in different temperature regimes, wind stirring, aerial influxes and grazer behavior between these

treatments. I think differences in wind stirring would be small, given the narrow width of the channels (15 cm) and the 1-3 cm of freeboard in each that projected above the water surface. Temperatures in all channels remained within 0.1 ^{o}C of the ambient river water temperature. Observations of grazers similarly did not show any change in abundances or behavior between treatments.

Epiphyte Density: Contributing Factors

Epiphyte density per unit host area depends on several factors, including the concentrations of epiphyte cells in the flow passing over the host area, their flow-related probability of settling over the target area, their local growth once settled, their probability of sloughing off, and host surface areal expansion with growth. Epiphyte and host growth rates should both increase with irradiance, perhaps as saturating functions. Epiphyte density should increase with local diatom immigration and reproduction and decrease with increasing host area.

Diatom immigration rates measured in streams range from 50-2500 cells•cm^{2}•d^{-1} (Stevenson and Peterson 1989). Epiphyte settling rates might be non-linearly related to flow velocity, with delivery from upstream enhancing colonization rates up to a point, after which cell sinking rates are not fast enough to counter rates of transport downstream. This transition may not have occurred over the low range of flows in my experiment (0-9 cm/s and 10-20 cm/s). At higher velocities (25-35 cm/s), Stevenson (1983) found increased impingement of diatoms on the substrate due to increased turbulence and thinning of the boundary layer. Higher velocities also led to increased propagule supply over the substrate, and increased reproduction of immigrated diatoms due to increased nutrient supply and waste clearance (Stevenson 1983, Stevenson and Peterson 1989). However, net diatom accrual fell ten-fold as velocities increased from 10 to 30 cm/s in reference streams, due to shear stress removing settled diatoms from the substrate (Stevenson 1983). The probability that epiphytes are exported after settling or multiplying on surfaces should in general increase monotonically with flow velocity.

I also need to consider changes in colonizable area of the host with changes in irradiance and flow velocity. Total host area depends on the number of filaments per basal pad, number of branches, filament length and width. Graham et al. (1982) and Tomlinson et al. (2010) have shown that an increase in peak irradiance from 150 to 1500 $\mu E \cdot m^{-2} \cdot s^{-1}$ leads to a doubling in *Cladophora* growth rate from 0.1 to 0.2 per day. For diatoms, the increase in growth rate is more significant, more than tripling from 0.3 to 0.9 per day (Bothwell 1989, Tuji 2000). This increased responsiveness of diatom growth rates to the higher irradiance levels in my unshaded treatments means that irradiance is likely to have a larger effect on local growth rates of diatom epiphytes than on increases of host surface area. However, peak maximum growth rates of *Cladophora* are significantly higher, estimated by Tomlinson et al. (2010) to be 1.54 per day under ideal irradiance, temperature and flow conditions, which is how host *Cladophora* is often able to outgrow its epiphytes above its saturating current velocity (Dodds 1991a).

Results from my modal length measurements show peak filament lengths 68% longer and mean filament lengths 40% longer in the unshaded channels compared with

shaded channels. However, this length effect was apparent 30 days after treatments were applied, and at this stage there were no significant differences in epiphyte densities for Rhopalodiaceae or total epiphytes. *Cocconeis* densities did show significant differences by the 30 days, but increases were in the unshaded and faster channels, while host filament length increased in the unshaded treatments and should thus have decreased *Cocconeis* densities.

Using these numbers as rough constraints and treating *Cladophora* cells as cylinders with surface area = length x 2π x (radius), I can estimate that, given constant host radii over time, total host area in the unshaded channels is 40% greater than host area in shaded channels. If I assume that diatom concentrations entering shaded versus unshaded channels is unchanged, I estimate that total epiphyte densities in the unshaded channels will be 40% lower based on increased host area alone.

Epiphytes and Water Velocity

Total epiphyte densities increased as expected in the low velocity treatments (as host *Cladophora* filaments senesced earlier in lower nutrient conditions and became overgrown with small late-successional, cyanobacteria such as *Chaemaesiphon* Braun et Grunow, and *Heteroleibleinia* (Geitler). The diatoms Rhopalodiaceae, and non-N-fixing *Achnanthidium minutissimum* (Kütz) Czarnecki also became more abundant. This is most likely due to increased immigration (impingement and settlement) of propagules through the boundary layer in the slower currents, reduced shearing of epiphytes, and host senescence (Stevenson 1983). There was no significant effect of water velocity on filament length, but I predicted a drop in diatom settling of ~10% due to less host branching. As there were ~63% more total epiphytes in slow channels compared with faster channels, it is unlikely that the effect I am seeing is due to the creation of less new settlement space by host filaments in slower channels.

Cocconeis spp. densities increased as predicted in the higher velocity treatments; *Cocconeis* is known to attach itself with a glue pad that would secure it against shear stresses from faster flows (Stevenson and Peterson 1989). However, Rhopalodiaceae epiphytes increased in the faster velocity treatments as well. I had predicted lower Rhopalodiaceae in the faster flow treatments, because of challenges settling, the loss of their N_2 fixing advantage if more TDN is delivered, and because host *Cladophora* might outgrow its epiphytes. Total epiphyte biovolume also increased in the higher velocity treatments, as the relatively larger *Cocconeis* and Rhopalodiaceaen diatoms had a larger influence on biovolume than the smaller but numerically more abundant late stage epiphytes *Achnanthidium*, *Chamaesiphon* and *Heteroleibleinia*.

The conflicting effects of water velocity on epiphyte growth and the differing settling velocities and colonization abilities of epiphytic taxa provides an explanation for these differential results. For example, Rhopalodiaceae may be capable of settling in faster flows because of their heavier frustules, while *Cocconeis* may resist export in faster flows due to its tighter attachment to its host.

An examination of species-specific traits in diatom immigration studies found that certain traits improved immigration success even with increasing flow velocity

(Stevenson and Peterson 1989), and that *Cocconeis*, in particular, was especially resistant to flow disturbance and shear. Adnate diatoms with smaller cell sizes are less susceptible to current stress because they do not protrude into faster flows above the boundary layers along their attachment substrates. *Cocconeis* spp. had smaller frustule sizes than most other diatoms counted in my stream channels, and also secretes a glue that secures its lower frustule to host cell walls (Stevenson et al. 1996). Diatoms with higher specific gravity, such as occurs with heavily silicified frustules (including Rhopalodiaceae), are better able to transit the boundary layer and settle on substrate, particularly in quiescent zones downstream of flow obstructions (Stevenson 1983), and their dense frustules may enable them to resist shear more effectively.

Diatoms with tight attachment to substrates can also resist shear stress and outcompete species with weaker attachments (Stevenson 1983). *Cocconeis* spp. have wider attachment sites than most species and are known for resistance to removal, often leaving behind the bottom valve long after the cell has died (*pers. observation)*. The ability to facilitate attachment by altering the substrate is another colonization enhancing trait (Stevenson 1983), clearly exhibited by Rhopalodiaceae species with their ability to stack upon each other in layers many cells deep. The presence of most of the key traits of good colonizers in *Cocconeis* and Rhopalodiaceae species, and the resultant ability to potentially out-compete other taxa in faster flow conditions, may explain how they have higher densities and biovolumes in the faster flow treatments in my stream channels.

Timing

The significantly delayed peak of *Cocconeis* accrual and relative biovolume in the Faster velocity treatments (7 days, Figure 7c) is consistent with an extended period of population growth (reaching 30-55% larger populations than Slow velocity treatments) in these higher nutrient- and higher propagule-supply conditions.

Epiphytes and Light

Cocconeis were more abundant in shaded than in light treatments, and reached peak relative biovolumes about a week later. This paradox may be due to their dilution in unshaded treatments, if their colonization and local growth was outpaced by the increased growth of the host *Cladophora.* However, as diatom settlement occurs on timescales much faster than filament elongation, and as filament length differences became significant about two weeks after most peaks in *Cocconeis* density, I believe the host area change to be less significant for *Cocconeis* than for later stage epiphytes.

Alternatively, this result may suggest that epiphytic diatoms are outcompeting their *Cladophora* host in low light conditions. *Cocconeis* species are likely to gain nutrients from their host due to their prostrate growth form (Burkholder and Wetzel 1990), and this might buffer their susceptibility to changes in ambient light. The increased photosystem efficiency of diatoms in low light compared to filamentous green algae (Dodds 1991 a, b, Stevenson 1996, Saunders 2009**)** is another factor. *Cocconeis* has been observed at increased abundances in lower irradiance environments in prior studies (Goldsborough 1994, Saunders 2009), and this has been attributed to the adnate form, thinner pervalvar

profile and flattened plastids of the genus, and recent studies have also shown a higher susceptibility to photoinhibition in marine *Cocconeis* taxa (Salleh and McMinn 2011). *Cocconeis* species, being early-successional taxa, also arrive before other epiphytes, and can tolerate earlier season conditions, including more turbid, deeper water and lower incident PAR, giving them a competitive advantage over host cells in adverse light conditions (Burkholder and Wetzel 1990, Marks and Power 2001).

The lack of a significant response to light manipulation for Rhopalodiaceae and Total Epiphyte densities and biovolume per mm^2 host area is contrary to my predictions, although peak relative biovolumes of Rhopalodiaceae were marginally higher in unshaded channels compared to shaded channels ($P = 0.07$), presumably due to the light-intensive nature of N-fixation (Floener and Bothe 1980).

In the density per host area and biovolume measurements, substantial increases in host area (and biovolume) due to increased filament growth in the unshaded channels may obscure any increase in epiphytes due to reproduction.

The moderate but statistically insignificant increase in total epiphyte and Rhopalodiaceae densities and biovolumes in unshaded compared to shaded treatments may reflect an increase in epiphyte growth under higher light conditions as expected (Dodds 1991a,b) that is obscured by the projected ~40% increase in host *Cladophora* area. If I assume that the densities of epiphytes in these channels were uniform over the host filaments, a 40% increase in host filament area would lead to higher total loads of Rhopalodiaceae and total epiphytes per total filament as follows:

Mean epiphyte biovolume per 440 μm of filament (unshaded) = 5,704,859 μm^3 = 12,966 μm^3 per μm host filament. Multiply by mean length of filaments in unshaded treatments: 12,966 μm^3 per μm x 265,250 μm = 3.44×10^9 μm^3 of epiphyte biovolume per host filament in unshaded channels.

Mean epiphyte biovolume per 440 μm of Filament (shaded) = 5,103,345 μm^3 = 11,599 μm^3 per μm host filament. Multiply by mean length of filaments in shaded treatments: 11,599 μm^3 per μm x 157,500 μm = 1.83×10^9 μm^3 of epiphyte biovolume per host filament in unshaded channels. There is thus an 88% increase in total epiphyte biovolume per filament in unshaded channels!

If I perform a two-way ANOVA on each mean biovolume multiplied by each mean filament length in shaded and unshaded channels, I find that the mean biovolume of total epiphytes per filament is significantly higher in unshaded vs. shaded channels (7.50×10^8 vs. 3.88×10^8 μm^3 per host filament, $F = 5.17$, $P = 0.025$, $df = 1,79$).

While I recorded my data using host filament lengths, and did not observe significant changes in filament width, the total colonizable area of attached algae on each cobble increased significantly in the unshaded channels. If the supply of diatoms is limiting, then epiphyte densities could be strongly affected by changes in host area. Future experiments could sample diatom concentrations over time, ideally every two hours upstream of the experiment site (Stevenson and Peterson 1989), and total host area could be tracked on each cobble throughout the experiment to further resolve this issue.

Reduced light levels were experienced during several weeks of the experiment due to statewide wildfires in late June and early July 2008 in California. While ashfall was

minimal at the experiment site, airborne particles reduced peak PAR levels about 40% during the week of June 28–July 5, 2008 according to the Total Solar Radiation data logged at the Angelo Meadow station (sensor.berkeley.edu). As this was during the peak growing season for algae at this location, this reduced light may have limited net growth of diatoms in all treatments, particularly shaded channels.

Finally, nitrogen-fixation is a light-intensive process (Floener and Bothe 1980), so light levels in shaded treatments may have been too low for Rhopalodiaceae to take advantage of low-nutrient and low-flow conditions.

CONCLUSIONS

The productivity of riverine aquatic food webs results from the interplay of physical factors, such as discharge timing and intensity, solar irradiance and turbidity, and biological factors such as predator suppression of grazers and competitive interactions between primary producers. Changes in the timing and intensity of scouring winter floods, for example, can determine whether armored grazers completely suppress algae (Power et al. 2008), while recruitment failure of epiphytic diatoms or cyanobacteria can delay host bloom senescence.

The specific effects of water velocity and light levels on host *Cladophora* and epiphytic diatom performance depend on the specific tolerances and optima for each species. For *Cladophora*, light levels are most significant, and accrual increased dramatically in high light treatments. Greater host accrual also led to higher epiphyte biovolumes per host filament, reflecting both the marginal increases in epiphytes and the significantly larger increases in *Cladophora* filament lengths in higher light. Among the epiphytes, *Cocconeis* spp. showed greater densities in shaded treatments, reflecting both increased relative growth in low irradiance, and possibly faster growth by host filaments in high irradiance treatments.

Water velocity, while important for nutrient supply and waste clearance, has complex and opposing effects on host bloom height and epiphyte colonization outside the extremes of stagnant water and sloughing thresholds. For total epiphytes, specific traits of each taxa led to conflicting effects on epiphyte density and biovolume: densities peaked in the lower velocity channels as expected, while total epiphyte biovolume peaked in the higher velocity channels. For individual taxa, differences in immigration abilities and resistance to export in faster flows led to major differences in biovolume of the host-epiphyte assemblage. For the early- and mid-to-late-stage epiphyte dominants *Cocconeis sp.* and *Epithemia sp.*, water velocity appears to have a positive relationship to colonization rates and densities. By host senescence, however, lower velocity channels became more heavily colonized with later-stage epiphytes, including abundant filamentous cyanobacteria.

Overall, the greater significance of light intensity for the green filamentous macroalga *Cladphora glomerata* is not surprising given the importance of photosynthesis in fueling its massive bloom sizes. For epiphytic diatoms, with their complex life cycle of overwintering, transport, settlement on filaments, and their ability to obtain nutrients from their host macroalga (Whitton 1970, Dodds 1991a, Lowe 2011b) and their

endosymbionts (Floener and Bothe 1980), the greater significance of water velocity is to be expected. The variations in responses of epiphytic taxa depends on their specific life histories and competitive traits, and underscores the complexity underlying riverine food web interactions.

As we have seen, subtle changes in summer irradiation or flow velocities can tip the balance of how long *Cladophora* gets to grow before it gets smothered by its epiphytes. If low flows and light lead to rapid *Cladophora* overgrowth and senescence early in the growing season, as I saw in my treatments, there will be less net productivity generated to feed consumers in the rivers, uplands, and coastal oceans. If high flows and light prolong *Cladophora* growth relative to its epiphytes, there will ultimately be more summer primary production of both host green algae and epiphytes. Under cooler flows, this production could supply high quality food to aquatic consumers. In warming rivers, however, this production might senesce, decay, and support harmful cyanobacterial blooms with the potential to make it out to the ocean (Kudela 2011, Paerl and Huisman 2008). It is clear that changes in climatic conditions may have dramatic effects on the interactions and biomass of primary producers, and that environmental tolerances for specific taxa will have to be accounted for in projections of aquatic food web responses to climate change, if we are to accurately predict the fate of riverine productivity and its impacts on connected ecosystems.

Moving from reach to basin and from weekly to annual scales

By manipulating irradiance and flow in artificial stream channels, I attempted to understand how light levels and flow velocities affect interactions between the dominant macroalga *Cladophora* and its epiphytes, which together account for the bulk of biomass accrual in my study system, and how this affects productivity during the summer growing season. The specific questions addressed in my research were: How do water velocity and solar irradiance affect relative growth and colonization rates of hosts and epiphytes? Under what conditions can *Cladophora* outgrow its epiphytes? At what point in the season do epiphytes become dense enough to suppress the growth of their macroalgal host? What are the implications for total annual accrual of biovolume/biomass of primary producers? If *Cladophora* growth suppression and senescence happened early in the season, less total biomass of host-epiphyte assemblages would proliferate over the summer than if *Cladophora* grew longer, increasing surface area for later-colonizing epiphytes.

Based on published research (Auer and Canale 1982, Hill and Knight 1988 , Dodds 1991a,b, Peterson and Grimm 1992, Hill et al. 1995, and many others cited in Sculley et al. 2013a), I expected accrued algal biomass to depend on irradiance/PAR, discharge/flow velocity, temperature and grazing pressure, and made predictions for *Cladophora* filament length and key epiphyte densities in my stream channels (Table 1). As discussed in the stream channels chapter above, I found significant effects of light and flow on host and epiphyte biovolume. Faster flows and higher light levels produced the longest *Cladophora* filaments and highest epiphyte biovolumes, whereas slower flows and lower light levels led to earlier senescence of *Cladophora*, shorter filaments and lower epiphyte biovolume.

A simple upscaling of these results for my basin-wide frustule counts might lead one to expect saturating or quadratic positive relationships between algae height/frustule counts and discharge and precipitation. There is, however, a threshold dependence of *Cladophora* biomass on discharge, not a linear relationship (Power et al. 2008). Precipitation, while it may lead to scouring floods, may also lead to spring spates that can export algal filaments and exceptionally cloudy growing seasons may limit growth through lowered PAR. Similarly, one might expect a negative relationship between algae height/frustule counts and fog frequency and temperature, but a more complex relationship may be expected when algal photoinhibition and senescence are considered.

In my research developing a paleo-productivity proxy in the chapter below, I hypothesize that algal bloom height and hence frustule counts from the cores would be significantly influenced by the occurrence of one or more bankfull discharges per year (Table 2), but that responses to temperature, total annual discharge, precipitation and PAR were likely to be too complex to leave clear signals in the sedimentary record.

A new paleo-productivity indicator of river food web responses to inter-annual variation in discharge with implications for river-ocean linkages: Riverine diatom frustules in deep marine sediment cores

INTRODUCTION

Global warming is predicted to have dramatic impacts on rivers by altering precipitation and flow regimes, ground water and runoff temperatures, and the timing, quantity, and quality of runoff, with repercussions for riparian, upland, estuarine, and offshore marine ecosystems (IPCC 2007, Poff et al. 2002, PRBO 2011). Global warming will interact with significant cyclical climate phenomena such as El Niño-Southern Oscillation (ENSO) and the Pacific Decadal Oscillation (PDO). It is vitally important to obtain environmental data spanning multiple cycles of the climate phenomena, and multiple generations of various key riverine and riparian species, as background for assessing, interpreting, and forecasting change. Because we lack long direct observational and instrumental time-series for most river ecosystems, paleo-environmental indicators would be invaluable as proxy data for reconstructing environmental and ecological histories over older time periods.

Freshwater diatoms have proven extremely useful as paleo-environmental indicators in lake and marine environments, because their silica shells or frustules preserve well in sediments and retain taxonomically diagnostic characters that distinguish taxa with different environmental tolerances (Smol and Stoermer 2010, Smol et al. 2001). Long depositional sedimentary records are not often preserved in more erosional riverine environments, however.

In the Tagus River of Portugal, investigators surmounted this problem by looking at riverine sediments deposited offshore, in the Tagus pro-delta near the river mouth. Comparing river diatom counts with instrumental records of river discharge, they found that freshwater diatom stratigraphy accurately records both major floods and annual mean river discharge in this area (Gil et al. 2007).

The Eel River, which cuts through high relief topography along the tectonically active North Coast of California (Lisle 1990, Seidl and Dietrich 1992) has few depositional environments in its watershed, but offshore, a deep marine canyon carved at low sea stands provide near-ideal conditions for freshwater sediment deposition (Drexler et al. 2006). Sediment budget studies, using isotopic tracers and fixed ocean-floor monitors in the canyon entrances, confirm that the submarine Eel canyon receives up to 50% of the Eel River's sediment flux (Leithold 1989, Puig et al. 2003, Mullenbach and Nittrouer 2006) at rates high enough to limit bioturbation (Drexler et al. 2006). An extensive marine ocean drilling program (Nittrouer 1999) has yielded hundreds of cores of this sediment deposited onto the adjacent continental shelf, including some cores from an adjacent submarine canyon that can be resolved to annual strata over their first ~100 years (Drexler *et al.* 2006). I sampled these cores to determine whether freshwater diatoms could be recovered that would be useful in assessing the history of environmental and ecological changes in the river over the last century.

The Eel River is the third largest river in California, with a drainage area of 9540 km^2 (Figure 1) and is representative of mid-sized mountainous rivers that collectively account for ~45% of global sediment discharge to the ocean, despite representing only 18% of global discharge and 10% of global drainage area (Milliman and Farnsworth 2008). Rivers of this size class are understudied relative to smaller and larger rivers (Milliman and Syvitsky 1992). Twenty-five years of ecological research in the Eel River

basin has linked annual hydrologic regimes to alternative food web structures with constrasting algal abundance (Power 1990, Power et al. 2004, Power et al. 2008, Power et al. 2009). Extending these inferences to the century scale could be useful in understanding how river food webs under Mediterranean seasonality may respond to climate change (Sala et al. 2000, Gritti et al. 2006, Klausmeyer and Shaw 2009).

By 2070, climate projections (e.g. HadCM3, CM2.x and RegCM3) predict increases in means of maximum temperatures (2.5 ^{o}C warmer) and minimum annual temperatures (2.3 ^{o}C colder), averaging to a small (0.1 ^{o}C) increase in mean annual temperature in the Northwestern California region (Stralberg et al. 2009). Mean annual rainfall may decrease by 101-387 mm (7-28%), although these projections are more uncertain than for temperature (Cayan et al. 2008, PRBO 2011). Bell et al. (2004) projected that with a doubling of atmospheric CO2 there will be a significant increase in extreme temperature events on the North Coast. Modest increases in the number and intensity of large precipitation events are also projected (Cayan et al. 2008). Coastal fog is predicted to either increase if ocean upwelling intensifies under climate change (Snyder et al. 2003, Lebassi et al. 2009) or decrease, following currently observed trends (Johnstone and Dawson 2010). For non-snowmelt-dominated streams, including those in Northwestern California, later streamflow timing is projected, with the center of mass of annual flow shifted 5–25 days later (Stewart et al. 2005).

Climate change will influence rivers directly by altering hydrographs and thermal regimes, and indirectly through effects on vegetation and land use in watersheds. For California North Coast vegetation, climate envelope projections predict areal expansion of chaparral, oak and pine vegetation and a decrease overall in conifer dominated communities over the coming decades (PRBO 2011).

In rivers under Mediterranean seasonality like the Eel, there is great seasonal and interannual variation in accrual of primary production. The filamentous macroalga *Cladophora glomerata* (L.) Kutz, and epiphytic diatoms that grow on *Cladophora* (Figure 2), as well as epiphytic diatoms attached to coarse stony substrates, dominate primary production in larger, sunlit channels draining > 100 km^2. These algae proliferate during the summer low flow season, and are scoured away during winter floods. Over twenty-five years of observations in the Eel River have revealed striking contrasts between "big algae years" when cobble, boulder, and bedrock substrates support large blooms of attached filamentous algae with seasonal peaks in length over 50 cm in height, and "low algae years" when all substrates remain relatively barren, with algal filaments generally less than 5-15 cm in length. These contrasting states shift with the magnitude of the previous winter floods, which in turn govern food web controls on algae (Power et al. 2008). Bed scouring floods obliterate large armored or sessile invertebrate grazers, which are not otherwise controlled by local predators, and demolish algae early in its summer growth season.

When released from grazing, *Cladophora* becomes covered with epiphytes that show a predictable seasonal succession. Earlier summer assemblages of epiphytic diatoms on *Cladophora* are dominated by adnate, low profile diatoms (*Cocconeis placentula* (Her.), *C. pediculus* (Ehrenb.) Kütz., *Achnanthidium minutissimum* (Kützing) Czarnecki), and stalked diatoms (*Rhoicosphenia curvata* (Kütz) Grun. ex Rabh., *Gomphonema* Ehrenb.

spp.). Towards mid- and late summer, two diatoms in the genus *Epithemia* (Rhopalodiaceae): *Epithemia turgida* (Ehrenb.) Kütz. and *E. sorex* Kütz. dominate these epiphyte assemblages (Power et al. 2009). *Epithemia adnata* (Kütz) Bréb. is also common in flocs around stony river substrates (P. Furey, pers. comm.). Because of its distinctive, robust frustule, *Epithemia* spp. was predicted to be a good candidate marker for big algae years in sediment cores that recorded annual deposition (Figure 3). Diatom frustule counts in the annually-resolved sediment cores from the Eel River offshore canyons potentially extend time series information about the correlations between big algal blooms and bed-scouring floods back nearly a century.

I measured freshwater diatom frustules in several cores collected during the STRATAFORM project, an extensive marine sedimentary coring project that was conducted directly offshore of the Eel River mouth (Figure 4) by the US Geological Survey, the University of Washington and the Office of Naval Research (Nittrouer 1999). Drexler et al. (2006) collected 87 push cores at depths ranging from 132m to 735m from the Eel canyon in August 2001. I developed an 84-year record of freshwater diatoms exported from the Eel River to Eel canyon sediments and evaluated their utility as a proxy for biomass accrual of *Cladophora* blooms in the Eel River basin by examining the dependence of freshwater diatom frustule counts in annual varves on algal bloom size, river discharge peaks during winters preceding and following given summer growth seasons, and various other climatic and hydrological parameters.

Materials and methods

Core Collection

T. Drexler, C. Nittrouer, and B. Mullenbach collected and dated all cores analyzed here during their research for the Office of Naval Research STRATAFORM Project (Fig. 4, Drexler et al. 2006). They used a remotely operated vehicle (ROV), the R/V Ventana, operated from shipboard in August 2001 to collect 87 push cores from the four channels that comprise the head of the Eel Canyon (Drexler et al. 2006). Core recovery depths ranged from 138–735 m and core lengths were 30–101 cm. Shipboard and bottom acoustic beacons were used to precisely position the core sites in canyon walls and thalwegs. Cores were sealed and brought back to the University of Washington for processing. Core halves were x-rayed for physical analysis and dates were obtained using ^{210}Pb, ^{137}Cs and ^{7}Be radioisotope techniques (Drexler et al. 2006). STRATAFORM researchers measured ^{210}Pb activity at precise intervals down the cores, and used the appearance and disappearance of bomb radioisotopes (e.g. ^{137}Cs) to provide upper or lower age boundaries based on known years of bomb testing (Drexler et al. 2006). Sediment accumulation rates for all canyon cores were calculated using ^{210}Pb activity along with ^{137}Cs and ^{7}Be (Drexler et al. 2006).

Core Selection

After my exploratory sampling revealed abundant, clearly recognizable freshwater and marine diatom frustules in ten core samples, C. Nittrouer and T. Drexler kindly provided us with three intact core halves for further analysis (Table 1). I chose these cores on the basis of two criteria: (1) maximum core strata preservation and (2) precisely constrained sediment accumulation rates. In the Eel Canyon, as in many submarine canyons incised into continental shelves, these two goals are often conflicting. Bioturbation is the main cause of core strata degradation in these regions (Drexler et al. 2006) and in nearby shelf sediments, marine polychaete worms rapidly degrade event strata within a timescale of 5-10 years (Leithold et al. 2003). In certain settings such as the Eel Canyon, however, high sediment accumulation rates suppress the worms and inhibit bioturbation. These areas, typically shallower canyon thalwegs, show high preservation of physical stratification due to low bioturbation, but poorly constrained sediment accumulation rates (Figure 5). This may be due to episodic increases in sediment deposition during storm events (Drexler et al. 2006, Mullenbach and Nittrouer 2000, Puig *et al.* 2003). Steady (and easily constrainable) sedimentation rates are generally low (<4 mm/yr) because the transport mechanisms (e.g. hemipelagic sedimentation) are slow and steady, but low rates permit worms to thrive. Heavy sedimentation (e.g. turbidity flows down thalwegs) suppresses worms but is generally episodic. Pulsed or irregular sedimentation make it very hard to constrain sedimentation rates.

An exception to this conflict, core L10C3, was collected from the Shemp Channel thalweg (see Site L10 marked with arrow on Fig 4) . Here locally steep canyon walls confine the thalweg to a width of ~40 m (Drexler et al. 2006). Bioturbation is minimal, with greater than 90% preservation of physical structures. The sediment accumulation rate is well constrained, approaching steady-state, with a rate change occurring partway down the core from 4 mm/yr ($r^2 = 0.82$) below 45 cm to 11 mm/yr ($r^2 = 0.73$) above 45 cm core depth. This unique combination of high preservation of strata and well-constrained sediment accumulation rates made core L10C3 an ideal candidate for freshwater diatom accumulation rate analysis.

Slide Preparation and Frustule Counting

Following Abrantes (1988) and Smol et al. (2001), I made slides from core sediments by adding 1 g of sediment to 20 ml deionized water in a 20 ml glass scintillation vial, stirring or agitating for 1 minute to fully suspend the sediment, immediately withdrawing 0.2 ml of suspension and placing it on coverslip. I dried coverslips overnight, and mounted them on microscope slides, using Naphrax (Brunel Microscopes, www.brunelmicroscopes.co.uk). For the exploratory L1C3, L1C5, L1C8 and L1C9 core subsamples, I simply added 1 g of loose sediment to each vial. For the intact L10C3 core, care was taken to withdraw the 1g of sediment from the full depth of the annual varve interval, measured using a micrometer. In the deeper/older section of the core, an

annual depth of 4 mm was used to match the sedimentation rate. In the shallower/younger section of the core an 11 mm depth was taken to match the higher sedimentation rate. To keep a constant sediment mass of 1 g, therefore, a wider cross section was used in the 4 mm annual depth than in the 11 mm section. Care was also taken to ensure that the sediment was fully suspended and disaggregated. As this core has a high fraction of fine sand (>17%) and a low fraction of clay (<28%) compared with other STRATAFORM cores (Drexler et al. 2006), this was not difficult, and visual inspection confirmed that simple stirring and agitation sufficed. Before placing my suspension sample on the coverslip, I pre-weighed each coverslip and weighed it again after sample drying, so that I could measure frustules counted per mg of dry sediment. This also enabled us to convert to frustules deposited per cm^2 per varve (or year) (Gil et al. 2007).

Because freshwater diatoms were much less abundant in cores than marine diatoms, I counted all freshwater diatoms on each entire slide and subsampled the common marine taxa (Smol and Stoermer 2010). Diatoms on each slide were counted in columns from right to left using the movable stage of the Olympus microscope. Column passes were made at 400x, and frustules were identified to species (most freshwater diatoms) or genus (most marine diatoms—for < 5% of marine diatoms, cells could only be identified to family). I measured cell diameters using an ocular Whipple grid. When needed for identification, an oil immersion eyepiece was used at 1000x. Due to the paired nature of diatom frustules, and their tendency to separate during transport, I counted each frustule separately then divided by two to estimate the total number of diatoms. I converted my diatom totals from each slide to the numbers I estimate for the entire varve as follows: I counted all frustules in the subsample, estimated the proportion of the total varve weight per cm^2 represented by the subsample (typically ~1/400), and multiplied the subsample totals by this proportion to get the totals for each varve (Gil et al. 2007).

Algal transect surveys in Upper South Fork Eel River 1988-2001

Diatom frustule densities in cores were compared with the magnitude of algal proliferations repeatedly surveyed by M. Power across four permanent cross-stream transects during summer from 1988 through 2001. These transects were established at 1 to 1.5 km intervals along the upper South Fork Eel River within the Angelo Coast Range Reserve, about 210 km upstream from the mouth of the Eel River. To survey algae, we stretched a meter tape between nails benchmarking each transect (nail to nail distance varied < 2 cm between surveys), and visually assessed dominant and subdominant macroscopic algal taxa using a diving mask or plexiglass view box. We recorded the modal height of attached filaments (or the length from point of attachment of strands of algae floating on the water surface, if these obscured view of the bed). Algal damp mass (w, g cm^{-2}) = 0.026 algal field height (cm) -0.295, ($r^2 = 0.80$, n = 36, $P < 0.0001$) (Power, unpublished data). We also estimated the % cover and condition of algae within an estimated ~100 cm^2 area under each transect point (Power et al. 2008, Power 1992a, Power and Stewart 1987 give further methodological details).

Climatologic Data

Mean annual temperature and precipitation data were obtained from National Weather Service stations Eureka WSO (NWS Code 42910) and Ukiah (NWS Code 49122) at the National Climate Data Center (www.ncdc.noaa.gov). Fog frequency data were obtained from Arcata, California airport records using frequency of cloud height ≤ 400m, JUN-SEP, as a proxy for summer fog frequency (Johnstone and Dawson 2010). ENSO phase is represented by the multivariate ENSO index (MEI) computed every month, using information recorded during the preceding 2 months. (The MEI time series is available online at http://www.cdc.noaa.gov/~kew/MEI.). PDO indices were downloaded from the University of Washington Joint Institute for the Study of the Atmosphere and Ocean (JISAO) (www.jisao.washington.edu).

Results and Discussion

Freshwater frustule counts in core varves dated to years when contemporary records of Eel River discharge and algal bloom survey data were available generally tracked both antecedent winter peak discharge and summer algal bloom magnitudes. Where there were discrepancies, the frustule counts followed the actual algal bloom magnitudes more closely than river discharge. These results held both for a 10 year analysis of three cores sampled for exploratory analysis and for the longer (1988-2001) record analyzed from Core L10C3, in which rates of sedimentation were best constrained, and annual strata were best preserved.

Ten-year record-- Comparison with Upstream Algae Surveys: 1991-2001

In the three exploratory L1C5, L1C8 and L1C9 cores (5 subsampled depths/years, Table 1) from the Larry entrance to the submarine Eel canyon (Fig 4, see Table 1), frustule counts in strata over a 10-year record (1991–2001) tracked peak antecedent winter discharge loosely, with 2/3 of the highest counts following flood years. Frustule counts tracked peak summer algal bloom height more closely, with all of the highest frustule counts occurring during "big" algae years (years with peak averaged modal height > 50 cm). In some years the general relationship between high antecedent winter discharge and large summer algal blooms did not hold. For example, during a drought year for 2000-1, when a small bloom would be expected (Power et al. 2008), a large algal bloom in fact occurred. The core frustule count for that year matches expectations for a large bloom size. Abundances of Rhopalodiaceaen diatoms (*Epithemia* spp.) and abundances of other freshwater diatom taxa were generally correlated in varves, with one exception, when in the drought year of 1991-2, other taxa of freshwater diatoms were unusually high, but counts of Rhopalodiaceae were low.

Thirteen-year record--Comparison with Upstream Algae Surveys: 1988-2001

Analysis of the record from core L10C3 over the same time period from the Shemp canyon entrance further supports and quantifies the relationship with bloom height and with peak antecedent winter discharge (Table 3). Figure 7 shows the period of overlap with the annual algae surveys. Qualitatively, freshwater diatom records both for *Epithemia* spp., and all freshwater diatoms, track the algae bloom record fairly well. Overall the *Epithemia* frustule signal captures over 47% of the variation in Peak Averaged Modal Bloom Height:

The best fit linear regression yields the following expression for converting total freshwater diatom frustule counts into peak algal bloom heights:

$$y\ (\text{algal peak bloom height}) = 0.0119\ (x,\ \text{frustules per varve}) - 284,\ r^2=0.33,\ p = 0.03,\ n = 13$$

The best fit linear regression yields the following expression for converting Rhopalodiaceae diatom frustule counts into peak algal bloom heights:

$$y\ (\text{algal peak bloom height}) = 0.0223\ (x,\ \text{frustules per varve}) - 104,\ r^2=0.47,\ p < 0.01,\ n = 13$$

Despite the suggestion of an asymptote (Figure 9 and 10), a quadratic equation did not significantly improve the fit.

Correlations with Environmental Variables using the Entire Core: 1918-2001

Freshwater diatoms recovered from the entire length of Core L10C3 (Fig 8) show interannual variation as peaks and valleys, but markedly higher frustule abundance during the earliest part of the core (1918-1931), as well as elevated abundances from 1948 to 1966, during a period of major flooding in the Eel Basin, of which the highest discharges on record occurred during the great floods of 1955 and 1964. A large individual peak also occurred in 1976-1977.

I examined the relationship between frustule abundances in strata older than our algal transect record (which started in 1988) with hydrologic records and other environmental parameters. If the relationship between frustule density in an annual varve and the peak algal bloom height during a given year was similar before 1988 to that documented during the period of coincident record (equation (1)), we would expect similar relationships of frustule densities with hydrologic events and other environmental factors influencing algal accrual.

In algal surveys conducted from 1988-2005 along a 4.5 km of river reach at the Angelo Reserve on the upper South Fork of the Eel River, large *Cladophora* blooms (defined *a priori* as exceeding 50 cm in peak modal height) tended to follow winters with floods exceeding bankfull discharge (P = 0.03, Fisher's exact test, n=18) (Power et al. 2008). In rivers with gravel and coarser substrates, bed-mobilizing floods (events that would destroy over-wintering armored grazers) are quasi-threshold events that are typically initiated by discharges that equal or exceed bankfull stage (Parker 1978). Myregression equation (1) predicts that a large, > 50 cm peak modal height "large" algal bloom occurs when the counts exceed 21 *Epithemia* frustules per sample, or 8,524 frustules per varve. For total freshwater diatoms the threshold is 70 frustules per sample or 28,067 frustules per varve.

Extensive surveys throughout the South and Middle Forks, and down the entire Eel River mainstem (M. Power, C. Ng, and J. Sculley, unpublished data) have documented a similar taxonomic composition of attached algae throughout the basin, with *Cladophora glomerata* as the dominant macroalga, and the diatoms *Cocconeis, Achnanthidium*, and *Rhoicosphenia*, as dominant earlier successional, and *Epithemia* spp. as dominant later-stage diatom epiphytes. *Dicosmoecus gilvipes*, the large armored caddisfly that is defended from most predators during its late instars during summer, but can be greatly suppressed by scouring winter floods, is also widespread throughout the basin, but tends to enter prepupation diapause earlier in warmer (e.g. downstream, less forested) portions of the basin (Hannaford 1998, Resh et al. 2011).

Given the basin-wide distributions of these key producer and grazer taxa, we would expect that hydrologic mediation of algae-based food webs across the entire Eel River basin would cause large frustule densities to follow large floods through the entire length of the hydrologic and core-based frustule records. I used the Leggett gage (USGS Station 11475800) and the Scotia gage (USGS Station 11477000) for hydrologic data, and core L10C3 (1918-2001) for frustule records for the periods 1965-2001 (Leggett gage) and 1918-2001 (Scotia gage). For the period of record, all three gages' discharge records are strongly correlated: Branscomb (South Fork Eel within the Angelo Reserve where transects were surveyed) with Leggett (R = 0.97), Branscomb with Scotia (R = 0.94) and Leggett with Scotia (R = 0.87). The 1.5-year recurrence interval ($Q_{1.5}$) can be used as an estimate of bankfull (gravel bed mobilizing) floods (Dunne and Leopold 1978). For the Leggett gage, the 1.5-year recurrence threshold for peak daily discharge was 565 m^3/s, and for the Scotia gage, it was 3,540 m^3/s. I used these thresholds to define a bankfull discharge in the following analysis.

In fifteen of the sixteen summers following winters with recorded peak discharges exceeding bankfull at the Leggett gage (over the whole available discharge record of 36 years), *Epithemia* and *Rhopalodia* frustule counts met or exceeded the 21 frustule threshold, leading to the inference that across the Eel River basin, 15 out of 16 summers following a winter with peak bankfull discharge had large *Cladophora* blooms. Unexpectedly, frustule counts > 21 did occur in 11 out of 20 drought years. Overall, however, I found a significant tendency for large blooms (as defined by the *Epithemia* frustule threshold) to follow winters with peak flows that equaled or exceeded estimated bankfull discharge (Table 4; $\chi^2 = 6.65$, df = 1, p = 0.01.). In thirty-five out of the thirty-seven summers following winters with recorded peak discharges exceeding bankfull at the Scotia gage (over the whole record of 84 years), *Epithemia* frustule counts met or exceeded the 21 frustule threshold, leading to the inference that across the Eel River basin, 35 out of 37 summers following a winter with peak bankfull discharge had large *Cladophora* blooms. Overall, large blooms (as defined by the *Epithemia* frustule threshold) tended to follow winters with peak flows that equaled or exceeded estimated bankfull discharge (Table 5; $\chi^2 = 4.26$, df = 1, p = 0.039). A positive relationship was expected because algae bloom height has been shown to be positively associated with peak discharges in excess of 120 m^3/s at the Branscomb gage (Power et al. 2008).

Evidence against Multi-year Retention of frustules in the river

One possible complication for interpreting the riverine diatom record in marine cores is whether a summer's diatom production might be stored in deep pools, off channel deposits, or other storage elements in the basin. Inferring environmental and ecological conditions from frustule abundance in dated varves would have to account for time lags if, for example, production were stored over low-flow winters until flushed during a subsequent high flow year. As a canyon-bound, incised river, the Eel lacks major off-channel storage areas, but some of its pools are rather deep (5-7 m), particularly where flow is impeded by large bedrock formations. If interannual storage were important, I would expect the density of frustules in a varve to increase with the magnitude of the peak winter flood that follows a given summer growth period.

However, regression of Rhopalodiaceae and total freshwater diatom frustules with the discharge of floods following a given summer season yielded weak negative but marginally significant relationships; Total Freshwater Diatoms vs. Scotia Peak Subsequent Discharge ($r^2 = 0.048$, $p < 0.05$) (Figure 11); and Rhopalodiaceae vs. Scotia Average Growing Season Discharge (defined as average monthly discharge from May-Aug, $r^2 = 0.051$, $p < 0.04$) (Figure 12).

Each frustule "year" is defined as the year of deposition, measured from August 1 to July 30 to match the core collection date. We expect that the vast majority of a given growing season's frustules will be deposited in the offshore Eel canyon during the deposition year immediately following the preceding growing season, e.g. the May–August 2000 growing season frustules should be found in the August 2000–August 2001 varve. Geochronological techniques using ^{7}Be and ^{210}Pb document that Eel fluvial sediments are rapidly (weeks to a few months) deposited during winter following the onset of high river discharge (Mullenbach and Nittrouer 2006). Peak discharges are based on water years measured from October 1 to September 30. Average Growing Season Discharge has been defined here as May 1 to August 31.

The evidence presented here suggests that even with subsequent low-flow winters, multi-year retention does not occur. The positive and significant correlation of frustule deposition with prior-year discharge, and the weak negative relationship of frustule deposition with subsequent-year discharge, supports the hypothesis of discharge (and peak modal height) correlation with no retention, and refutes the hypothesis that frustules are retained (e.g. in deep pools), even during low flow (drought) winters.

In addition, mean frustule counts from consecutive flood years and flood years followed by drought years shows no significant difference (Table 6, $P = 0.11$) providing further evidence that multi-year storage of frustules in the river is not significant.

Other Environmental Parameters

Rhopalodiaceae frustules and total freshwater frustules were negatively related to mean annual precipitation (NWS Station Eureka WSO P_{mean}) (Figures 13 and 14). A negative relationship between Rhopalodiaceae frustules, total freshwater frustules and mean annual temperature (NWS Ukiah T_{mean}) was also observed (Figures 15 and 16). No significant relationships were found with other environmental variables, including precipitation, ENSO and PDO index values and fog. However, a comparison of frustule counts from years with positive ENSO and PDO indices, negative indices, and mixed indices did show a significant difference between in-phase and out-of-phase years. Years with PDO and ENSO indices that were either both positive or both negative had significantly higher Rhopalodiaceae frustule counts than years with indices that were of opposite sign ($p < 0.05$, Table 7). The mechanisms for this difference are unclear, but there is evidence that peak floods in the Eel basin are more frequent, of higher intensity and carry more sediment during in-phase years than out-of-phase years (Andrews and Antweiler 2012), which may more thoroughly export or crush armored grazers and permit *Cladophora* blooms to escape grazing pressure at earlier and/or longer intervals, leading to larger bloom sizes.

The regressions between freshwater diatom frustules and mean annual precipitation as well as mean annual temperature have slopes close to zero (Figures 13-16) as well as somewhat weak negative correlation coefficients. The weak negative relationship of freshwater diatom frustrules with mean annual precipitiaton does suggest that release of algae from top-down grazer control by single-event, bed scouring floods, rather than persistent higher flows and water tables, which might enhance bottom-up factors like nutrient loading from the watershed, underlie the contrast between years with large algal blooms and summers when algae are suppressed. Other potential mechanisms for negative relationships between annual production and precipitation include lower insolation due to turbidity (and cloudiness) associated with extended rainy seasons. Growing season storms can cause runoff and sediment loading into stream channels with associated turbidity that lowers benthic irradiance and photosynthesis. Late spring spates additionally can cause shearing and export of *Cladophora* filaments (Power et al. 2008) prior to the development of epiphyte communities. The combined negative effects of precipitation during the growth season apparently offset any positive effects over the entire Eel River basin, whether through the direct effects above or through some other indirect mechanism. Lower temperatures due to late storms, abundant summer fog or other inclement weather can reduce algal growth rates whereas fair weather and warmer temperatures should increase productivity and potentially standing biomass (Dodds 1991a,b). Delayed algal senescence in cooler water may offset growth reductions by increasing persistence and epiphyte colonization of algal blooms. Both relationships could be non-linear due to increased evapotranspiration and water temperatures during extended sunny periods, and heat stress on *Cladophora* at very low flows and high temperatures. In the Eel River basin as a whole, increased temperatures apparently have a net negative affect on maximum bloom height.

Upscaling

For the period 1988 to 2001, freshwater Rhopalodiaceae frustules recovered from marine core L10C3 provide a good proxy for algal biomass at the algal survey sites along the South Fork of the Eel River near Branscomb, CA. The abundance of Rhopalodiaceae frustules in a varve for a given year was significantly related to surveyed *Cladophora* peak averaged modal height, and this relationship was stronger than the relation of Rhopalodiaceae frustules for a given year to that water year's peak discharge. We would expect these results if these cores had been recovered just downstream from the SFE study reaches, (there were no such cores). It was surprising, however, that frustule counts representing annual flux out of the entire 9540 km^2 Eel basin were so strongly related to bloom heights surveyed over a relatively small (5 km) study reach in the upper portion of the South Fork Eel River (at reaches draining 116–130 km^2). For Rhopalodiaceae and other freshwater diatom counts in annual varves in the deep marine canyons offshore to adequately index basin-wide annual algal production, the following conditions would appear to be required: (1) basin-wide coherence in the annual hydrologic mediation (via food web controls) of algal bloom sizes across the Eel River; (2) lack of storage in depositional environments (deep pools, off channel water bodies or wetlands) so most annual diatom frustule production is exported offshore during the same water year, and (3) basin-wide similarity of light levels, temperature, nutrients, water

velocity and other factors that influence *Cladophora*, *Epithemia,* and other epiphytic diatom accrual during a given year.

Mechanism (1), hydrologic mediation via food web interactions, has been established as a major mechanism of *Cladophora* blooms in the Upper South Fork Eel River basin (Power et al. 2008). In this present study, increased Rhopalodiaceae frustules recovered from marine core L10C3 during summers following bankfull winter floods provide evidence that across the entire Eel River basin during the interval recorded in the core, large algal blooms tended to follow bed-scouring winter floods. There are two algal growth responses to hydrologic mediation that could drive up Rhopalodiaceae counts: (a) longer streamer lengths (bloom height) following scouring floods as *Cladophora* grows under reduced grazing pressure early in the growing season and therefore provides more colonizable area for epiphytes, and (b) higher Rhopalodiaceae densities per unit length of host *Cladophora*. Response (a) has been documented directly (Power et al. 2008) and by proxy in this study. Response (b) would likely depend on how much late-summer *Cladophora* persists to be exported. Because *Epithemia* is highly selected by most grazers in the river (Power et al. 2009), controls over the late summer food web should influence *Epithemia* densities on hosts. However, since in the vast majority of the Rhopalodiaceae frustule counts, variation correlates with *Cladophora* bloom height, the second epiphyte density response may be of secondary importance.

The geomorphology of the Eel as a steep, canyon bound river, and the apparent lack of frustule storage even over drought winters discussed above suggest that there is only one depositional trap in the whole basin – the offshore canyons.

Surveys suggest broad similarity of biota and environmental conditions through the basin, but this interpretation is preliminary and should be treated with caution. While it appears that growing conditions over the entire Eel River basin may vary seasonally in a somewhat synchronous fashion over the year (Sculley *unpublished data*), the river warms more rapidly in the less forested areas downstream from the Angelo Reserve and in the eastern basin. Earlier warming would send the grazer *Dicosmoecus* in to earlier summer diapause (Hannaford 1998, Resh et al. 2001), potentially decoupling summer drought from the grazer's top-down control of late summer <u>*Cladophora*</u> and diatom blooms. Temperature differences between the cool, forested Angelo Reserve where the algal surveys were conducted, and the warmer, less forested Eel basins, may explain why large frustule accumulations following drought winters were more common for output from the entire Eel Basin than were large *Cladophora* blooms following drought winters in the Angelo Reserve surveys.

Conclusions

Significance for Climate-Food Web Analyses

Freshwater diatom frustules recovered from deep marine canyon cores appear to be useful as a paleo-productivity (bloom size) proxy of algae and algae-based food web dynamics going back nearly a century. My results suggest that we can use *Epithemia* and

other freshwater epiphytic diatoms to extend temporal inferences about hydrologically mediated food web responses, e.g. the bimodal algae bloom response to bankfull discharge regimes, back to 1918 for the L10C3 core. The results are also encouraging for spatial upscaling. Algal surveys from 1988-2001 performed in a relatively small portion of the upper Eel River basin (draining 116–137 km^2) correlated well with diatom frustule abundances integrating fluxes from the entire 9540 km^2 Eel River basin over this period. Following a winter with scouring (bankfull) floods, algae are released from suppression by predator-resistant grazers and typically achieve large (> 50 cm) bloom sizes, proliferating in an effectively one-level food chain before other consumers establish grazing pressure in late June–July. This effect on algal biomass depends on peak discharge exceeding the bankfull threshold, and apart from this there is a poor correspondence between algal biomass (and associated frustule loads) and peak and mean discharge (compare Figures 11 and 12 with Tables 4 and 5). In contrast to the threshold nature of algal proliferations and persistence on discharge dependence, the frustule values yield quantitative estimates of bloom size that can be recovered from longer millennial cores.

Based on frustule recovery from marine cores, we are able to estimate the actual size attained by past algal blooms, and therefore the energy available for primary consumers and predators. This should help elucidate food web dynamics in comparable river basins where predator-resistant grazers, *Cladophora* and its epiphytic diatoms occur with well-constrained downstream sediment trap(s) over the temporal- and spatial scales recoverable in sediment cores. Paleo-proxies such as this that provide a record of primary production may greatly expand the time domain of food web analyses beyond the period of not only researcher surveys but also of the instrumental record. As many potential drivers of food web dynamics have periods of decades to centuries, paleo-production proxies may open up new ecosystems to food web analysis and increase our understanding of food web dynamics over longer periods of time.

With the increased understanding of the importance of long-period climate cycles such as the Pacific Decadal Oscillation for marine and freshwater food webs, the need for high-fidelity paleo-productivity proxies has become more apparent. The widespread geographic dominance of *Cladophora glomerata* in temperate freshwater rivers and lakes globally (Whitton 1970, Dodds 1991a, Guiry and Guiry 2012) suggests that its freshwater epiphytic diatoms could be used as proxies in other temperate rivers where depositional records have accumulated at the mouth, in reservoirs or off-channel lakes, or within depositional sub-basins. These records would greatly increase the spatial and temporal scales of inferences linking food webs to environmental change, enhancing our understanding of how river webs may respond to future changes in climate, land cover, and other factors affecting riverine runoff and conditions.

Finally, the development of a paleoproductivity proxy using freshwater diatoms recovered from marine sediments provides a quantitative tool for measuring the transfer of freshwater nutrients into marine ecosystems, and may lead to a more sophisticated understanding of the linkages of freshwater and marine productivity not only in the California Current System but in other marine systems influenced by river inputs worldwide.

From multi-annual to multi-decadal inferences

Global climate change is projected to increase the intensity and frequency of ENSO and PDO events, as well as the occurrence of heat waves, floods and droughts (IPCC 2012). I have confirmed that peak discharge, which itself is influenced by ENSO and PDO state, is the main control on algal bloom size in my proxy data analysis and based on prior research (Power et al. 2008), but other direct climatic effects from fog, precipitation and temperature were marginal or insignificant. The lack of evidence for multi-year retention of frustules in the Eel River basin (Cores Chapter, Table 6) implies that multi-year patterns of frustule counts following sequential droughts and flood years should not be apparent, and this is consistent with my findings. If there were retention of frustules in deep pools or off-channel sedimentary deposits, then multiyear droughts would result in extended sequences of low frustule counts followed by much higher frustule counts at the end of each drought, while frequent floods would be represented by initial flushing of sedimentary frustule deposits followed by threshold blooms of large algal biomass so long as the scouring threshold was exceeded. Without retention each drought or flood year is reflected in frustule counts from the varved sediments of that year. Memory in the frustule proxy record is effectively year to year.

I attempted to determine if the frustule proxy for bloom size differs significantly during and following multi-year phenomena such as ENSO, extreme climate events such as extended droughts, and during and following multi-decadal phenomena such as PDO. I did not make a prediction based solely on ENSO, because precipitation and discharge at the intermediate latitudes of the Eel River basin do not vary consistently with ENSO phase (Background Chapter, Tables 1-2; see Tootle and Piechota 2006 for regional discussion). A recent study has shown that most of the sediment transport in the Eel River occurs during cold phases of the PDO and ENSO (Andrews and Antweiler 2012), presumably as the largest flood events occur when these phases overlap (Table 3; see Milliman and Farnsworth 2008 for regional discussion). This led me to hypothesize that the highest frustule counts might be found in layers deposited during simultaneous cold or warm phases of ENSO and PDO. I found that frustule counts were significantly higher in both cases and I hypothesize this to be potentially related to the higher peak discharges associated with these periods (Cores chapter, Tables 5-6).

Extreme climate events, such as the megafloods of 1955 and 1964, as well as the droughts of the 1930's and late 1970's, may be recognizable not only in core sediments but also in frustule counts, and provide markers to help calibrate dates of deposition. For example, the sedimentation rate of the key core of my study, L10C3, changes from 4 mm/yr to 11 mm/yr following the megafloods of mid-century, as confirmed by radiocarbon dating of these sediments. I found higher frustule counts for a sustained period from the early 1950's to the late 1960's that may correspond to intense flood scour and larger algal blooms during a period of strong cold PDO and ENSO. Other high frustule count periods from 1917-33 may reflect the intense cold PDO of 1917-24 followed by a switch to a warm phase marked by the 1925-6 El Niño. The pronounced low counts in the 1970's may reflect the marked drought of that period. Transient peaks in the frustule record also occur following peak floods associated with ENSO ('+': El Niño, '–': La Niña) and other high-precipitation events in 1925-6(+), 1954-56(–), 1972-3(+), 1973-6(–), 1982-3(+), 1986, 1988-9(–), 1992, 1997-8(+) and 1999.

The influence of riverine nutrients from a coastal California watershed on winter marine phytoplankton blooms in the California Current ecosystem: Preliminary results from sedimentary cores and satellite data.

INTRODUCTION

Primary production in the Eel River has been established by isotopic studies to feed local aquatic and terrestrial food webs (Finlay et al. 2002) before being exported by winter high flows to the estuary, continental shelf and submarine canyons by the following summer (Drexler et al. 2006). Satellite and shipboard data document the offshore transport of sediments from the Eel River basin in a large freshwater plume extending ten kilometers or more offshore (Figure 1) (Geyer et al. 2000) into the California Current System (CCS), which contains one of the world's largest productive marine ecosystems (Checkley and Barth 2009). One of five key eastern boundary current systems, which together account for 20% of global fisheries yield (Chan *et al.* 2008), its productivity is fueled by wind-driven upwelling of nutrient rich waters into coastal photic zones (Hickey 1998).

Ship surveys (*e.g.* Bruland et al. 2001) and satellites (*e.g.* Abbott and Zion 1985) have documented this productivity for decades using a variety of metrics, most typically as chlorophyll *a*, an essential pigment ubiquitous in phytoplankton. Satellite measurements of these marine plankton blooms began from 1978 - 1986 with the Coastal Zone Color Scanner (CZCS) mission (Gregg et al. 2002), and recommenced in 1997 through the present with the SeaWIFs (McClain et al. 2004) and Aqua-MODIS satellite missions (Salomonson et al. 2002). While the main chlorophyll *a* peaks are during the late-spring to summer upwelling period, a substantial winter to early spring peak exists, accounting for 20-33% of the total annual chlorophyll *a* produced (Wetz et al. 2006, Henson and Thomas 2007). The source of nutrients and other conditions that trigger this winter productivity peak has been the source of some controversy and several research papers (*e.g.* Bruland et al. 2001, Henson and Thomas 2007, Checkley and Barth 2009). The early spring peak occurs during predominantly downwelling conditions, so upwelled nutrients are unlikely to be a significant source for these blooms (Wetz et al. 2006).

River plumes have been posited as a possible source of nutrients; nitrogen, iron and silica have been measured in river plumes off the California and Oregon coasts (Geyer et al. 2000, Bruland et al. 2001, Wetz et al. 2006). River plumes also provide a uniquely clement habitat for nascent plankton blooms: a stable buoyant surface layer rich in nutrients and high in the photic zone (Hickey et al. 2010). Elevated populations at all levels of the marine foodweb have been documented for regions influenced by the Columbia River plume (Emmett et al. 2006).

The Eel River mouth is located just north of Cape Mendocino near the center of the CCS. Despite its relatively small size (9540 km^2), it delivers more sediment per unit watershed area than any river in the coterminous United States (Brown and Ritter 1971), and surveys have documented extensive deposits on the nearby continental shelf (Wheatcroft and Borgeld 2000, Mullenbach et al. 2006).

As described above, I used freshwater diatom frustules recovered from datable sedimentary layers in the submarine Eel canyon to assemble an 84 year record of algal productivity and export for the Eel River basin. Here I examine the evidence for the influence of Eel River nutrients on winter marine phytoplankton blooms on the nearby continental shelf using satellite chlorophyll measurements, meteorological time series and diatom proxy data.

BACKGROUND

Oceanographic Context

The mouth of the Eel River empties into the bight between Cape Blanco, Oregon, to the north, and Cape Mendocino, California, to the south, directly into one of the most productive sections of the central California Current System (CCS) (Henson and Thomas 2007). Poleward winds predominate in winter due to the seasonal strengthening and southward position of the Aleutian Low, while equatorward winds take hold in the summer as the North Pacific High strengthens and moves north (Figure 2). Cyclonic precipitation-bearing frontal systems are frequent from October to April, and can alter predominant wind directions on time scales of 1-5 days (Geyer et al. 2003).

The California Current System (CCS) contains one of the most productive large marine ecosystems in the world (Checkley and Barth 2009 and references therein). One of five key eastern boundary current systems, which together account for 20% of global fisheries yield (Chan *et al.* 2008), its productivity is mainly fueled by wind-driven upwelling of nutrient rich waters into coastal photic zones (Hickey 1998).

The primary driver of high productivity in the CCS is upwelling. Upwelling in this region is driven by pressure gradient forcing of north to south winds along the eastern boundary of the North Pacific gyre, driving Ekman pumping of surface waters westward (offshore), which brings deep, cold, nutrient-rich waters from below to replace them along the shoreline (Diffenbaugh et al. 2004, Barth et al. 2007, Chan et al. 2008). This effect is enhanced by flow divergence south of major points of land such as Cape Mendocino and Trinidad Head (Checkley and Barth 2009) (Figure 2).

The marine diatom genus *Chaetoceros* (Ehrenberg) (Figure 3) has been associated with upwelling zones globally (Smol and Stoermer 2010). The resting spores of this genus are heavily silicified and thought to be characteristic of turbulent waters rich in nutrients of upwelling areas (Abrantes 1988). In the Tagus River study cited above (Gil et al. 2007), *Chaetoceros* abundance from marine box cores was linked to upwelling events.

However, downwelling conditions predominate north of Cape Mendocino (Checkley and Barth 2009) during the fall and winter months as poleward winds and the salinity-forced Davidson countercurrent force water towards the coastline. According to Checkley and Barth, Cape Blanco forces the strong coastal upwelling jet offshore, creating a region of less intense upwelling, a "shadow zone" which may serve as a retention zone for marine organisms. In the region between Cape Blanco and Cape Mendocino, where the Eel River mouth is located, increased marine productivity is spurred by this retention zone, as well as submarine canyons, alternating periods of upwelling and downwelling, offshore banks and extensions of the continental shelf as well as the plume of nutrient-rich freshwater from the Eel River itself (Hickey and Banas 2008).

Measurements of water in coastal river plumes extending into the California Current ecosystem have shown the presence of labile carbon, nitrogen, phosphorus, iron and silica, especially during storm events (Hickey et al. 2010). Just offshore of the Eel River

mouth, a highly productive region of the California Current ecosystem extends from Cape Blanco to the north, southwards past Cape Mendocino to the south (Figure 2). Sediment surveys along the nearby continental shelf have documented large quantities of river sediment deposited during floods (Wheatcroft and Borgeld 2000).

Satellite Measurements of Chlorophyll a

The first satellite sensor to measure ocean color on a near-global, continuous basis was the Coastal Zone Color Scanner (CZCS) multi-channel scanning radiometer launched aboard the Nimbus 7 satellite in October 1978. Designed to operate as a proof-of-concept for one year, it measured reflected solar energy in six channels, which allowed mapping of chlorophyll, salinity and temperature, among other parameters (NSSDC 2013). The resulting dataset contains chlorophyll data in units of mg/m^3 in 9 km pixels from 1978 to 1986. Thermal degradation of the main sensor towards the end of the mission as well as failure of one of the sensors used to reconstruct aerosol abundance led to several data reprocessing efforts, including the blended analysis of Gregg et al. (2002) that combined *in situ* measurements of chlorophyll and other ground-truthing techniques to improve the accuracy of CZCS data. The Sea-viewing Wide Field-of-view Sensor (SeaWiFS) instrument was developed as a follow-on to the CZCS to measure ocean color at higher resolutions and with total global coverage (Figure 4). It was launched onboard the SeaStar spacecraft in 1997 and recorded reflected solar energy in eight channels, with chlorophyll data recorded in 4 km and 9 km resolution datasets. The Moderate-Resolution Imaging Spectroradiometer (MODIS) instrument was launched on NASA's Aqua satellite in 2002, and provides the highest resolution ocean color data yet in 36 spectral bands.

RESEARCH QUESTIONS

We are interested in applying our understanding of the climatic, discharge and trophic controls on riverine algal productivity, and our diatom proxy record of algal biomass produced in the Eel River basin and exported offshore, to explore the relationship between freshwater and marine productivity in this region. After examining the available datasets including upwelling, river discharge, SeaWiFS, MODIS and CZCS satellite measurements, PDO and ENSO indices, upstream algal surveys and published shipboard measurements of nutrients, I developed six research questions:

(1) How often do we see marine chlorophyll peaks outside the upwelling season?

(2) What is the temporal correlation between marine chlorophyll, river discharge and upwelling?

(3) Is there a correlation between marine chlorophyll and upstream surveyed algal bloom heights?

(4) Is there a correlation between *Epithemia* frustules exported to the Eel Canyon, and the size of the annual and spring marine phytoplankton blooms as observed in the SeaWIFS, MODIS and CZCS satellite chlorophyll data?

(5) On an annual basis, how does this correlation compare with that between marine chl *a* and *Chaetoceros*, a marine diatom used as an upwelling indicator?

(6) Does the ENSO or PDO Regime have any influence on marine chlorophyll and its dependence on upwelling, discharge, and river algae?

METHODS

Diatom Frustule Counts

Freshwater diatoms deposited in marine cores were identified to species and counted as described in the Cores chapter above. Frustule counts per annual varve for *Epithemia* spp. and total freshwater diatoms were totaled for the entire 84 year record recovered in core L10C3. I also counted frustules of the marine diatom *Chaetoceros* in sedimentary cores and regressed its abundance against peak and cumulative annual upwelling to test its utility as an upwelling indicator off the mouth of the Eel.

Discharge and Upwelling Data

Discharge data for the Eel River was downloaded from the USGS National Water Information System (nwis.usgs.gov). I used the Leggett gage (USGS Station 11475800,) and the Scotia gage (USGS Station 11477000,) for hydrologic data, and core L10C3 (1918-2001) for frustule records for the periods 1965-2001 (Leggett gage) and 1918-2001 (Scotia gage). Upwelling data was downloaded from the Pacific Fisheries Environmental Laboratory (www.pfeg.noaa.gov) using monthly mean pressure fields to calculate the offshore Ekman transport of surface waters due to geostrophic wind stress at two locations bracketing the Eel River mouth (42°N, 125°W and 39°N, 125°W).

SeaWiFS chlorophyll a data

SeaWiFS and Aqua/MODIS chlorophyll a data was obtained from the Ocean Color website maintained by NASA's Goddard Space Flight Center (oceancolor.gsfc.nasa.gov) using the Giovanni agent to compile daily, monthly and annual mean chlorophyll *a* concentrations over a ½ x ½ degree latitude ~2400 km^2 square (124.41 to 124.91°W, 40.75 to 41.25°N) offshore of the Eel River mouth (Figure 1) from 1997 to 2001, the period of overlap between this satellite mission and the STRATAFORM core data.

CZCS chlorophyll a data

CZCS satellite chlorophyll a data were obtained from the National Oceanographic Data Center (www.nodc.noaa.gov) maintained by the National Oceanographic and Atmospheric Administration using the blended analysis method of Gregg et al. (2002) to improve data quality and overcome some of the limitations of the older sensor, including inadequate aerosol sensing and thermal sensor degradation. Monthly and annual chlorophyll data over the same ½ x ½ degree latitude square (~2400 km^2) offshore of the Eel River mouth were extracted using an NIH data viewer over the entire period of the mission from 1978 to 1986.

Data Analysis

I regressed independent variables (discharge, upwelling) against dependent variables (frustules of all freshwater diatoms, *Epithemia* and *Chaetoceros)* against each other and

against SeaWiFS and CZCS chlorophyll *a* annual peaks and mean monthly values. I used regression, t-tests and χ^2 tests to determine if mean chl a, mean discharge, peak modal bloom height of *Cladophora* and upwelling varied significantly with each other and between PDO and ENSO phases. I analyzed SeaWIFS/MODIS chl a data to look for evidence of stronger marine blooms in late summer during years after flood years, offset from periods of strong coastal upwelling. I also looked for strong secondary algal blooms during wet, flooding winters, to see if there was evidence that inorganic nutrient delivery by river water was important.

RESULTS AND DISCUSSION

To determine whether nutrients transported offshore in the Eel River plume might be fertilizing offshore plankton blooms, I first plotted marine chlorophyll *a* in the ½ x ½ degree latitude square offshore of the Eel mouth with upwelling over the period from September 1997 to September 2011 to identify peaks in marine productivity that occurred during downwelling or neutral periods. I found "non-upwelling peaks" in 10 out of 15 years in my data (Figure 5), defined as being at least 33% of the summer peak and occurring between December 1 and April 30 and, and of these at least 9 are in or directly following distinctly downwelling periods with substantial river input. There were fall peaks during downwelling phases 5 out of 15 years, with substantial coincident river discharge.

Using regression, I found a significant strong positive correlation between upwelling and annual chlorophyll *a* (r^2=0.25, p<0.0000001) and a weak negative correlation between river discharge and annual chlorophyll *a* (r^2=0.08, p<0.0001). The association with upwelling is expected and reflects the contribution of upwelled nutrients during the summer upwelling-season bloom. The negative association with discharge may reflect the greater importance of algal-mediated transport of nutrients over abiotic mineral resources present in the river plume. There were no significant correlations between peak and cumulative annual discharge with peak and cumulative annual chlorophyll.

There was no significant correlation between Rhopalodiaceae or total freshwater diatom frustules and upwelling (r^2=0.01, p=0.33 and r^2=0.02, p=0.27, n=55). However, a low but significant correlation is present between both categories of freshwater diatoms and mean annual discharge (r^2=0.05, p=0.03, n=84).

Chaetoceros is an important genus of marine diatom commonly associated with upwelling zones (Gil et al. 2007), and I counted its frustules in the marine sedimentary cores and regressed it against peak and cumulative annual upwelling to test its utility as an upwelling indicator. While *Chaetoceros* is not a particularly good indicator of peak upwelling strength (r^2=0.24, p=0.21, n=55) in my data, it is a good indicator of cumulative annual upwelling (r^2=0.66, p=0.01, n=31) (Figure 6). *Chaetoceros* is also significantly correlated with annual chlorophyll *a* in both the SeaWiFS data (r^2=0.55, p=0.05, n=5) (Figure 7) and the CZCS data (r^2=0.64, p<0.01, n=9) (Figure 8).

There was a significant correlation between mean monthly marine chlorophyll *a* and ENSO state (+/–, t-test) ($p = 0.03$). The difference in means was 2.5 vs. 1.96 mg/m^3 chlorophyll, or a 28% increase in marine chlorophyll during El Niños versus La Niñas. The mechanism for this correlation is unclear, as the correlation between ENSO state and discharge or upwelling is not significant ($p = 0.23$ and 0.28 respectively). I also found a significant association (t-test, $p < 0.05$) between "non-upwelling peaks" in marine chlorophyll and flood years (defined per Dunne and Leopold (1978) as water years at the Scotia USGS gage with peak discharge greater than the 1.5 year recurrence interval, or 3,540 m^3/s) (Figure 9).

Using my definition of winter-spring "non-upwelling peaks", I found a significant and strongly positive correlation of these peaks with peak averaged modal *Cladophora* bloom height from upstream algal surveys during the period of overlap with the satellite record (1998-2011) ($r^2=0.44$, $p<0.02$) (Figure 10). Using the proxy record of freshwater diatom frustules for basin-wide algal productivity, I find a strong but marginally significant correlation of annual mean monthly chlorophyll *a* with *Epithemia* frustules and with total freshwater frustules for the SeaWiFS data period of 1997-2001 ($r^2=0.69$, $p=0.08$ and $r^2=0.62$, $p=0.11$) (Figures 11-13). The correlation of average annual chlorophyll *a* with *Epithemia* frustules for the CZCS data period of 1978-1986 is even stronger, with $r^2=0.75$, $p=0.002$ (Figure 14-15). Total freshwater frustules are also significantly correlated with average annual chlorophyll *a* ($r^2=0.70$, $p=0.005$) (Figure 16).

Taken together, these results imply a connection between riverine algae and the offshore marine ecosystem. While upwelling is clearly the major driver of marine chlorophyll concentrations, my data support a role for freshwater-derived nutrients in winter/spring marine productivity. The finding that the upwelling indicator *Chaetoceros* is not as good an indicator of marine chlorophyll *a* as *Epithemia* frustules underlines the importance of the potential role of freshwater algae in this system. Winter/spring chlorophyll peaks appear to be associated with both downwelling and significant river discharge in my system (Figure 6). Downwelling and higher discharge are common features of cyclonic winter storm systems at the Eel mouth (Geyer et al. 2003).

It is unclear whether the mechanism is mainly hydrologic, or involves riverine algae directly, but the correlation of chlorophyll data with both the upstream annual algal surveys and core-derived freshwater frustules implies a complex role for riverine algae. The significant correlation of winter/spring peak chlorophyll implies a direct role for riverine nutrients—as algae from the summer growing season is entrained in higher winter flows, significant biomass of *Cladophora* and its epiphytes is delivered in the buoyant Eel River plume to the adjacent coastal ocean. Several studies of river plumes at the Eel, the Columbia River, and other rivers along the Oregon coast have found higher concentrations of nitrogen, phosphorus, iron, and silicon in the buoyant river water than the surrounding ocean, particularly during downwelling or neutral periods (Geyer et al. 2000, Bruland et al. 2001, Wetz et al. 2006) and increased abundances of producer, consumer and predator taxa (Emmett et al. 2006, Hickey et al. 2010).

Depending on the nutrient in question, changes in peak and mean discharge could influence the delivery of nutrients to the offshore California Current ecosystem (Bruland et al. 2001, Geyer et al. 2000, Hebert 2001, Hickey and Banas 2008, Hickey et al. 2009). The long-term delivery of algal-derived and terrestrial nutrients to the offshore marine

ecosystem would be enhanced by regular flood scour of Eel River basin sediments, and inhibited by lack of scouring floods. For predominantly abiotic nutrients such as silica and iron, mean discharge should be more important (Wetz et al. 2006), and extended periods of flood and drought, regardless of whether or not scouring floods occur, could impact nutrient delivery.

SUMMARY AND CONCLUSIONS

Taken together, my results paint a complex portrait of the production and fate of riverine algae. Beginning with early season growth on cobble and bedrock substrates, *Cladophora glomerata* blooms are subject to a complex series of hydrologic, climatic and biotic controls that strongly influence the biomass that is available to connected ecosystems both within the watershed and in estuarine and nearshore habitats.

Artificial stream channel experiments have shown that irradiance and current velocity strongly affect primary production through their effects on host-epiphyte interactions. Higher irradiance and faster velocities release *Cladophora* from smothering by epiphytes and lead to the longest filaments and by inference largest biovolumes of host and epiphytes, which are then available to connected food webs. Lower irradiance and slower velocities lead to early smothering of *Cladophora* by its epiphytes, earliest senescence, shortest filaments, and by inference, least biovolumes of host and epiphytes. Irradiance has more important effects on host *Cladophora*, fueling larger blooms, while water velocity (in my treatment ranges) proved to have more important effects on epiphytes, leading to dominant taxa outcompeting other epiphytes under ambient flows.

Through my recovery and analysis of freshwater diatoms in STRATAFORM marine cores, I have established that Rhopalodiaceae and total freshwater frustules from marine sediments accurately track basin-wide algal bloom heights over the entire period of record. This proxy for paleo-productivity has enabled us to make inferences about primary production and food-web dynamics across a larger area and longer timescales than either investigator surveys or the instrumental record have previously made possible. My inferences include the consistent bi-modal response of *Cladophora* bloom height to scouring floods across the Eel River watershed extending back to 1917, the increased bloom height during in-phase ENSO and PDO, and the lack of retention of significant algal production within the watershed on an interannual basis.

Extending frustule-proxy-based inferences to connected marine ecosystems, I have found that freshwater diatom frustules are better predictors of chlorophyll *a* in plankton blooms directly offshore of the Eel River mouth than marine upwelling proxies like *Chaetoceros*. Two sets of satellite data suggest a correlation between *Cladophora* bloom size and freshwater productivity in the Eel basin (measured as Rhopalodiaceae and freshwater diatoms) and marine plankton productivity (measured as chlorophyll *a*). Twenty-five years of annual algal surveys combined with fifteen years of satellite measurements of marine chlorophyll reveal a strong and significant correlation of algal bloom height and winter/spring peaks in marine chlorophyll.

By integrating analyses of upwelling, river discharge, satellite measurements of chlorophyll and direct and proxy measurements of freshwater algal productivity, I have established the presence of a recurrent winter/spring phytoplankton bloom that is not associated with significant upwelling, is frequently preceded by high river discharge events, and has a strong and significant association with freshwater river algal inputs.

The development of a proxy measure for paleo-productivity in temperate rivers has thus enabled a wide range of upscaled inferences about species interactions and responses of productivity to climatic, hydrologic and biotic controls. When integrated with local manipulative experiments, instrumental records and remotely sensed datasets, this tool may enable insights into large-scale and long-term responses of food webs to climate change and cross-ecosystem subsidies that are not otherwise easily obtained. As I have shown, the utility of this proxy should not be limited to the Eel River, but due to the presence of *Cladophora* and similar epiphytic and grazer taxa in temperate rivers worldwide (Whitton 1970, Guiry and Guiry 2012), and the frequent occurrence of submarine canyons in river-shelf sedimentary systems (Drexler et al. 2006), I expect that these techniques will may open up new ecosystems to food web analysis and increase our understanding of food web dynamics over longer periods of time.

This type of multiscale synthesis of manipulative studies, proxy and remotely sensed data may help enhance our understanding of how river webs may respond to future changes in climate, improve our understanding of how the energy flow and biogeochemical fluxes that they mediate may change with climate change, and may lead to a more sophisticated understanding of freshwater and marine productivity linkages in other marine systems influenced by river inputs worldwide.

LITERATURE CITED

Abbott, M. R., and P. M. Zion. 1987. Spatial and temporal variability of phytoplankton pigment off northern California during coastal ocean dynamics experiment. Journal of Geophysical Research 92:1745–1755.

Abrantes, F. 1988. Diatoms assemblages as upwelling indicators in surface sediments off Portugal. Mar. Geol. **85**:15–39.

Andrews, E. D., R. C. Antweiler, P. J. Neiman, and M. F. Ralph. 2004. Influence of ENSO on Flood Frequency along the California Coast. Journal of Climate **17**(2):337-348.

Andrews, E.D., and R.C. Antweiler. 2012. Sediment fluxes from California coastal rivers: the influences of climate, geology and topography. Journal of Geology, **120**:349-366.

Auer, M. T., and R. P. Canale. 1982. Ecological studies and mathematical modeling of Cladophora in Lake Huron: III. The dependence of growth rates on internal phosphorus pool size. Journal of Great Lakes Research **8**:93-99.

Bahls L.L., and E. E. Weber. 1988. Ecology and distribution in Montana of *Epithemia sorex* Kutz, a common nitrogen fixing diatom. Proceedings of the Montana Academy of Sciences **48,** 15-20.

Battarbee, R. W. 1986. Diatom analysis. Pages 527-570 *in* Handbook of Holocene Palaeoecology and Palaeohydrology. B. E. Berglund, editor. Wiley Interscience, Chichester, UK.

Baumgartner, T.R., A. Soutar, and V. Ferriera-Bartrina. 1992. History of Pacific sardine and northern anchovy populations. CalCOFl Reports **33**:24-40.

Bergey, E. A., C. A. Boettiger, and V. H. Resh. 1995. Effects of water velocity on the architecture and epiphytes of *Cladophora Glomerata* (Chlorophyta). Journal of Phycology **31**: 264-271.

Bode, C. 2013. PAR modeling at the Angelo Coast Range Reserve. *In prep.*

Boles, G. L., R. F. Clawson, and R. D. Lallatin. 1977. Some physical, chemical, and biological characteristics of the Eel River estuary. Memorandum Report, June 1977. California Department of Water Resources. Sacramento, California.

Bothwell, M. L. 1989. Phosphorus-limited growth dynamics of lotic periphytic diatom communities: areal biomass and cellular growth rate responses. Canadian Journal of Fisheries and Aquatic Sciences **46**:1293-1301.

Bruland, K. W., E. L. Rue, and G. J. Smith. 2001. Iron and macronutrients in California coastal upwelling regimes: Implications for diatom blooms. Limnology and Oceanography **46**:1661-1674.

Burkholder J.M., and R.G. Wetzel R.G. 1990. Epiphytic alkaline phosphatase on natural and artificial plants in an oligotrophic lake: re-evaluation of the role of

macrophytes as a phosphorus source for epiphytes. Limnolology and Oceanography **35**:736–746.

Cane, M.A. 1992. Tropical Pacific ENSO Models. Pages 583-614 *in* Climate System Modeling, K. Trenberth, editor. Cambridge University Press. Cambridge, UK.

Carpenter, S. R., S. G. Fisher, N. B. Grimm, and J. F. Kitchell. 1992. Global change and freshwater ecosystems. Annu. Rev. Ecol. Syst. **23**:119-139.

Cayan, D. R., and R. H. Webb. 1992. El Niño/Southern Oscillation and streamflow in the western United States, p. 29-69. *In* El Niño, Historical and paleoclimatic aspects of the Southern Oscillation. Cambridge Univ. Press.

Cayan, D. R., E. P. Maurer, M. D. Dettinger, M. Tyree, and K. Hayhoe. 2008. Climate change scenarios for the California region. Clim. Change **87**:S21–S42.

Checkley, D. M., Jr., and J. A. Barth. 2009. Patterns and processes in the California Current System. Progress in Oceanography:doi:10.1016/j.pocean.2009.07.028

Decamps, H. 1993. River margins and environmental change. Ecological Applications **3**:441-445.

Diffenbaugh, N.S., M.A. Snyder, and L.C. Sloane. 2004. Could CO2-induced land-cover feedbacks alter near-shore upwelling regimes? Proceedings of the National Academy of Sciences. **101**(1):27-32.

Dodds, W. K. 1991a. Community interactions between the filamentous *Cladophora glomerata* (L.) Kutzing, its epiphytes and epiphyte grazers. Oecologia **85**: 572-580.

Dodds, W. K. 1991b. Factors associated with dominance of the filamentous green alga *Cladophora glomerata.* Water Res. **25**: 1325-1332.

Dodds, W. K., and D. A. Gudder. 1992. The ecology of Cladophora. Journal of Phycology **28**:415-427.

Drexler, T. M., C. A. Nittrouer and B. L. Mullenbach. 2006. Sedimentation in the Eel Canyon. J. Sed. Res. **76**:839-852.

Duffy, P. A., J. E. Walsh, J. M. Graham, D. H. Mann, and T. S. Rupp. 2005. Impacts of Large-Scale Atmospheric-Ocean Variability on Alaskan Fire Season Severity. Ecological Applications **15**(4): 1317-1330.

Dunne, T., and L. P. Leopold. 1978. Water in environmental planning. W.H. Freeman and Co., San Francisco, CA.

Emmett, R.L., G. K. Krutzikowsky and P. Bentley. 2006. Abundance and distribution of pelagic piscivorous fishes in the Columbia River plume during spring/early summer 1998–2003: Relationship to oceanographic conditions, forage fishes, and juvenile salmonids Progress in Oceanography **68**:1–26.

Fairchild G.W., and R. L. Lowe. 1984. Artificial substrates which release nutrients: effects on periphyton and invertebrate succession. Hydrobiologia, **114**:29-37.

Farnsworth, K.L., and J.D. Milliman. 2003. Effects of climatic and anthropogenic change on small mountainous rivers: The Salinas river example. Global and Planetary Change **39**:1-2, 53-64.

Finlay, J.C., S. Khandwala, and M.E. Power. 2002. Spatial Scales of Carbon Flow in River Food Web. Ecology **83**:1845-1859

Floener L., and H. Bothe. 1980. Nitrogen fixation in *Rhopalodia gibba*, a diatom containing blue-greenish includions symbiotically. Pages 541-552 *in* Endocytobiology, endosymbiosis, and cell biology. W. Schwemmler, and H.E.A. Schenk, editors. Walter de Gruyter & Co., Berlin.

Gasith A., and V. H. Resh. 1999. Streams in Mediterranean climate regions: Abiotic influences and biotic responses to predictable seasonal events. Annual Review of Ecology and Systematics:**30,** 51-81.

Gell, P., J. Tibby, J. Fluin, P. Leahy, M. Reid, K. Adamson, S. Bulpin, A. MacGregor, P. Wallbrink, G. Hancock, and B. Walsh. 2005. Accessing limnological change and variability using fossil diatom assemblages, South-East Australia. River Research and Applications **21**: 257-269.

Geyer, W. R., P. Hill, T. Milligan, and P. Traykovski. 2000. The structure of the Eel River plume during floods. Continental Shelf Research **20**:2067-2093.

Gil, I. M., F. Abrantes, and D. Hebbeln. 2007. Diatoms as upwelling and river discharge indicators along the Portuguese margin: instrumental data linked to proxy information. The Holocene **17**(8): 1245-1252.

Giller, S., and B. Malmqvist. 1998. The Biology of Streams and Rivers. Oxford Univ. Press.

Goldsborough, L. G. 1994. Heterogeneous spatial distribution of periphytic diatoms on vertical artificial substrata. Journal of the North American Benthological Society **13**:223-236.

Goni, M. A. 2011. Controls on the fluxes and composition of organic matter across the land-ocean continuum – what can we learn from sedimentary records in different depositional environments? Invited Lecture presented at 2011 Fall Meeting, AGU, San Francisco, Calif., 5-9 December.

Gregg, W.W., M. E. Conkright, J. E. O'Reilly, F. S. Patt, M. H. Wang, J. A. Yoder, and N. W. Casey. 2002. NOAA–NASA Coastal Zone Color Scanner Reanalysis Effort. Applied Optics **41**(9):1615-1628.

Gresens, S. E. 2001. Thermal sensitivity of ingestion and digestion in larvae of a eurythermal chironomid. Journal of the North American Benthological Society **20**:68-83.

Grimm, N.B. 1987. Nitrogen dynamics during succession in a desert stream. Ecology **68**:1157-1170.

Guiry, M.D., and G.M. Guiry. 2012. AlgaeBase. World-wide electronic publication, National University of Ireland, Galway. http://www.algaebase.org; last accessed on 14 January 2012.

Hannaford, M. 1998. Development and Comparison of Biological Indicators of Habitat Disturbance for Streams and Wetlands. Ph.D. Dissertation. University of California, Berkeley.

Harrington, R., I. Woiwod and T. Sparks. 1999. Climate change and trophic interactions. TREE **14**:146-150.

Hayward, T.L. 1997. Pacific Ocean climate change: atmospheric forcing, ocean circulation and ecosystem response. TREE **12**(4):150-154.

Henson, S. A., and A. Thomas. 2007. Interannual variability in timing of bloom initiation in the California Current System. Marine Sciences Faculty Scholarship. Paper 63.

Herbert, T.D., J.D. Schuffert, D. Andreasen, L. Heusser, M. Lyle, A. Mix, A. C. Ravelo, L. D. Stott, and J.C. Herguera. 2001. Collapse of the California Current during glacial maxima linked to climate change on land. Science **293**:71-76.

Hickey, B.M., and N. S. Banas. 2008. Why is the northern end of the California current system so productive? Oceanography **21** (4), 90–107.

Hickey, B.M., R. McCabe, S. Geier, E. Dever, and N. Kachel. 2009. Three interacting freshwater plumes in the northern California current system. Journal of Geophysical Research **114** (C00B03). doi:10.1029/2008JC004907.

Hill W.R., and A. W. Knight. 1988. Nutrient and light limitation of algae in two northern California streams. Journal of Phycology **24**:125-132.

Hill, W.R. Effects of Light. 1996. Pages 121-148 *in* Benthic Algal Ecology in Freshwater Ecosystems. R.J. Stevenson, M.L. Bothwell, and R.L. Lowe, editors. Academic Press, San Diego, USA.

Hill, W.R., M. G. Ryon, and E. M. Schilling. 1995. Light limitation in a stream ecosystem: Responses by primary producers and consumers. Ecology **76**:1297-1309.

Hondzo, M., and H. Wang. 2002. Effects of turbulence on growth and metabolism of periphyton in a laboratory flume. Water Resources Research **38**:13-1–13-9.

Hopkinson, C. S., I. Buffam, J. Hobbie, J. Vallino, M. Perdue, B. Eversmeyer, F. Prahl, J. Covert, R. Hodson, M. A. Moran, E. Smith, J. Baross, B. Crump, S. Findlay, and K. Foreman. 1998. Terrestrial inputs of organic matter to coastal ecosystems: An intercomparison of chemical characteristics and bioavailability. Biogeochemistry **43**: 1037-1054.

Hu, F.S., B.P. Finney, and L.B. Brubaker. 2001. Ecosystems **4**:358-368.

IPCC. 2007. Contribution of Working Groups I, II and III to the Fourth Assessment Report of the Intergovernmental Panel on Climate Change. Core Writing Team. R.K. Pachauri and A. Reisinger, editors. IPCC.

IPCC. 2012: Summary for Policymakers. , Pages 1-19 *in* Managing the Risks of Extreme Events and Disasters to Advance Climate Change Adaptation [Field, C.B., V. Barros, T.F. Stocker, D. Qin, D.J. Dokken, K.L. Ebi, M.D. Mastrandrea, K.J. Mach, G.-K. Plattner, S.K. Allen, M. Tignor, and P.M. Midgley (eds.)]. A Special Report of Working Groups I and II of the Intergovernmental Panel on Climate Change. Cambridge University Press, Cambridge, UK, and New York, NY, USA.

Johnstone, J. A., and T. E. Dawson. 2010. Climatic context and ecological implications of summer fog decline in the coast redwood region. Proceedings of the National Academy of Sciences 107(10):4533-4538.

Kiffney, P.M., J.P. Bull, and M.C. Feller. 2002. J. Am. Water Res. Assoc. **38**:1437-1451.

Kishi, D., M. Murakami, S. Nakano, and K. Maekawa. 2005. Freshw. Biol. **50**:1315-1322.

Kudela, R. M. 2011. Characterization and deployment of Solid Phase Adsorption Toxin Tracking (SPATT) resin for monitoring of microcystins in fresh and saltwater. Harmful Algae 11:117-125.

Lebassi, B., J. Gonzalez, D. Fabris, E. Maurer, N. Miller, C. Milesi, P. Switzer, and R. Bornstein. 2009. Observed 1970–2005 cooling of summer daytime temperatures in coastal California. Journal of Climate **22**(13):3558–3573.

Leithold, E. L, and R. S. Hope. 1999. Deposition and modification of a flood layer on the northern California continental shelf: lessons from and about the fate of terrestrial particulate organic carbon. Mar. Geol. **154**: 183-195.

Leithold, E. L., D. W. Perkey, N. E. Blair, and T. N. Creamer. 2005. Sedimentation and carbon burial on the northern California continental shelf: the signatures of land-use change. Continental Shelf Research **25**: 349-371.

Leithold, E.L. 1989. Depositional processes on an ancient and modern muddy shelf, northern California. Sedimentology, **36**, 179–202.

Lisle, T. E. 1990. The Eel River, northwestern California; high sediment yields from a dynamic landscape. Pages 311-314 *in* The Geology of North America. Volume O-1. Surface Water Hydrology. M.G. Wolman, and H.C. Riggs, editors. Geological Society of America. Boulder, Colorado, USA.

Lowe R.L., and Y. Pan. 1996. Benthic algal communities and biological monitors. Pages 705-739 *in* Algal ecology: Freshwater benthic ecosystems. R.J. Stevenson, M.J. Bothwell, and R.L. Lowe), editors. Academic Press, San Diego, California, USA.

Lowe, R. L. 2011. Algae Counting Protocol. http://ib.berkeley.edu/labs/power

Lowe, R. L. 2011b. The importance of scale in understanding the natural history of diatom communities. Pages 293-311 *in* The Diatom World. J. Seckbach, and J. P. Kociolek, editors. Springer, New York, USA.

Mantua, N. J. 2012. PDO Index. http://jisao.washington.edu/pdo/PDO.latest

Mantua, N. J., S. R. Hare, Y. Zhang, J. M. Wallace, and R. C. Francis. 1997. A Pacific interdecadal climate oscillation with impacts on salmon production. Bulletin of the American Meteorological Society **78**:1069-1079.

Markovic, D., U. Scharfenberger, S. Schmutz, F. Pletterbauer, and C. Wolter. 2013. Variability and alterations of water temperatures across the Elbe and Danube River Basins. Climatic Change doi 10.1007/s10584-013-0725-4.

Marks J.C. and M. E. Power. 2001. Nutrient induced changes in the species composition of epiphytes on *Cladophora glomerata* Kutz. (Chlorophyta). Hydrobiologia **450**:187-2001.

McCarty, J. P. 2001. Ecological consequences of recent climate change. Conservation Biology **15**:320-331.

Meehl, G. A., F. Zwiers, J. Evans, T. Knutson, L. Mearns, and P. Whetton. 2000. Trends in Extreme Weather and Climate Events: Issues Related to Modeling Extremes in Projections of Future Climate Change. Bulletin of the American Meteorological Society **81**(3):427-436.

Miller, A.J., and N. Schneider. 2000. Progr. Oceanogr. **47**:355-379.

Milliman, J. D., and K. L. Farnsworth. 2008. River Discharge to the Coastal Ocean: a global synthesis. Cambridge University Press, Cambridge, UK.

Milliman, J. D., and P. M. Syvitski. 1992. Geomorphic/Tectonic control of sediment discharge to the ocean: the importance of small mountainous rivers. Journal of Geology **100**:525-544.

Minobe, S. 1997. A 50-70 year climatic oscillation over the Pacific and North America. Geophysical Research Letters **24**:683-686.

Mullenbach, B. L., and C. A. Nittrouer. 2000. Rapid deposition of fluvial sediment in the Eel Canyon, northern California. Continental Shelf Research **20**:2191–2212.

Mullenbach, B. L., and C.A. Nittrouer. 2006. Decadal record of sediment export to the deep sea via Eel Canyon. Continental Shelf Research **26:**2157–2177.

Mullenbach, B.L., Nittrouer, C.A., Puig, P., and Orange, D.L. 2004. Sediment deposition in a modern submarine canyon: Eel Canyon, northern California. Marine Geology **211**:101–119.

Nakagawa, H., and O. G. Opitz. Inducing cellular senescence using defined genetic elements. Methods in Molecular Biology **371**:167-178.

Nittrouer, C.A. 1999. STRATAFORM: overview of its design and synthesis of its results. Marine Geology **154**:3–12.

Paerl, H. W., and J. Huisman. 2008. Blooms like it hot. Science 320:57-58.

Parker, G. 1978. Self-formed straight rivers with equilibrium banks and mobile bed. Part Q. The gravel river. Journal of Fluid Mechanics **89**:127-146.

Parker, M. S., M. E. Power, and J. T. Wootton. 2002. Effects of substrate composition, stream-bed stability, and sediment supply on survival and trophic role of a dominant stream grazer. Verhandlugen-Internationale Vereinigung fur Theoretishce und Angewandte Limnologie **28**:238–241.

Parmesan, C. 2006. Ecological and evolutionary responses to recent climate change. Annu. Rev. Ecol. Evol. Syst. 2006. 37:637–669.

Perkins, D. M., J. Reiss, G. Yvon-Durocher, and G. Woodward. 2010. Global change and food webs in running waters. Hydrobiologia doi 10.1007/s10750-009-0080-7

Petersen, J. H., R. Reisenbichler, and G. R. Gelfenbaum. 2003. Historical changes in the Columbia River estuary using sediment cores. USGS Final Report May 8, 2003. Wfrc.usgs.gov.

Peterson C. G., and N. B. Grimm. 1992. Temporal variation in enrichment effects during periphyton succession in a nitrogen-limited desert stream ecosystem. Journal of the North American Benthological Society **11**:20-36.

Poff, N. L., M. M. Brinson, and J. W. Day, Jr. 2002. Potential impacts on inland freshwater and coastal wetland ecosystems in the United States. Pages 1-56 *in* Aquatic ecosystems and global climate change: Pew Center on Global Climate Change, Washington, DC, USA.

Post, D. M., M.L. Pace, and N.G. Hairston 2000. Ecosystem size determines food-chain length in lakes. Nature **405**:1047-1049.

Power, M. E. 1990a. Seasonal and hydrologic controls of algal blooms in Northern California rivers. Water Resources Center, University of California at Riverside, Riverside, California.

Power, M. E. 1990b. Benthic turfs versus floating mats of algae in river food webs. Oikos **58**:67-79.

Power, M. E. 1991. Shifts in the effects of tuft-weaving midges on filamentous algae. American Midland Naturalist **125**:275-285.

Power, M. E. 1992. Hydrologic and trophic controls of seasonal algal blooms in northern California rivers. Archiv fur Hydrobiologie **125**:385-410.

Power, M. E., and A. J. Stewart. 1987. Disturbance and recovery of an algal assemblage following flooding in an Oklahoma stream. Am. Midland Nat. **117**:333-345.

Power, M. E., M.S. Parker, and W.E. Dietrich. 2008. Seasonal reassembly of a river food web: Floods, droughts, and impacts of fish. Ecological Monographs **78**(2):263-282.

Power, M. E., R. Lowe, P. C. Furey, J. Welter, M. Limm, J. Finlay, C. Bode, S. Chang, M. Goodrich, and J. Sculley. 2009. Algal mats and insect emergence in rivers under Mediterranean climates: Towards photgrammetric surveillance. Freshwater Biology **54**:2101-2115.

Power, M. E., W.E. Dietrich, and J.C. Finlay. 1996. Dams and downstream aquatic biodiversity: Potential food web consequences of hydrologic and geomorphic change. Environmental Management **20**:887-895.

Power, M. E., W.E. Rainey, M.S. Parker, J. L. Sabo, A. Smyth, S. Khandwala, J.C. Finlay, F.C. McNeely, K. Marsee, and C. Anderson. 2004. River to watershed subsidies in an old-growth conifer forest. G.A. Polis M.E. Power, and G. Huxel, editors. Food webs at the landscape level. University of Chicago Press, Chicago, Illinois, USA.

PRBO Conservation Science. 2011. Projected Effects of Climate Change in California: Ecoregional Summaries Emphasizing Consequences for Wildlife. Version 1.0. http://data.prbo.org/apps/bssc/climatechange (Accessed <1/20/2012>).

Puig, P., A. S. Ogston, B. L. Mullenbach, C. A. Nittrouer, and R. W. Sternberg. 2003. Shelf-to-canyon sediment transport processes on the Eel continental margin (northern California). Marine Geology **193**:129–149.

Quinlan, R., M.S.V. Douglas, and J.P. Smol. 2005. Global Change Biology **11**:1381-1386.

Resh, V. H., M. Hannaford, J. Jackson, K., G. A. Lamberti, and P. K. Mendez. 2011. The biology of the limnephilid caddisfly Dicosmoecus gilvipes (Hagen) in Northern California and Oregon (USA) Streams. Zoosymposia **5**:413–419.

Roberts, G. C., M. Ramana, A. Pham, and V. Ramanathan. La Jolla Fog Study. Invited Lecture presented at 2002 Fall Meeting, AGU, San Francisco, Calif., 5-9 December.

Root, T. L., and S.H. Schneider. 1995. Ecology and climate: Research strategies and implications. Science **269**:334-341.

Rosenzweig, C., A. Iglesius, X. B. Yang, P. R. Epstein, and E. Chivian. 2001. Climate change and extreme weather events: Implications for food production, plant diseases, and pests. *NASA Publications.* Paper 24.

Round, F. E. 1973. The Biology of the Algae (2nd edition), Edward Arnold, Ltd, London, UK.

Round, F. E. 1984. The Ecology of Algae. Cambridge University Press, Cambridge, UK

Round, F. E. 1991. Diatoms in river water-monitoring studies. Journal of Applied Phycology **3**(2):129-145.

Round, F. E., R. M. Crawford, and D. G. Mann. 2007. The Diatoms: biology and morphology of the genera. Cambridge University Press, Cambridge, UK.

Salleh, S., and A. McMinn. 2011. The effects of temperature on the photosynthetic parameters and recovery of two temperate benthic microalgae, *Amphora* CF. *Coffeaeformis* and *Cocconeis* CF. *Sublittoralis* (Bacillariophyceae). J. of Phycology **47**(6): 1413-1424.

Salomonson, V.V., W. Barnes, J. Xiong, S. Kempler, and E. Masuoka. 2002. An Overview of the Earth Observing System MODIS Instrument and Associated Data Systems Performance. Geoscience and Remote Sensing Symposium. 2002 IEEE International **2**:1174-76.

Saunders, L. L. 2009. Metaphyton mat conditions and their effects on filamentous algal communities and their diatom epiphytes. Ph. D. Thesis. Drexel University, Philadelphia, Pennsylvania, USA.

Scheffer, M., D. Straile, E.H. van Nes, and H. Hosper. 2001. Limnology and Oceanography **46**:1780-1783.

Schindler, D. W., K.G. Beaty, E.J. Fee, D.R. Cruikshank, E.R. DeBruyn, D.L. Findlay, G.A. Linsey, J.A. Shearer, M.P. Stainton, and M.A. Turner. 1990. Effects of climatic warming on lakes of the central boreal forest. Science **250**: 967-970.

Schindler, D.W. 2009. "Lakes as sentinels and integrators for the effects of climate change on watersheds, airsheds and landscapes." Limnology and Oceanography **54** (6 part 2): 2349-2358.

Seidl, M. A., and W. E. Dietrich. 1992. The problem of channel erosion into bedrock. Catena Supplement **23**:101-124.

Smol, J. P., and E. F. Stoermer. 2010. The Diatoms: Applications for the Environmental and Earth Sciences. Cambridge University Press, Cambridge, UK.

Smol, J. P., H. J. Birks, and W. M. Last, editors. 2001. Tracking Environmental Change Using Lake Sediments. Kluwer Academic.

Snyder, M. A., and L. C. Sloan. 2005. Transient Future Climate over the Western United States Using a Regional Climate Model. Earth Interactions **9**(11):1-21.

Snyder, M. A., L.C. Sloan, N.S. Diffenbaugh, and J.L. Bell. 2003. Future climate change and upwelling in the California Current. Geophysical Research Letters **30**(15): 1823.

Sommerfield, C. K., A. S. Ogston, B. L. Mullenbach, D. E. Drake, C. R. Alexander, C. A. Nittrouer, J. C. Borgeld, R. A. Wheatcroft, and E. L. Leithold. 2007. Oceanic dispersal and accumulation of river sediment. Pages 157-212 *in* Continental-Margin Sedimentation: Transport to Sequence. C. Nittrouer, J. Austin, M. Field, M. Steckler, J. Syvitski, and P. Wiberg, editors. Blackwell Scientific. Oxford, UK.

Sommerfield, C. K., and Nittrouer, C.A. 1999. Modern accumulation rates and a sediment budget for the Eel shelf: a flood-dominated depositional environment. Marine Geology **154**, 227–241.

Sommerfield, C. K., D.E. Drake, and R.A. Wheatcroft. 2002. Shelf record of climatic changes in flood magnitude and frequency, north-coastal California. Geology **30**:395-398.

Steinman, A. D. 1996. Effects of grazers on freshwater benthic algae. Pages 341-373 *in* Benthic Algal Ecology in Freshwater Ecosystems. R.J. Stevenson, M.L. Bothwell and R.L. Lowe, editors. Academic Press, San Diego, California, USA.

Stevenson, R. J. 1983. Effects of current and conditions simulating autogenically changing microhabitats on benthic diatom immigration. Ecology **64**:1514-1524.

Stevenson, R. J., and C. G. Peterson. 1989. Variation in benthic diatom (Bacillariophyceae) immigration with habitat characteristics and cell morphology. Journal of Phycology **25**:120-129.

Stevenson, R. J., and E. F. Stoermer. 1982. Seasonal abundance patterns of diatoms on *Cladophora* in Lake Huron. Journal of Great Lakes Research **8**:169-183.

Stevenson, R. J., and J. P. Smol. 2002. Use of algae in environmental assessments. Pages 775-804 *in* Freshwater Algae in North America: Classification and Ecology. J.D. Wehr, and R.G. Sheath, editors. Academic Press, San Diego, California, USA.

Stevenson, R. J., M. J. Bothwell, and R. L. Lowe. 1996. Algal ecology. Academic Press, San Diego, California, USA.

Stewart, I. T., D. R. Cayan, and M. Dettinger. 2005. Changes toward earlier streamflow timing across Western North America. J. Clim. **18**:1136-1155.

Stralberg, D., D. Jongsomjit, C. A. Howell, M. A. Snyder, J. D. Alexander, J. A. Wiens, and T. L. Root. 2009. Re-Shuffling of Species with Climate Disruption: A No-Analog Future for California Birds? Plos One **4**.

Thompson, D.W.J., and J.M. Wallace. 2000. J. Clim. **13**:1000-1016.

Tomlinson, L. M., M. T. Auer, H. A. Bootsma, and E. M. Owens. 2010. The Great Lakes *Cladophora* Model: Development, testing and application to Lake Michigan. Journal of Great Lakes Research **36**:287-297.

Tootle, G. A., and T. C. Piechota. 2006. Relationships between Pacific and Atlantic ocean sea surface temperatures and U.S. streamflow variability. Water Resources Research **42**:W07411.

Tuji, A. 2000. The effect of irradiance on the growth of different forms of freshwater diatoms: implications for succession in attached diatom communities. Journal of Phycology **36**:659-661.

Walther, G. R. 2010. Community and ecosystem responses to recent climate change. Philosophical Transactions of the Royal Society B **365**:2019-2024.

Wetz, M. S., B. Hales, Z. Chase, P. A. Wheeler, and M. M. Whitney. 2006. Riverine input of macronutrients, iron, and organic matter to the coastal ocean off Oregon, U.S.A., during the winter. Limnology and Oceanography **51**(5): 2221-2231.

Whitford, L. A., and G. J. Schumacher. 1961. Effect of current on mineral uptake and respiration by a freshwater alga. Limnology and Oceanography **6**:423-425.

Whitford, L. A., and G. J. Schumacher. 1964. Effect of a current on respiration and mineral uptake in *Spirogyra* and *Oedogonium*. Ecology **45**:168-170.

Whitton, B. A. 1970. Biology of *Cladophora* in freshwaters. Water Research **4**:457-476.

Winder, M., and D.E. Schindler. 2004. Global Change Biology **10**:1844-1856.

Wolfe, A. P. 1997. On diatom concentrations in lake sediments: results from an inter-laboratory comparison and other tests performed on a uniform sample. J. Paleolimnol. **18**:261-268.

Woodward, G., D. M. Perkins, and L. E. Brown. 2010. Climate change and freshwater ecosystems: impacts across multiple levels of organization. Phil. Trans. R. Soc. B. **365**:2093-2106.

Wooton, J.T., and M.E. Power. 1993. Productivity, consumers and the structure of a river food chain. PNAS **90**:1384-1387.

Zhang, Y., J.M. Wallace, and D.S. Battisti. 1997. J. Clim. **10**:1004-1020.

TABLES

Background Chapter

Year X / Year X+1	Flood	Drought
Flood	High production, Low retention → High frustule counts	Low production, Low retention → Intermediate frustule counts
Drought	High production, High retention → Low frustule counts	Low production, High retention → Low frustule counts

Table 1. Projected count distributions depend on both algal production and export, which in turn depend on discharge during winters prior to and following a given growing season, assuming some algal retention occurs in pools along the Eel during drought years. If no retention occurs, as the accompanying research implies, this becomes a one row table, with High production leading to High frustule counts and Low production leading to Low frustule counts.

	ENSO	PDO
Eel River Annual Peak Discharge-Scotia	r^2 = .001, p = .77	r^2 = .026, p = .14
Eel River Annual Peak Discharge-Leggett	r^2 = .014, p = .48	r^2 = .015, p = .49
Eel River Annual Peak Discharge-Branscomb	r^2 = .156, p = .20	**r^2 = .348, p = .03**
Eel River Mean Monthly Discharge-Scotia	**r^2 = .007, p = .005**	r^2 = .0001, p = .72
Eureka Precipitation	**r^2 = .058, p = .03**	r^2 = .006, p = .48

Table 2. Correlation coefficients for Eel River peak annual and mean monthly discharge (USGS Gage Station 11477000 Scotia) and precipitation (Eureka, CA NWS Station 42910) with corresponding ENSO and PDO annual and monthly index values.

	PDO Warm, ENSO Warm	PDO Warm, ENSO Cold	PDO Cold, ENSO Warm	PDO Cold, ENSO Cold
Mean Discharge (cms)	8339	5759	6900	7381
Peak Discharge (cms)	4755	5044	6294	4857
Top Ten Floods (# events in top10)	4	1	2	3

Table 3. Annual data for Eel River discharge and peak events (USGS Gage Station 11477000 Scotia) and precipitation (Eureka, CA NWS Station 42910) with ENSO and PDO annual mean phases over the period 1917-Present.

t-tests: Two Sample, Unequal Variance, for difference of means in monthly discharge	Mean A	Mean B	Effect Size	P(T<=t) two-tailed	df
In Phase/ Out of Phase	7937	6459	**1,478**	**0.03**	792
Warm/Cold PDO	7737	7188	549	0.44	1076
Warm/Cold ENSO	7870	6901	969	0.17	986

Table 4. Results of t-tests (Two-Sample, Unequal Variances) for significant difference in mean monthly discharge for months with "in-phase" PDO and ENSO (warm/warm and cold/cold) versus "out of phase" PDO and ENSO indices (warm/cold and cold/warm); warm PDO (warm/warm and warm/cold) versus cold PDO (cold/warm and cold/cold); and warm ENSO (warm/warm and cold/warm) versus cold ENSO (cold/cold and warm/cold). The only significant difference in mean monthly discharge is with in-phase versus out of phase indices: in-phase PDO and ENSO months had significantly higher mean discharge than out of phase months, with an effect size of nearly 1500 cm/s.

Flow velocity/ light	**0-9 cm s^{-1}**	**0-9 cm s^{-1}**	**10-20 cm s^{-1}**	**10-20 cm s^{-1}**
	Cladophora	*Epiphytes*	*Cladophora*	*Epiphytes*
150 $\mu E \cdot m^{-2} \cdot s^{-1}$	Shortest filaments;	Intermediate total epiphyte densities	Intermediate filament length	Intermediate total epiphyte densities
	Earliest senescence	Intermediate Rhopalodiaceae	Intermediate senescence	Fewest Rhopalodiaceae
1500 $\mu E \cdot m^{-2} \cdot s^{-1}$	Intermediate Filament lengths	Highest total epiphyte densities	Longest filament length	Intermediate total epiphyte densities
	Intermediate senescence date	Intermediate Rhopalodiaceae	Latest senescence	Fewer Rhop. More Cocconeis

Table 1. Predicted relative growth period duration and maximum length of *Cladophora* hosts, and densities of total and Rhopalodiacean epiphytes. Senescence is commonly defined as the loss of a cell's ability to divide and grow (Nakagawa and Opitz 2007). I empirically define senescence as the loss of greater than half of the chloroplast contents of a host *Cladophora* cell.

Chn	Treatment S: Slow, D: Dark F: Fast, L: Light	6/9: T_0 Mean±SD A, B, C, D	6/24: T_1 Mean±SD A, B, C, D	7/8: T_2 Mean±SD A, B, C, D	7/21: T_3 Mean±SD A, B, C, D	8/4: T_4 Mean±SD A, B, C, D
1	SD	**12.25±3.1** 8, 15, 14, 12	**10.75±1.5** 13, 10, 10, 10	**5.75±6.2** 3, 3, 2, 15	**2.75±1.7** 1, 2, 3, 5	**1.875±2.1** 5, 0.5, 1, 1
2	FD	**8.25±4.3** 9, 14, 5, 5	**8.75±2.9** 9, 12, 5, 9	**7.0±5.4** 15, 5, 3, 5	**1.875±1.5** 2, 1, 0.5, 4	**0.875±.25** 1, 1, 0.5, 1
3	FL	**9.25±2.5** 10, 9, 12, 6	**9.25±2.2** 12, 8, 10, 7	**12.0±9.3** 4, 19, 21, 4	**5.5±3.3** 3, 10, 6, 3	**2.75±1.3** 3, 4, 3, 1
4	SL	**9.5±2,4** 7, 12, 11, 8	**9.75±1.7** 12, 10, 9, 8	**13.0±10.9** 22, 3, 23, 4	**3.25±2.5** 7, 2, 2, 2	**1.13±0.63** 1, 2, 0.5, 1
5	FD	**8.75±1.5** 8, 11, 8, 8	**10.75±2.8** 9. 8, 12, 14	**4.25±2.2** 2, 5, 3, 7	**2.0±0.8** 1, 2, 3, 2	**1.0±0.7** 0.5, 2, 0.5, 1
6	FL	**10.75±2.1** 12, 13, 9, 9	**8.25±2.6** 8, 12, 6, 7	**18.5±15.9** 6, 5, 25, 38	**16.0±16.7** 3, 1, 25, 35	**2.13±2.0** 1, 0.5, 2, 5
7	SL	**7.75±0.96** 7, 9, 8, 7	**7.0±0.8** 8, 6, 7, 7	**21.25±10.3** 32, 8, 26, 19	**8.25±9.3** 5, 2, 22, 4	**5.5±6.5** 4, 1, 15, 2
8	SD	**7.25±1.3** 7, 7, 6, 9	**9.5±0.6** 10, 9, 10, 9	**6.75±4.1** 12, 7, 2, 6	**3.0±0.8** 4, 3, 3, 2	**0.875±0.3** 1, 1, 0.5, 1
9	SL	**11.25±2.1** 13, 13, 9, 10	**11.25±1.7** 12, 11, 9, 13	**41.75±20.2** 31, 62, 55, 19	**36.75±19.5** 43, 60, 30, 14	**11.5±13.8** 2, 32, 5, 7
10	FD	**6.25±0.5** 6, 6, 7, 6	**10.25±1.5** 9, 11, 12, 9	**4.0±1.4** 3, 4, 6, 3	**6.25±3.4** 2, 9, 9, 5	**1.5±1.2** 0.5, 3, 2, 0.5
11	FL	**8.75±0.96** 8, 10, 9, 8	**8.75±2.2** 12, 8, 8, 7	**33.5±10.5** 45, 37, 32, 20	**28.25±16.1** 40, 30, 38, 5	**4.5±4.4** 2, 11, 2, 3
12	SD	**10.0±0.8** 11, 9, 10, 10	**10.0±0.8** 11, 10, 9, 10	**15.75±12.5** 6, 7, 17, 33	**11.5±11.4** 2, 4, 13, 27	**1.25±0.5** 2, 1, 1, 1
13	SD	**9.0±1.6** 7, 9, 9, 11	**9.0±1.4** 11, 8, 9, 8	**29.5±28.1** 71, 22, 9, 16	**19.0±19.2** 45, 6, 3, 22	**2.0±1.4** 1, 2, 1, 4
14	FL	**7.75±1.7** 8, 7, 10, 6	**9.25±2.6** 8, 7, 13, 9	**39.25±7.4** 38, 34, 50, 35	**22.5±8.6** 18, 21, 35, 16	**13.25±9.2** 17, 9, 24, 3
15	FD	**8.75±2.5** 9, 8, 6, 12	**8.5 ±2.6** 7, 12, 9, 6	**29.5±32.1** 21, 77, 12, 8	**15.0±10.9** 16, 30, 6, 8	**4.75±4.3** 11, 4, 2, 2
16	SL	**6.75±0.96** 6, 6, 7, 8	**8.25±2.9** 9, 6, 6, 12	**37.5±18.2** 23, 30, 64, 33	**27.0±11.5** 10, 32, 35, 31	**12.0±10.6** 1, 5, 20, 22
17	SL	**7.75±2.5** 11, 7, 5, 8	**8.25±2.8** 11, 10, 5, 7	**21.25±10.2** 17, 24, 34, 10	**10.25±10.9** 4, 9, 26, 2	**4.75±6.2** 1, 3, 14, 1
18	FD	**8.5±1.7** 11, 8, 7, 8	**8.5±3.0** 12, 6, 6, 10	**12.0±8.3** 23, 10, 12, 3	**2.25±0.5** 2, 3, 2, 2	**1.13±0.5** 2, 1, 1, 0.5
19	FL	**6.75±1.7** 7, 6, 5, 9	**9.5±1.9** 8, 12, 10, 8	**12.5±8.6** 5, 7, 14, 24	**4.75±3.8** 4, 4, 1, 10	**1.5±1.2** 2, 0.5, 0.5, 3
20	SD	**9.25±2.2** 8, 12, 10, 7	**9.5±2.4** 6, 11, 10, 11	**6.75±2.1** 9, 5, 8, 5	**5.375±8.4** 0.5, 2, 18, 1	**0.625±0.3** 0.5,1,0.5, 0.5
	All FL	**8.65±0.68**	**9.0±0.22**	**23.15±5.59**	**15.4±4.62**	**4.83±2.16**
	All SL	**8.60±0.80**	**8.90±0.73**	**26.95±5.43**	**17.10±6.33**	**6.96±2.09**
	All FD	**8.10±0.47**	**9.35±0.49**	**11.35±4.76**	**5.48±2.52**	**1.85±0.73**
	All SD	**9.55±0.81**	**9.75±0.30**	**12.9±4.53**	**8.33±3.10**	**1.33±0.27**

Table 2. *Cladophora* filament growth across all channels and light and velocity treatments

Total Epiphyte Abundances (frustules)

Chn	Treatment S: Slow, D: Dark F: Fast, L: Light	6/9: T_0	6/24: T_1	7/8: T_2	7/21: T_3	8/4: T_4
6	FL	89.4	1119.7	727.34	1272.9	1228.6
19	FL	147.64	1070.62	3126.23	2147.3	2500.5
14	FL	210.61	659.33	1591.5	2556	2844.8
11	FL	62.62	461.36	1409.6	2082.5	2920.7
All FL	**Mean±SE**	**127.6±33**	**827.8±160**	**1713.7±506**	**2014.7±269**	**2373.7±392**
10	FD	54.6	550.65	2552.25	1127.1	1630
15	FD	109.66	446.36	1954.95	2141	2748
18	FD	77.68	386.16	1842.34	1089.2	3094.5
5	FD	139.95	185.34	1883.22	2020.1	1780.8
All FD	**Mean±SE**	**95.4±19**	**392.1±77**	**2058.2±166**	**1594.4±282**	**2313.3±359**
9	SL	80.17	588.76	924.56	1565	1062.2
7	SL	194.57	144.98	1786.67	3595.9	8130.4
17	SL	219.1	342.12	1288.69	3088.1	6865.2
16	SL	199.11	176.87	1952.44	4176.7	2386.8
All SL	**Mean±SE**	**173.2±31**	**313.2±102**	**1488.1±235**	**3106±560**	**4611±1708**
20	SD	241.36	376.39	985.82	835.7	3261.8
12	SD	33.66	443.15	2536.41	2974.6	2818.6
8	SD	55	327.29	1270.19	1758.6	2211.9
13	SD	298.84	433.25	1565.73	1287.7	4114.8
All SD	**Mean±SE**	**157±66**	**395±27**	**1589.5±337**	**1714.2±461**	**3101.8±400**

Table 3a. Total densities of *all* epiphytes across all channels, light and velocity treatments, in frustules per square millimeter of host surface area.

Total Epiphyte Biovolumes

Chn	Treatment S: Slow, D: Dark F: Fast, L: Light	6/9: T_0	6/24: T_1	7/8: T_2	7/21: T_3	8/4: T_4
6	FL	282,372	4,666,627	1,573,676	4,932,648	2,423,247
19	FL	557,447	8,387,800	2,982,895	5,269,133	2,976,247
14	FL	999,953	2,431,685	4,811,429	6,630,025	4,578,408
11	FL	163,178	1,750,464	4,737,987	6,883,245	7,233,870
All FL	**Mean**	500,737	4,309,144	3,526,497	5,928,763	4,302,943
	±SE	185,756	1,495,407	776,089	485,641	1,078,564
10	FD	272,773	1,615,599	5,481,148	4,976,208	5,346,482
15	FD	119,962	1,895,012	5,625,863	7,484,717	6,760,213
18	FD	256,778	1,661,315	5,214,057	2,592,251	5,784,650
5	FD	449,149	535,562	4,126,398	5,901,516	4,471,033
All FD	**Mean**	274,666	1,426,872	5,111,867	5,238,673	5,590,594
	±SE	67,516	303,338	339,381	1,022,925	475,979
9	SL	354,657	2,152,605	3,283,472	5,419,798	2,713,784
7	SL	772,630	323,457	2,865,642	1,879,412	1,591,279
17	SL	262,702	1,101,088	4,699,447	3,232,789	4,221,921
16	SL	475,335	513,696	5,469,639	2,256,969	1,867,007
All SL	**Mean**	466,331	1,022,711	4,079,550	3,197,242	2,598,498
	±SE	110,994	411,386	607,175	793,820	591,493
20	SD	681,703	1,685,012	3,089,366	1,729,697	1,713,015
12	SD	145,466	2,204,570	4,398,310	2,454,344	2,270,606
8	SD	264,922	684,253	2,907,742	5,150,269	3,054,299
13	SD	1,418,303	984,072	2,369,723	2,274,897	3,536,788
All SD	**Mean**	627,599	1,389,477	3,191,285	2,902,302	2,643,677
	±SE	287,537	343,197	430,374	764,998	405,336

Table 3b. Total biovolumes of total epiphytes across all channels, light and velocity treatments, in cubic microns.

Rhopalodiaceae Epiphyte Abundances (frustules)

Chn	Treatment S: Slow, D: Dark F: Fast, L: Light	6/9: T_0	6/24: T_1	7/8: T_2	7/21: T_3	8/4: T_4
6	FL	7.5	2.74	4.65	155.5	128.6
19	FL	10.26	427.76	31.55	326.4	100.9
14	FL	47.12	1.45	21.06	588.1	323.1
11	FL	7.33	9.48	18	119.2	892.7
All FL	**Mean±SE**	**18.1±9.7**	**110±106**	**18.8±5.5**	**297±107**	**361.3±184**
10	FD	5.83	1.9	6.21	93.8	81.6
15	FD	8.42	2.49	8.32	171.6	517.2
18	FD	1.32	8.11	47.54	27.4	389.4
5	FD	13.25	6.2	11.02	55.4	199.4
All FD	**Mean±SE**	**7.2±2.5**	**4.7±1.5**	**18.3±9.8**	**87.1±31**	**296.9±97**
9	SL	8	7.91	31.37	240.1	58.8
7	SL	30.85	0	19.86	82.8	106.3
17	SL	1.45	10.53	59.78	119	172
16	SL	11.11	0.76	37.91	26.5	135.2
All SL	**Mean±SE**	**12.9±6.3**	**4.8±2.6**	**37.2±8.4**	**117±45**	**118±24**
20	SD	0	8.03	24.41	39.1	104.2
12	SD	2.77	6.45	1.55	56.2	28.2
8	SD	7.29	0.66	0.54	345.8	65.8
13	SD	8.88	5.43	42.39	46.3	61.9
All SD	**Mean±SE**	**4.7±2**	**5.1±1.6**	**17.2±10**	**122±75**	**65.0±16**

Table 4a. Total abundances of Rhopalodiaceae epiphytes across all channels, light and velocity treatments, in frustules per square millimeter of host surface area.

Rhopalodiaceae Epiphyte Biovolumes

Chn	Treatment S: Slow, D: Dark F: Fast, L: Light	6/9: T_0	6/24: T_1	7/8: T_2	7/21: T_3	8/4: T_4
6	FL	39,427	52,965	82,037	463,932	1,263,049
19	FL	134,328	7,115,832	365,823	865,029	744,346
14	FL	410,887	25,620	121,788	2,226,728	1,189,319
11	FL	50,728	88,267	184,057	1,125,565	4,525,899
All FL	**Mean**	158,843	1,820,671	188,426	1,170,314	1,930,653
	±SE	86,639	1,765,100	62,748	377,512	872,635
10	FD	37,701	5,178	117,014	388,529	396,055
15	FD	18,150	40,155	52,237	1,693,296	3,036,740
18	FD	1,726	168,253	277,447	224,212	1,681,327
5	FD	84,815	78,585	31,795	392,735	1,615,818
All FD	**Mean**	35,598	73,043	119,623	674,693	1,682,485
	±SE	17,978	35,099	55,655	341,794	539,549
9	SL	50,000	52,237	378,200	1,356,142	839,141
7	SL	295,623	0	73,839	389,635	529,356
17	SL	15,588	39,427	588,093	381,086	1,092,617
16	SL	66,099	1,726	394,461	187,509	718,460
All SL	**Mean**	106,828	23,348	358,648	578,593	794,893
	±SE	63,807	13,247	106,233	263,351	117,951
20	SD	0	120,466	169,521	156,793	651,095
12	SD	30,124	115,288	27,346	323,241	164,318
8	SD	64,915	12,810	1,726	2,560,319	521,565
13	SD	53,963	6,904	250,049	305,279	380,007
All SD	**Mean**	37,250	63,867	112,160	836,408	429,246
	±SE	14,385	31,224	58,944	575,846	104,224

Table 4b. Total biovolumes of Rhopalodiaceae epiphytes across all channels, light and velocity treatments, in cubic microns.

Cocconeis Epiphyte Abundances (frustules)

Chn	Treatment S: Slow, D: Dark F: Fast, L: Light	6/9: T_0	6/24: T_1	7/8: T_2	7/21: T_3	8/4: T_4
6	FL	56.49	1093	490.48	998.1	179.9
19	FL	66.68	278.79	869.71	1301.3	576.9
14	FL	100.1	636.27	1393.35	1367.5	685.6
11	FL	41.53	435.1	1195.17	1545.4	568.3
All FL	**Mean±SE**	**66±12**	**610.8±177**	**987.2±198**	**1303±114**	**503±111**
10	FD	5.43	524.5	2486.37	922.9	1260.7
15	FD	15.69	425.09	1827.4	1836.5	1203.8
18	FD	21.91	355.9	1640.95	735.3	1485.1
5	FD	54.6	157.45	1660.4	1837.5	1125.9
All FD	**Mean±SE**	**24.4±11**	**365.7±78**	**1904±199**	**1333±293**	**1269±77**
9	SL	12.82	571.62	717.66	807.1	554.7
7	SL	48.73	125.42	1077.92	330.2	41.9
17	SL	52.45	305.86	1114.61	888	432.1
16	SL	118.55	121.1	1493.75	533.2	330.3
All SL	**Mean±SE**	**58.1±22**	**281±106**	**1101±159**	**640±128**	**340±109**
20	SD	87.9	355.25	857.46	456.5	132.5
12	SD	25.66	425.06	1756.44	429.7	713.3
8	SD	8.33	313.88	1202.22	801.6	532.5
13	SD	90.75	421.52	648.44	592.9	807.4
All SD	**Mean±SE**	**53.2±21**	**378.9±27**	**1116±242**	**570.2±85**	**546.4±149**

Table 5a. Total densities of *Cocconeis* epiphytes across all channels, light and velocity treatments, in frustules per square millimeter of host surface area.

Cocconeis Epiphyte Biovolumes

Chn	Treatment S: Slow, D: Dark F: Fast, L: Light	6/9: T_0	6/24: T_1	7/8: T_2	7/21: T_3	8/4: T_4
6	FL	236,641	4,601,390	1,455,023	4,353,320	602,192
19	FL	247,025	1,108,852	2,486,129	4,160,714	2,083,660
14	FL	338,366	2,403,342	4,664,062	4,315,068	2,543,072
11	FL	105,866	1,621,600	4,520,842	5,536,078	2,017,996
All FL	**Mean**	231,975	2,433,796	3,281,514	4,591,295	1,811,730
	±SE	47,846	769,986	786,134	317,667	419,755
10	FD	37,364	1,590,280	5,343,617	4,509,564	4,756,411
15	FD	40,478	1,853,385	5,554,664	5,749,103	3,309,584
18	FD	87,184	1,489,394	4,909,448	2,337,662	3,888,554
5	FD	158,799	455,955	4,084,381	5,442,417	2,729,248
All FD	**Mean**	80,956	1,347,254	4,973,028	4,509,687	3,670,949
	±SE	28,339	306,845	325,240	770,489	432,335
9	SL	59,160	2,096,273	2,817,907	3,629,303	1,590,692
7	SL	102,752	315,730	2,737,992	1,207,355	158,877
17	SL	177,481	1,059,951	4,063,367	2,682,074	1,296,612
16	SL	359,119	496,199	5,011,108	1,942,142	920,273
All SL	**Mean**	174,628	992,038	3,657,593	2,365,219	991,613
	±SE	66,171	400,749	543,706	517,844	309,631
20	SD	280,233	1,561,522	2,882,639	1,401,017	424,337
12	SD	96,525	2,082,241	4,280,139	1,836,185	1,913,766
8	SD	369,503	671,039	2,895,160	2,402,715	1,269,105
13	SD	36,337	971,521	1,977,471	1,853,295	2,612,730
All SD	**Mean**	195,649	1,321,581	3,008,852	1,873,303	1,554,985
	±SE	77,774	313,837	475,112	205,164	466,158

Table 5b. Total biovolumes of *Cocconeis* epiphytes across all channels, light and velocity treatments, in cubic microns.

Losses due to Grazing, Rot and Export

Tuft	Treatment	Initial Wet Weight	Initial Damp Weight	Final Wet Weight	Final Damp Weight	Change in Wet Weight	Change in Damp Weight
1	SD	7.988	3.82	3.274	1.454	4.714	2.366
2	FD	6.894	3.35	4.221	1.392	2.673	1.958
3	FL	5.825	3.444	3.754	1.413	2.071	2.031
4	SL	4.683	3.074	5.797	2.076	-1.114	0.998
5	FD	8.88	3.755	4.846	1.735	4.034	2.02
6	FL	5.459	2.263	4.344	1.304	1.115	0.959
7	SL	6.29	2.781	5.288	1.667	1.002	1.114
8	SD	8.491	3.429	4.55	1.521	3.941	1.908
9	SL	8.286	3.711	7.256	2.31	1.03	1.401
10	FD	9.782	3.654	5.06	1.656	4.722	1.998
11	FL	8.753	3.739	LOST-BROKEN BAND			
12	SD	8.855	2.63	5.354	1.464	3.501	1.166
13	SD	8.024	2.925	3.431	1.06	4.593	1.865
14	FL	9.812	3.176	5.576	1.574	4.236	1.602
15	FD	9.004	3.053	5.703	1.951	3.301	1.102
16	SL	7.577	3.068	4.097	1.851	3.48	1.217
17	SL	10.075	3.656	8.397	2.511	1.678	1.145
18	FD	10.404	3.72	4.768	1.529	5.636	2.191
19	FL	10.57	3.92	4.55	1.456	6.02	2.464
20	SD	9.353	3.96	6.9	2.541	2.453	1.419

Table 6. Initial and final wet and damp weights of detached clumps of *Cladophora* strands placed in channels to evaluate losses from grazers, sloughing or export. Treatments are labeled as follows: S=Slow, D=Dark, F=Faster, L=Light. The clump for channel 11 was lost before measurement.

Summary of ANOVA Results

Variable	Source	F-Ratio	*P*	df
Cladophora: length	Velocity	0.5693	0.45	1,79
	Light	**10.3671**	**0.002**	**1,79**
" " : timing	Velocity	2.8377	0.096	1,79
	Light	**8.2579**	**0.005**	**1,79**
" " : width	Velocity	0.6141	0.52	1,79
	Light	0.4379	0.44	1,79
Rhopalodiaceae: mean density	**Velocity**	**4.7250**	**0.03**	**1,79**
	Light	1.9970	0.16	1,79
" " : maximum density	**Velocity**	**6.8087**	**0.02**	**1,15**
	Light	1.4727	0.25	1,15
" " : mean biovolume	**Velocity**	**16.8403**	**0.00012**	1,63
	Light	0.1753	0.67	1,63
" " : maximum biovolume	**Velocity**	**5.4912**	**0.037**	1,15
	Light	1.8109	0.20	1,15
" " : relative biovolume	Velocity	2.7644	0.12	1,15
	Light	3.8929	0.07	1,15
Cocconeis spp: mean density	**Velocity**	**7.2370**	**0.01**	**1,79**
	Light	1.8770	0.17	1,79
" " : maximum density	**Velocity**	**9.4345**	**0.01**	**1,15**
	Light	**4.5766**	**0.05**	**1,15**
" " : mean biovolume	**Velocity**	**14.5617**	**0.0003**	1,63
	Light	0.5633	0.46	1,63
" " : maximum biovolume	**Velocity**	19.7659	**0.0008**	1,15
	Light	0.0109	0.92	1,15
" " : relative biovolume	Velocity	0.1731	0.68	1,15
	Light	1.2127	0.29	1,15
" " : timing of max density	**Velocity**	**4.8000**	**0.05**	**1,15**
	Light	1.2000	0.29	1,15
" : timing of max rel. biovolume	Velocity	1.2	0.29	1,15
	Light	4.8	**0.049**	1,15
Total Epiphytes: mean	Velocity	0.9131	0.34	1,79
	Light	1.0327	0.31	1,79
" " : maximum	**Velocity**	**4.6970**	**0.05**	**1,15**
	Light	1.8904	0.19	1,15
" " : mean biovolume	**Velocity**	16.8403	**0.0001**	1,63
	Light	0.1754	0.68	1,63
" " : maximum biovolume	**Velocity**	14.2239	**0.003**	1,15
	Light	1.1124	0.31	1,15
" " : biovolume per filament	Velocity	0.4256	0.52	1,79
	Light	5.17	**0.025**	1,79

Table 7. Results from two-way ANOVA analysis assessing variation in *Cladophora* growth and the relative abundances and biovolumes of total epiphytes and two major epiphyte taxa across light and velocity treatments. Significant results are highlighted in boldface.

Core	L1C5	L1C8	Core L1C9	L10C3
Depth (m)	138	137	137	175
Channel/Site (Fig. 4)	Larry/L1	Larry/L1	Larry/L1	Shemp/L10
Environment	Wall	Wall	Thalweg	Thalweg
Length (cm)	65	74	88	62.3
Age Range	~1936-2001	~1927-2001	~1913-2001	~1918-2001
Preservation	75%	65%	95%	90%
Accumulation Rate (mm/yr)	7-14	7-14	7-14	11(0-45 cm) 4(45-63 cm)
Samples (cm)	2 (0-1, 9-10)	2 (2-3, 5-6)	2 (2-3, 8-9)	84 (annual)

Table 1. Summary of metadata for the four cores used in this study. Preservation refers to the preservation of physical strata compared with other STRATAFORM cores, and runs from 0 to 100%. *Note on Core L10C3 and Bimodal Sediment Accumulation:* Core L10C3 is somewhat unique in that it displays a bimodal sediment accumulation rate: 11 mm/yr in the upper section from 0 - 451mm depth (approximately 1960-2001 post big floods) and 4 mm/yr in the lower section from 451 – 623 mm depth (approximately 1918 – 1960). This difference has been attributed to changes in sediment supply or dispersal pathways (Drexler et al. 2006). Interestingly, the two largest flood events in recorded history along the Eel River neatly bracket this date: the first mega-flood occurred in 1955, while the second occurred in 1964. At about this time the sediment load per unit discharge increased dramatically on downstream reaches of the mainstem Eel River (Lisle 1981). This was attributed to devegetation of large sections of riverbank and activation of landslides, both increasing sediment supply of unbound sediment during subsequent flood events (Lisle 1981). Accumulated frustules track peak discharge patterns above and below the transition, supporting the unbound sediment hypothesis and the observation in Drexler et al. (2006) that the change in sediment accumulation rates was due to changes in watershed sediment supply and not to changes in subaqueous sediment delivery mechanisms to the offshore canyons.

Depth (cm)	Year	Core	Discharge Yr X, X+1 (m^3/s)	Spate (Date, m^3/s)	Bloom (cm)	Rhopalodiaceae (valves/yr)	Other FW (valves/yr)
0-1	**2000-1**	**L1C5**	**Drought, Drought 83, 53**	**11Mar 12.4**	**298**	**125,381**	**977,635**
2-3	**1998-9**	**L1C9**	**Flood, Flood 176, 136**	**25Mar 25.3**	**265**	**186,335**	**1,707,886**
5-6	**1995-6**	**L1C8**	**Flood, Flood 321, 129**	**23Mar 65.8**	**177**	**87,600**	**1,115,437**
8-9	**1991-2**	**L1C9**	**Drought, Drought 89, 45**	**23 Apr 6.3**	**25**	**34,028**	**1,529,312**
9-10	**1990-1**	**L1C5**	**Drought, Drought 102, 90**	**22May 24.3**	**34**	**64,716**	**351,716**

Table 2. Results from exploratory surveys of cores L1C5, L1C8 and L1C9 from the Larry entrance to the Eel canyon. Rhopalodiaceae and other freshwater frustule counts generally match discharge and bloom records, and where they disagree, the frustule counts follows the actual bloom magnitude, not the predicted bloom magnitude. Year-depth correspondence was estimated using ^{210}Pb constraint of 7-14 mm/yr (Drexler et al. 2006). A spate is defined (following Power et al. 2008) as a pulse of discharge that is elevated but less than bankfull.

Depth (mm)	Year	Discharge Yr X, X+1 (m^3/s)	Bloom (cm)	L10C3 Epithemia (frustules/ sample)	L10C3 FW Diat (frustules/ sample)
0-11	**2000-1**	**Drought, Drought 83, 53**	**Big 298**	**44**	**109**
11-22	**1999-00**	**Flood, Drought 136, 83**	**Big 108**	**38**	**95**
22-33	**1998-9**	**Flood, Flood 176, 136**	**Big 265**	**40**	**93**
33-44	**1997-8**	**Flood, Flood 418, 176**	**Big 127**	**30**	**70**
44-55	**1996-7**	**Flood, Flood 129, 418**	**Small 17.3**	**11**	**56**
55-66	**1995-6**	**Flood, Flood 321, 129**	**Big 177**	**34**	**94**
66-77	**1994-5**	**Drought, Flood 43, 321**	**Small 3.5**	**3**	**21**
77-88	**1993-4**	**Flood, Drought 240, 43**	**Big 50**	**19**	**33**
88-99	**1992-3**	**Drought, Flood 45, 240**	**Small 47**	**48**	**99**
99-110	**1991-2**	**Drought, Drought 90, 45**	**Small 25**	**28**	**136**
110-121	**1990-1**	**Drought, Drought 102, 90**	**Small 34**	**14**	**81**
121-132	**1989-90**	**Flood, Drought 157, 102**	**Big 57**	**14**	**36**
132-143	**1988-9**	**Flood, Flood 147, 157**	**Small 24**	**10**	**44**

Table 3. Results from period of overlap of core L10C3 with algae survey record

Discharge \ Bloom	Frustules > 21	Frustules < 21
Flood	**15**	**1**
Drought	**11**	**9**

Table 4. Fisher's Exact Test for Peak Modal Bloom Height (*Cladophora glomerata* using the core L10C3 Rhopalodiaceae frustule proxy of 21 frustules per sample for "Big" blooms) and Bankfull Discharge (using a USGS Leggett gauge threshold of 565 m^3/s for "Flood years, (USGS Station 11475800, 1965-Present)). P = 0.011.

Discharge ~~Bloom~~	Frustules > 21	Frustules < 21
Flood	**35**	**2**
Drought	**37**	**10**

Table 5. Fisher's Exact Test for Peak Modal Bloom Height (*Cladophora glomerata* using the core L10C3 Rhopalodiaceae frustule proxy of 21 frustules per sample for "Big" blooms) and Bankfull Discharge (using a USGS Scotia gauge threshold of 3540 m^3/s for "Flood years, (USGS Station 11477000, 1911-Present)). P = 0.036.

t-tests: Two Sample, Unequal Variance, for difference of means in monthly discharge	Flood-Flood Mean	Flood-Drought Mean	P(T<=t) two-tailed	df
Flood-Flood/Flood-Drought	55.7	47.5	0.5008	25

Table 6. Results from a t-test for difference in mean frustule counts in consecutive flood years and flood years followed by drought years. The insignificant difference in mean frustule counts provides further support for the hypothesis that year-to-year storage of frustules in the river basin (e.g. in deep pools) prior to deposition in the offshore canyon sediments is insignificant.

PDO/ENSO State	Warm/Warm	Warm/Cold	Cold/Warm	Cold/Cold	Warm/Warm or Cold/Cold	Warm/Cold or Cold/Warm
Mean Rhopalodiaceae frustules	59.77	32.33	48.78	57.20	59.03	43.83

t-tests: Two Sample, Unequal Variance, for difference of means in annual frustule counts	Warm/Warm or Cold/Cold Mean	Warm/Cold or Cold/Warm Mean	P(T<=t) one-tailed	df
In Phase/Out-of-phase	59.03	43.83	0.0459	41

Table 7. Mean Rhopalodiaceae frustules in years with different combinations of PDO and ENSO index polarity (sign) and results from a t-test for difference in mean frustule counts in years with in-phase and out-of-phase PDO and ENSO indices. A one-tailed test is justified here as the mean peak discharge in in-phase years is known to be larger than in out-of-phase years (Andrews and Antweiler 2012) leading to a predicted increase in crushing and export of armored grazers, larger *Cladophora* bloom sizes and higher frustule counts in these years.

FIGURES

Background Chapter

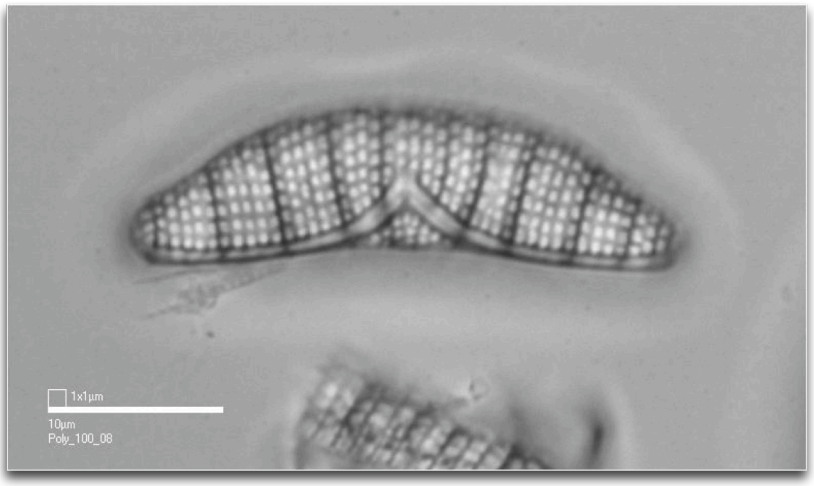

Figure 1. The genus *Epithemia* is in many ways highly suitable as a productivity marker or proxy because it is exclusively freshwater, it closely tracks its host *Cladophora*'s bloom size, it has a robust frustule that resists breaking and dissolution, and it is very recognizable (the "mustache" raphe seen above is diagnostic). Further, *Cladophora* is a dominant macroalga in temperate streams worldwide (Whitton 1970, Dodds 1991a, Guiry and Guiry 2012), and *Epithemia* appears to be a dominant late-successional epiphyte on *Cladophora* in nitrogen-limited freshwaters (Floener and Bothe 1980, Peterson and Grimm 1992, Power et al. 2009). Photo credit Rex Lowe.

Figure 2a. The canyon-bound, bedrock-based Eel has very few depositional environments. Bedrock and boulder substrate in the headwaters grades to cobbles, pebbles and gravel in the delta. Even at Fernbridge, a few kilometers from the mouth, the riverbed is gravel, and deposition is limited to a narrow estuarine zone before crossing the bar into the Pacific. Photo courtesy of NASA.

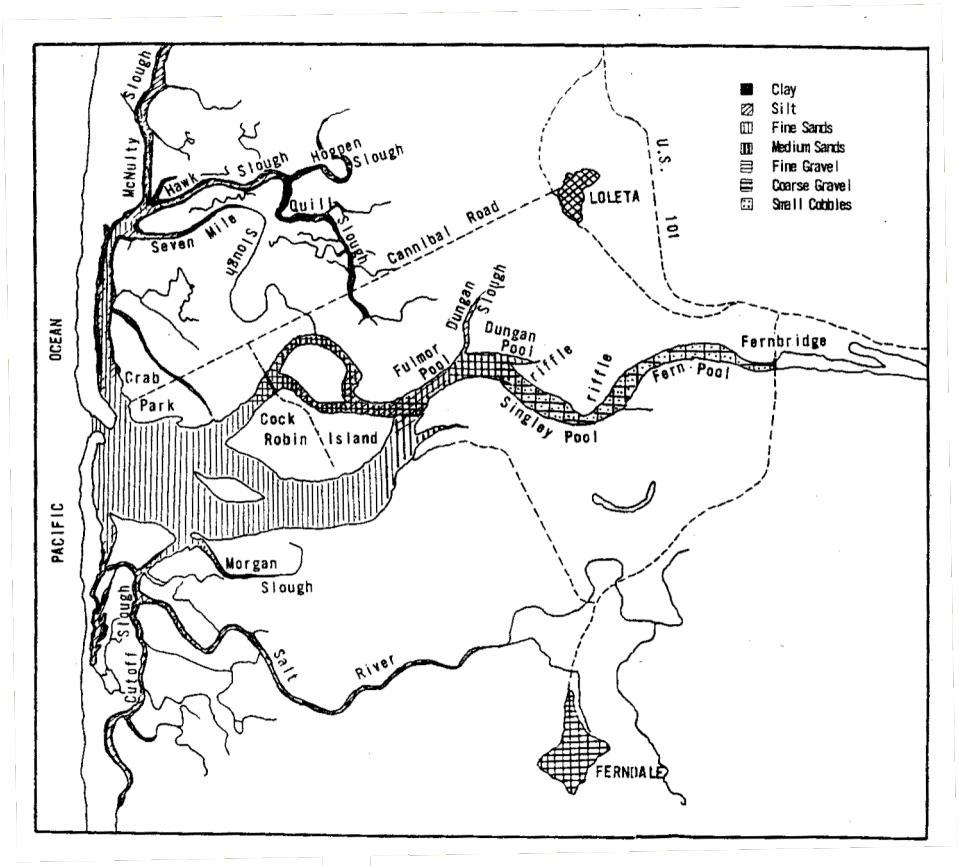

Figure 2b. The delta and estuary of the Eel River near Fernbridge, California. Bedrock and boulder substrate in the headwaters grades to cobbles, pebbles and gravel in the delta. Cobbles are present down to Singley Pool, represented by stipples. Even at Cock Robin Island, a few kilometers from the mouth, the riverbed is gravel, as shown by horizontal striping. Silt and clay-sized particle deposition is limited to the channels and sloughs north of Cock Robin Island and Crab Park. Map from Boles et al. (1977).

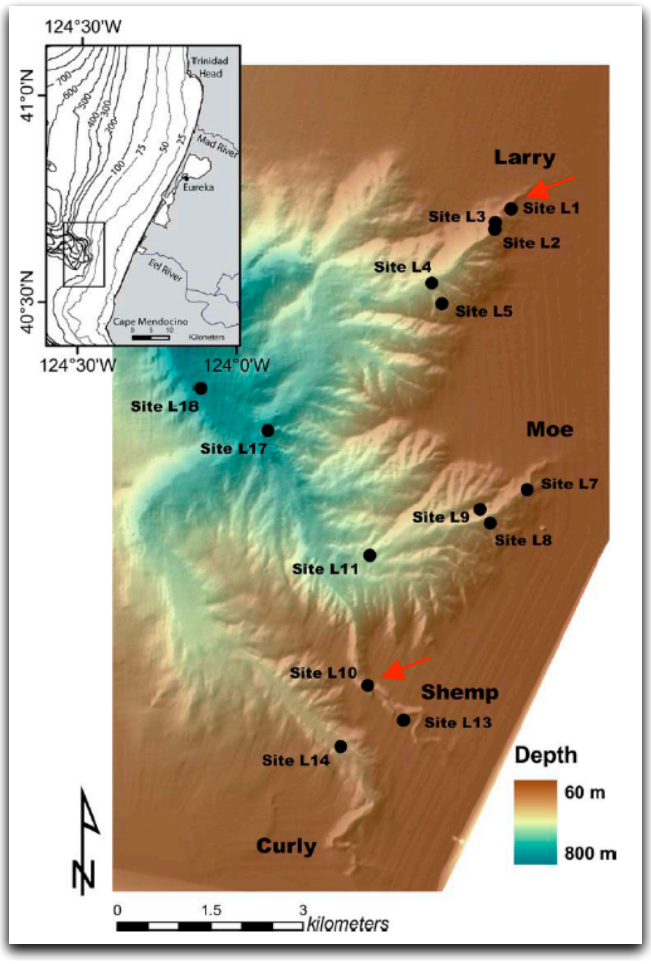

Figure 3. A topographic view of the submarine Eel Canyon. Sites used in this study are marked with red arrows, including L1, at the head of the Larry canyon entrance, and L10, halfway down the Shemp canyon entrance. Inset shows the location of the canyon about 15 km offshore of the Eel River mouth (Figure modified from Drexler *et al.* 2006, © Society for Sedimentary Geology).

.

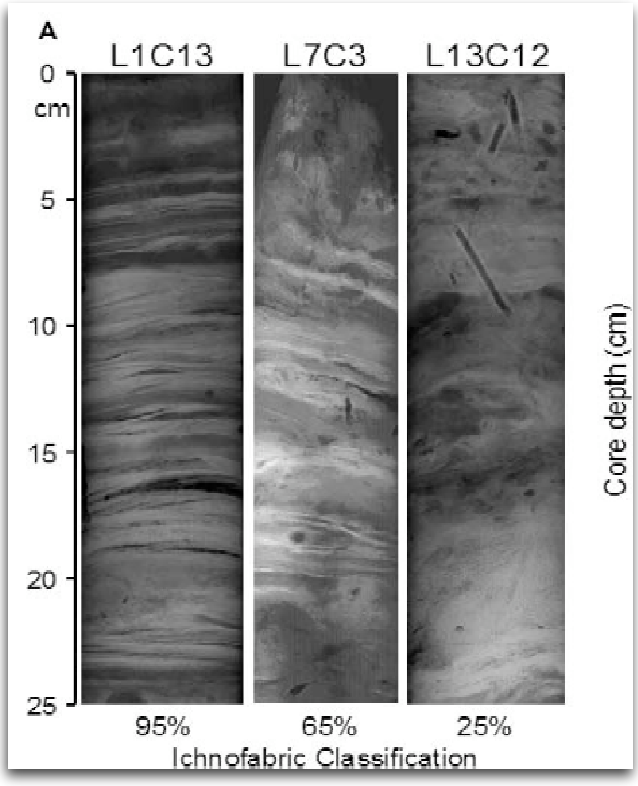

Figure 4. Representative cores showing differential sedimentary layer preservation: an "Ichnofabric classification" value is assigned to each core to indicate its level of preservation: thalweg cores range from 80-95%, and wall cores from 40-85%. On the left core L1C13 shows a high degree of bed preservation, while on the right core L13C12 shows extensive burrows and bioturbation. Isotopic analyses constrain accumulation rates, more precisely for wall cores. So there is a tradeoff between dating accuracy and preservation for all but a few cores (Figure from Drexler *et al.* 2006, © Society for Sedimentary Geology).

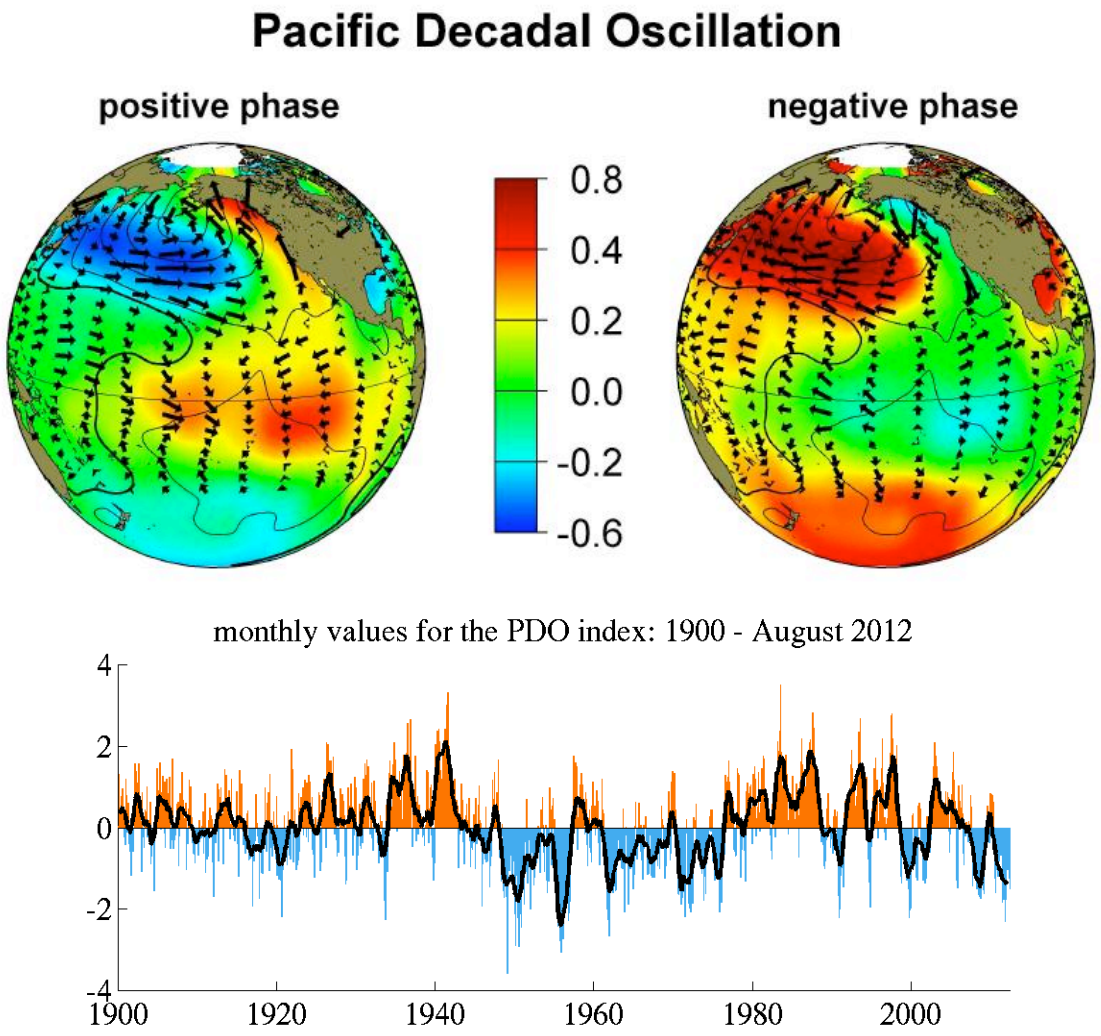

Figure 5. The Pacific Decadal Oscillation (PDO) spatial and temporal patterns. A regime shift in 1977 from colder conditions marked in blue to warmer conditions marked in red is now matched with the 2008 shift back to the colder state. PDO is an extratropical "ENSO-like" phenomenon shifting moisture and heat between Alaska and the Pacific Northwest. The warm phase weakens the California Current, warms SSTs, and reduces fog in Northern California. The cold phase exhibits opposite effects. The PDO has large effects on plankton-based food webs, and may be significant for algae-based river webs as well. At the Angelo, the PDO combines with ENSO and the Arctic Oscillation to "set the table" for discharge regimes, with additional effects on fog, temperature and sediment transport (Graphics from Mantua 2007, used with permission).

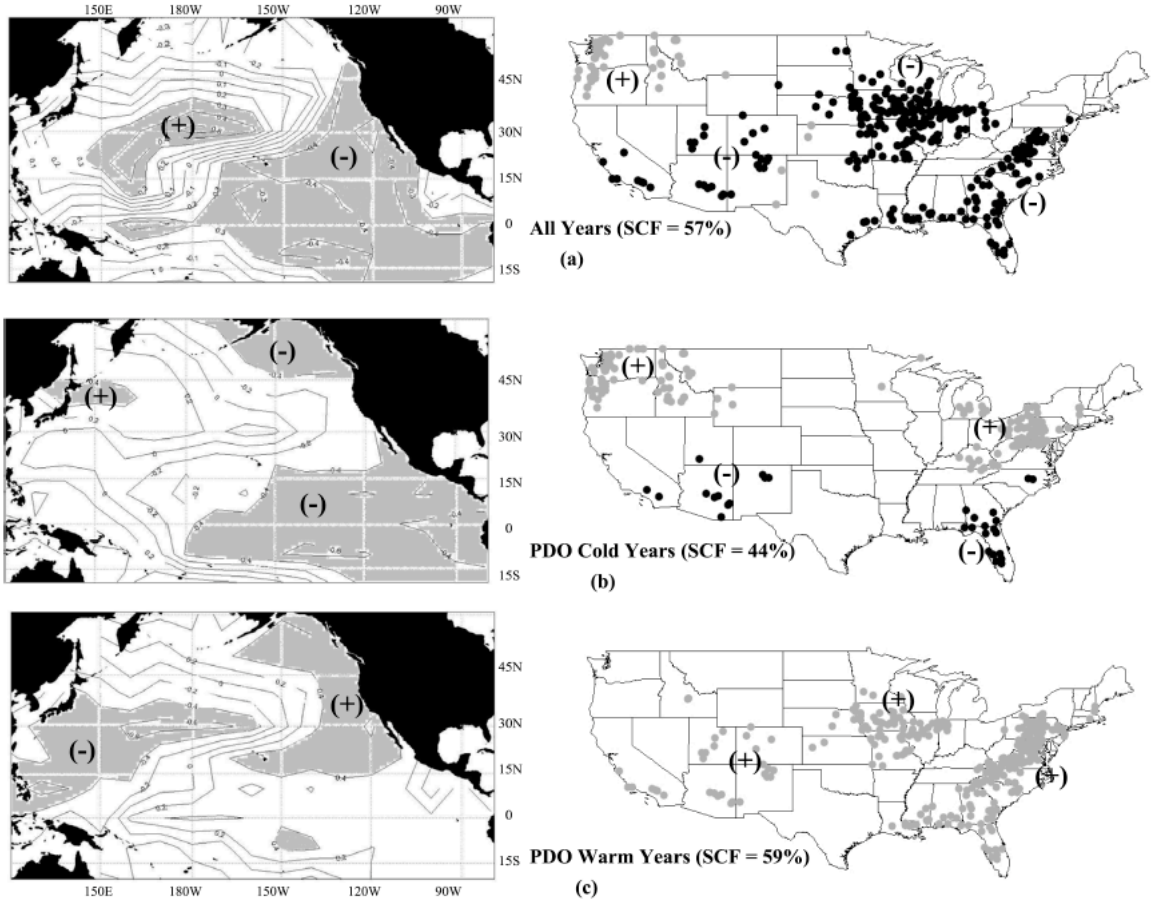

Figure 6. Heterogeneous correlation figures for SVD (first mode) for previous year spring-summer season Pacific Ocean SSTs and current water year U.S. streamflow for (a) all years, (b) PDO cold years, and (c) PDO warm years. Significant (>95%) SST regions were approximated by gray shading. Significant (>95%) negative (positive) streamflow stations were represented by black (gray) circles. Note the opposing responses to the north and south of approximately 40°N. (Figure from Tootle and Piechota 2006, used with permission).

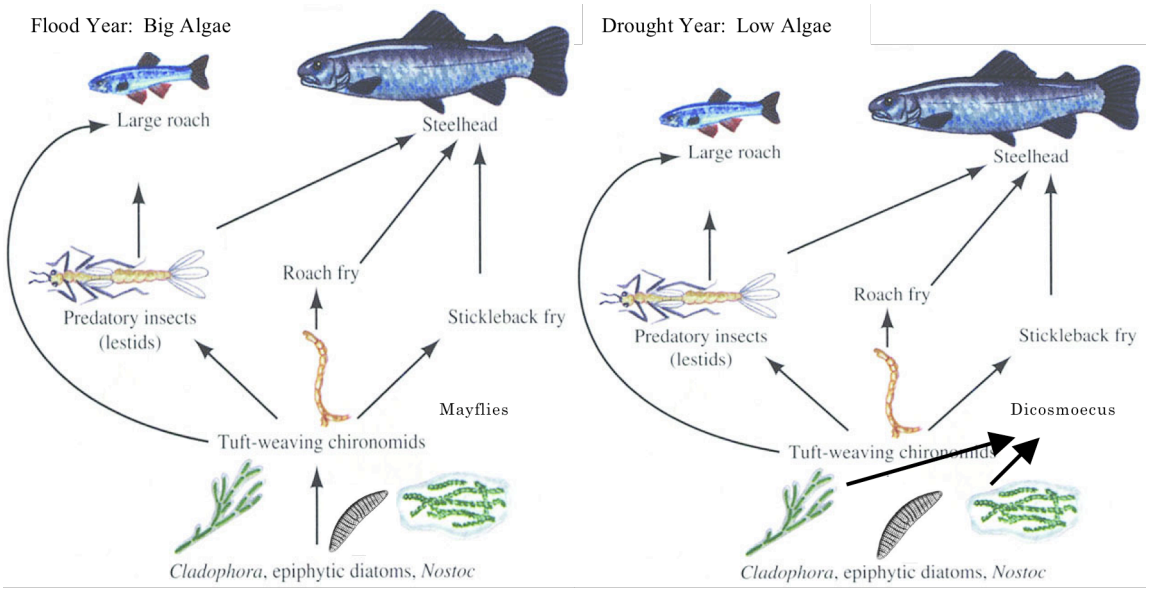

Figure 7. A 22-year record of surveys has identified a bimodal food web regime driven by peak winter flows interacting with food web controls on algae. An armored grazer, *Dicosmoecus gilvipes,* can suppress algal growth in drought years, but is crushed or exported by high winter floods. The resulting shifts in peak filament lengths for the dominant macroalga *Cladophora glomerata* are reflected in shifts of its dominant epiphytes, including the diatom genus *Epithemia*. Big algae years should produce more *Epithemia frustules* that are exported by subsequent winter flows, and may be discernable in downstream sedimentary deposits.

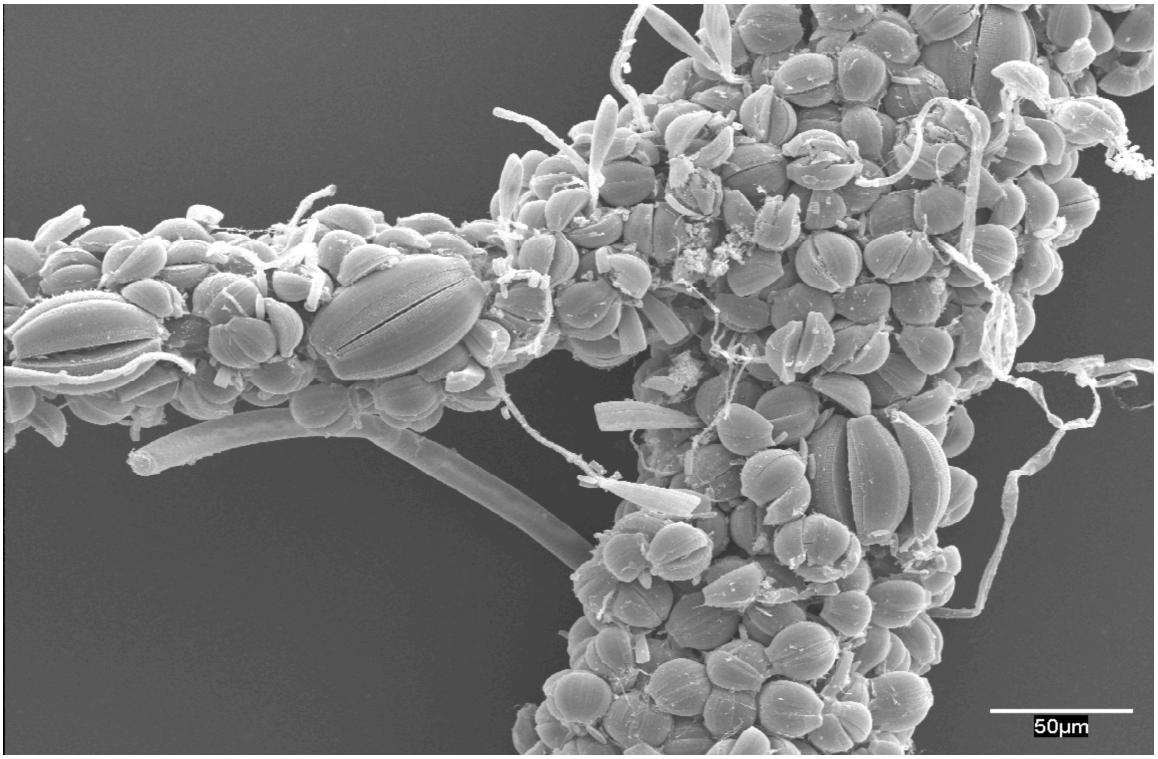

Figure 8. Scanning electron micrograph of heavily epiphytized strand of *Cladophora glomerata.* Almost all of the attached epiphytes are *Epithemia* spp. Photo credit Rex Lowe.

Figure 1. Stream Channel Experiment. View looking downstream, showing 20 channels in the South Fork Eel River. Each channel is 3 m long x 15 cm wide x 15 cm deep. The velocity gates are visible at the head of each channel, with those in the raised position on the Faster treatment channels and those in the lowered position for the Slow treatment channels. Shade cloth covers the Dark treatment channels. Cobbles and tiles are visible in the Light/unshaded channels. Five channels were randomly assigned to each treatment (channels are numbered from the left): *Slow, Dark*–channels 1, 8, 12, 13 and 20; *Faster, Dark*–channels 2, 5, 10, 15 and 18; *Slow, Light*–channels 4, 7, 9, 16 and 17; *Faster, Light*–channels 3, 6, 11, 14 and 19.

Figure 2. Cobble bearing *Cladophora* filaments in one of the artificial stream channels. River gravel was placed beneath the cobble to mimic the natural stream bed. A meter tape was placed on top of the lower channel wall for scale.

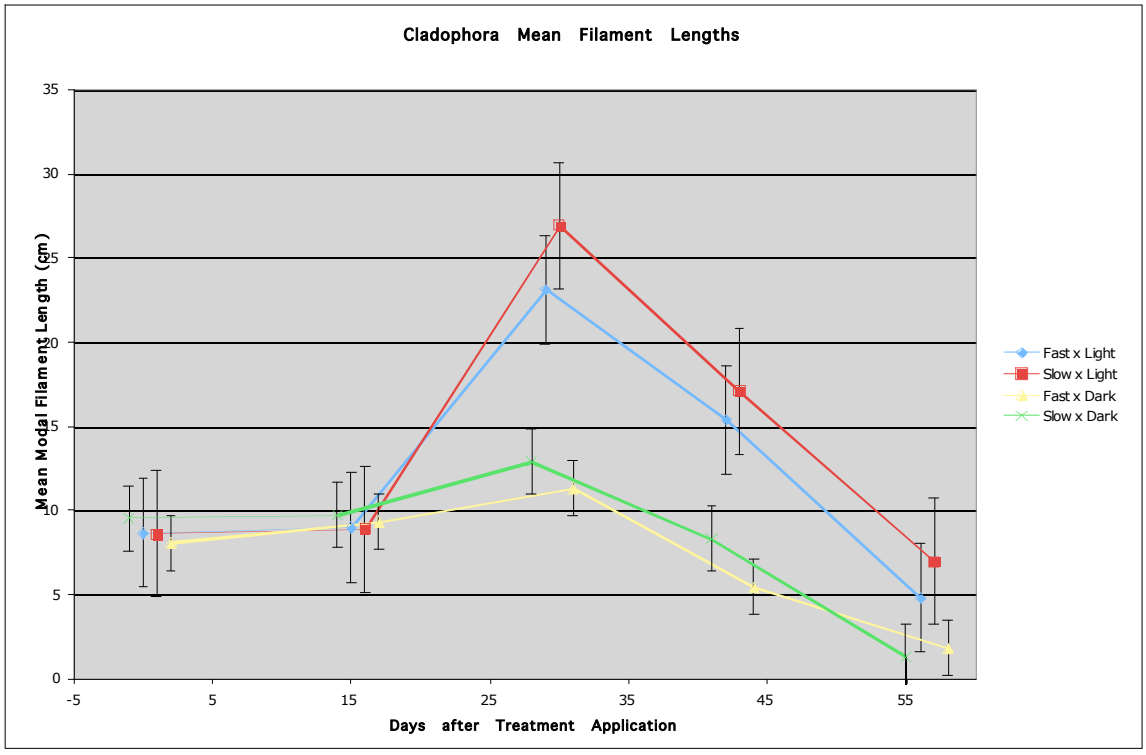

Figure 3a. *Cladophora glomerata* mean filament lengths over time. Values are mean modal filament lengths averaged over four observations in each channel per time interval, then averaged over all five channels in each treatment, and are shown ± one SE. Treatments were first applied on June 9, 2008.

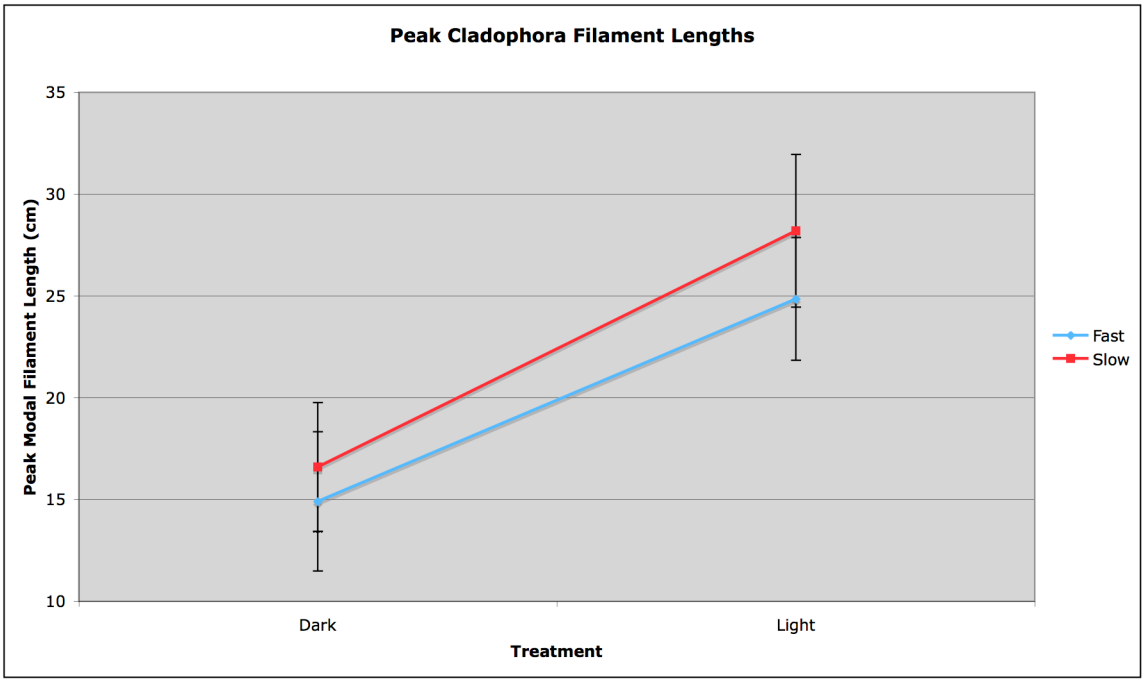

Figure 3b. Peak filament lengths for *Cladophora glomerata* attached to the 80 cobbles used across all stream channels in this experiment. Peak lengths were significantly longer in the light treatments (mean modal length = 26.53 cm) than the dark treatments (mean modal length = 15.75, F = 10.37, P = 0.002, df = 1, 79). Water velocity had no significant effect on peak length (p = 0.45). Bars are one standard error.

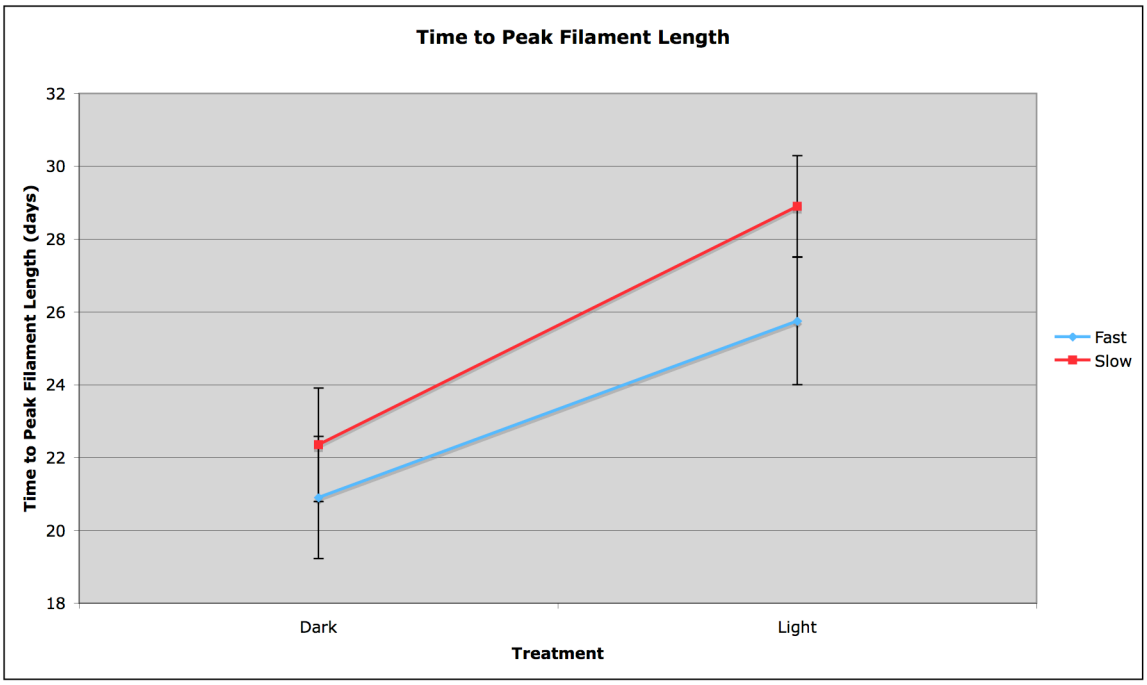

Figure 3c. Days after the application of all treatments to maximum streamer length for all 80 cobbles. Earlier peaks of 3-5 days tended to occur for Dark (F = 8.26, P = 0.005, df = 1,79) treatments and to a lesser extent for Faster velocity (F = 2.84, P = 0.09, df = 1,79) treatments. Bars are ± one SE.

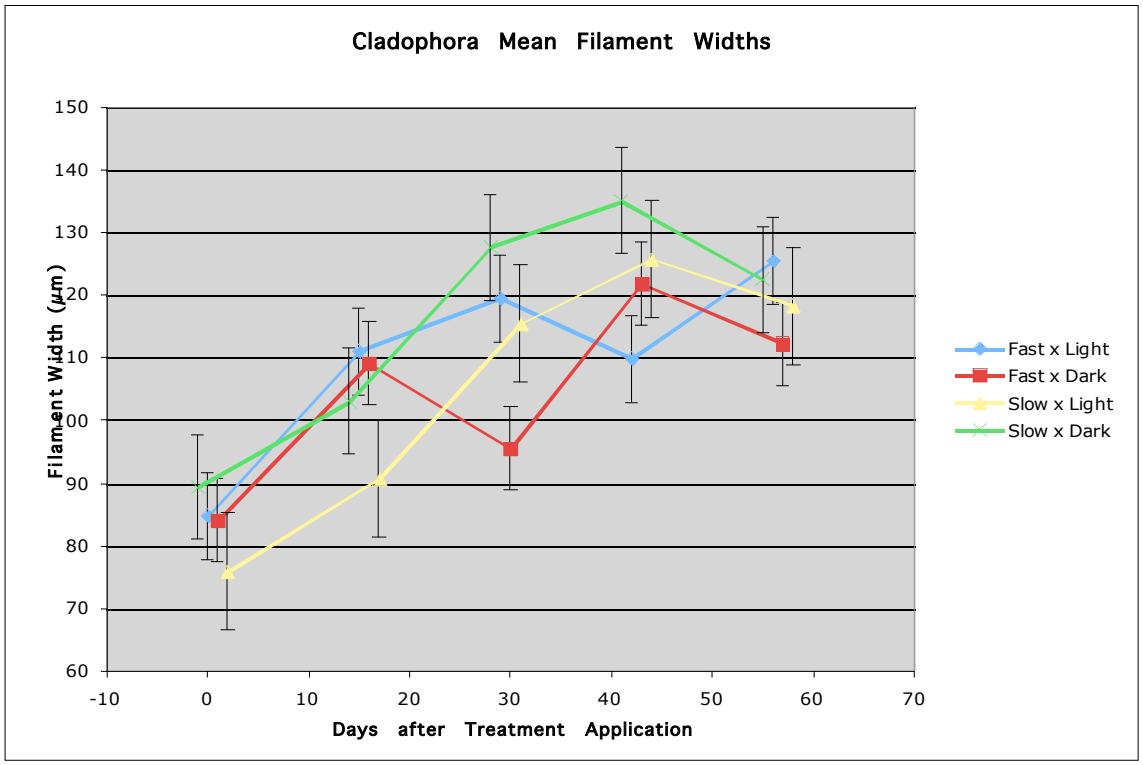

Figure 4a. *Cladophora glomerata* mean filament widths over the period of the experiment. Labels refer to the four light x velocity treatments. Values are mean filament widths averaged by channel and averaged by treatment for all 20 sampled cobbles with ±1 SE.

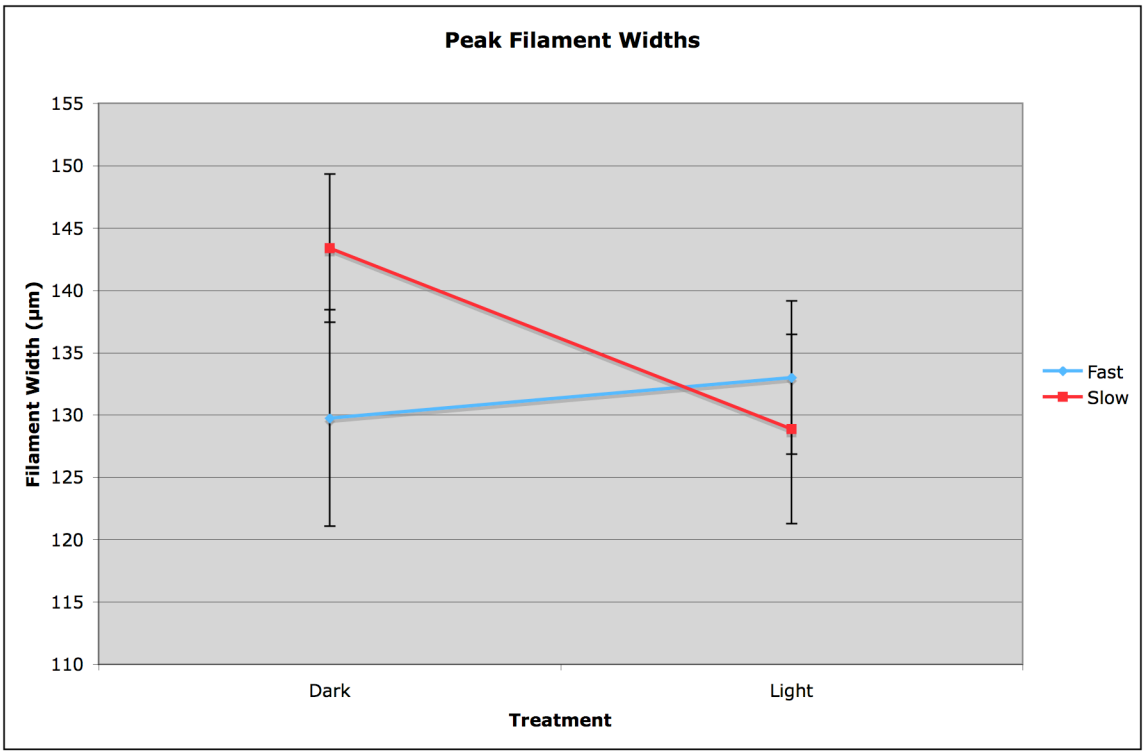

Figure 4b. Peak filament widths for *Cladophora glomerata* attached to the 16 sampled cobbles in each treatment. Widths did not vary among treatments (P = 0.45, P = 0.52)., although Slow x Dark treatment differences were marginally wider (P = 0.06). Bars are ± one SE.

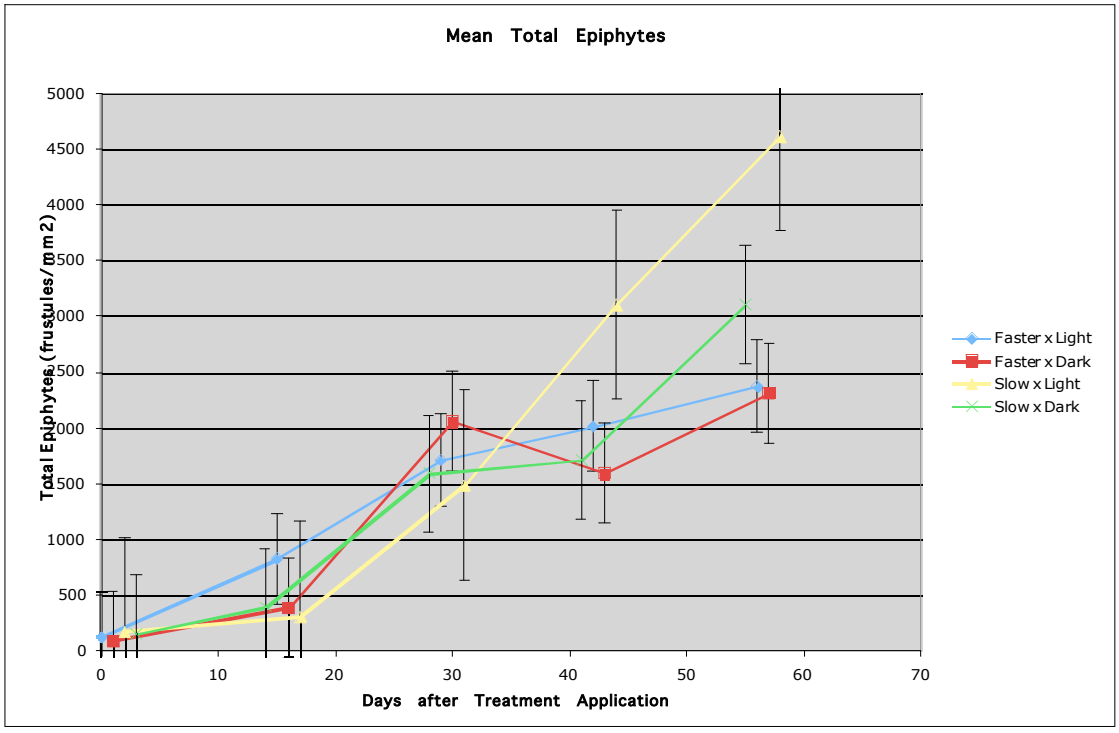

Figure 5a. Total Epiphytes (per square mm of host surface area) counted on 12 of 16 randomly selected cobbles from each treatment at time periods T_1 through T_4, values averaged over each channel and then averaged by treatment, means ± 1 SE. There was no significant association between mean total epiphytes and treatments (P = 0.20). Slow x Light treatment differences were marginally higher (P = 0.12).

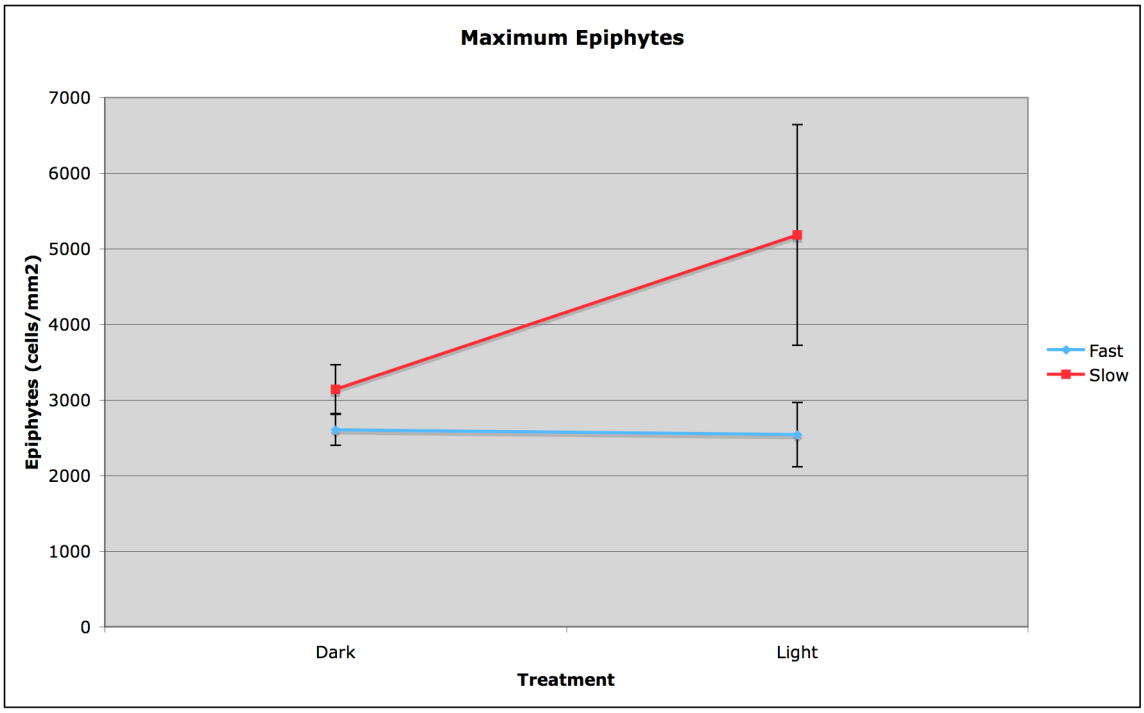

Figure 5b. Maximum total epiphyte loads (per mm^2 host) for replicates of the various treatments, means ± 1 SE. Maximum total epiphytes loads were significantly higher in Slow treatments (mean = 4163 frustules) than in Fast treatments (mean = 2572 frustules) ($F = 4.79$, $P = 0.05$, $df = 1,15$).

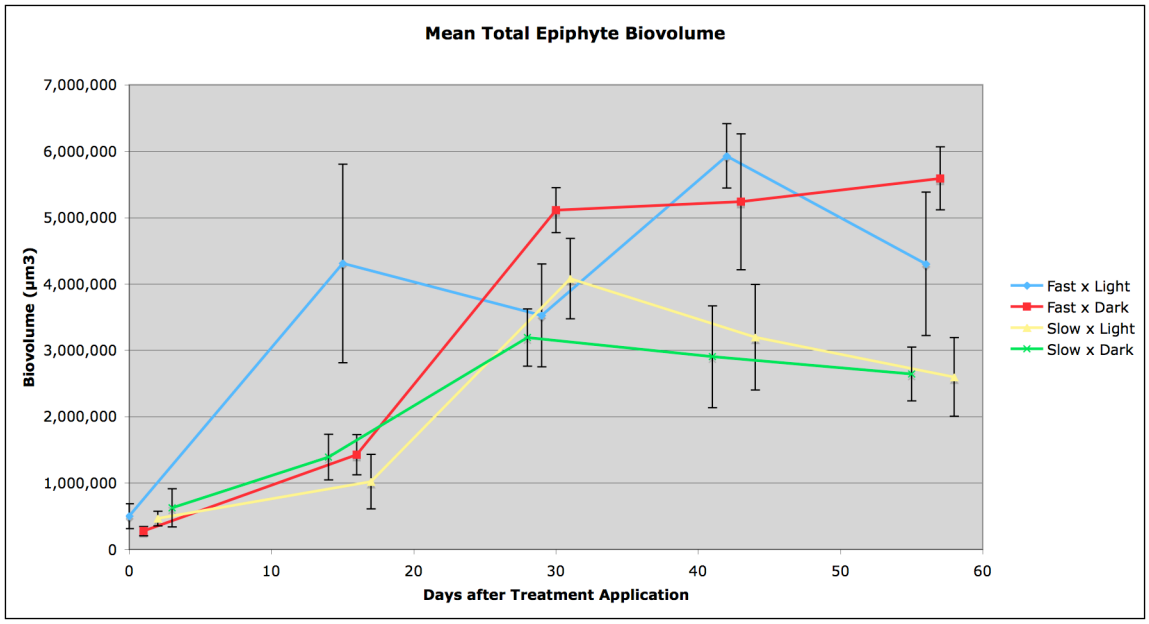

Figure 5c. Total Epiphyte Biovolume (in cubic microns) from each treatment at time periods T_1 through T_4, values averaged over each channel and then averaged by treatment, means ± 1 SE. Mean total epiphytes biovolume was significantly higher in Fast treatments (mean = 4,429,419 μm^3) than in Slow treatments (mean = 2,628,092 μm^3) ($F = 16.84$, $P = 0.0001$, $df = 1,63$).

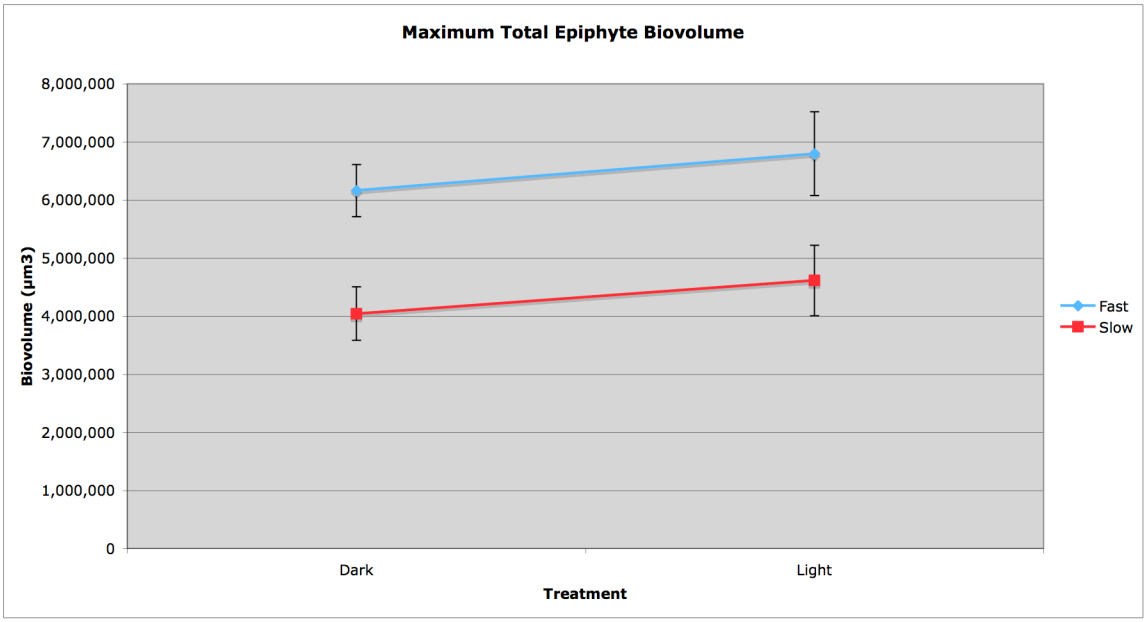

Figure 5d. Maximum total epiphyte biovolume (μm^3 per mm^2 host) for replicates of the various treatments, means ± 1 SE. Maximum total epiphyte biovolumes were significantly higher in Fast treatments (mean = 4,263,666) than in Slow treatments (mean = 2,554,685) ($F = 17.17$, $P = 0.001$, $df = 1,15$).

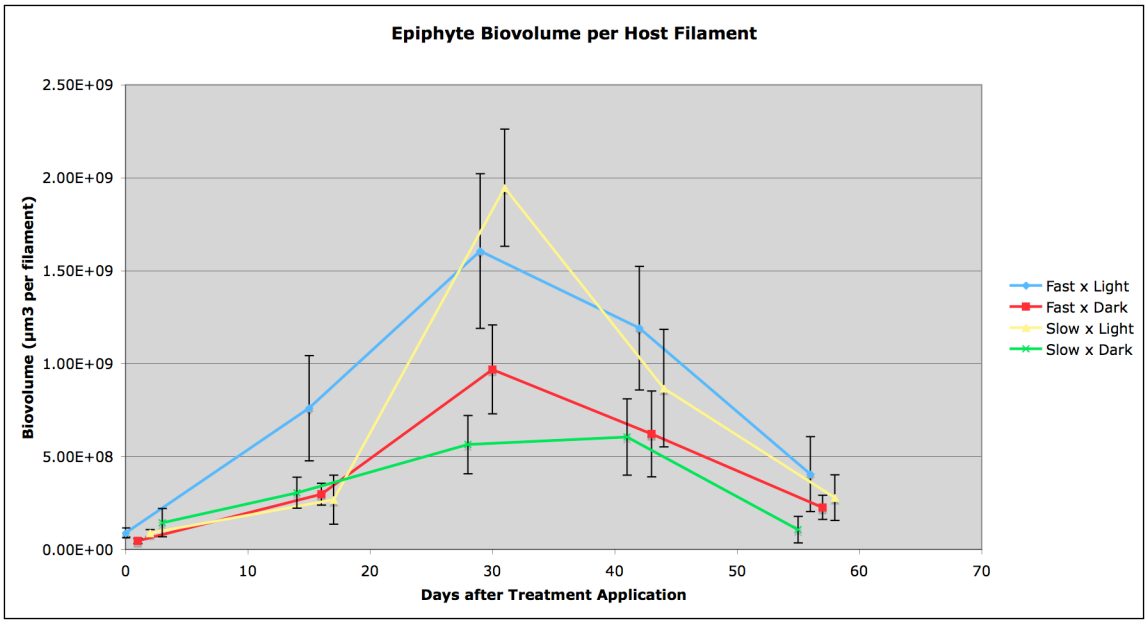

Figure 5e. Total epiphyte biovolume per host filament (in cubic microns) from each treatment at time periods T_1 through T_4, values averaged over each channel and then averaged by treatment, means ± 1 SE. Mean total epiphyte biovolume per filament was significantly higher in Light treatments (mean = 7.50×10^8 μm^3) than in Dark treatments (mean = 3.88×10^8 μm^3) ($F = 5.17$, $P = 0.025$, $df = 1,79$).

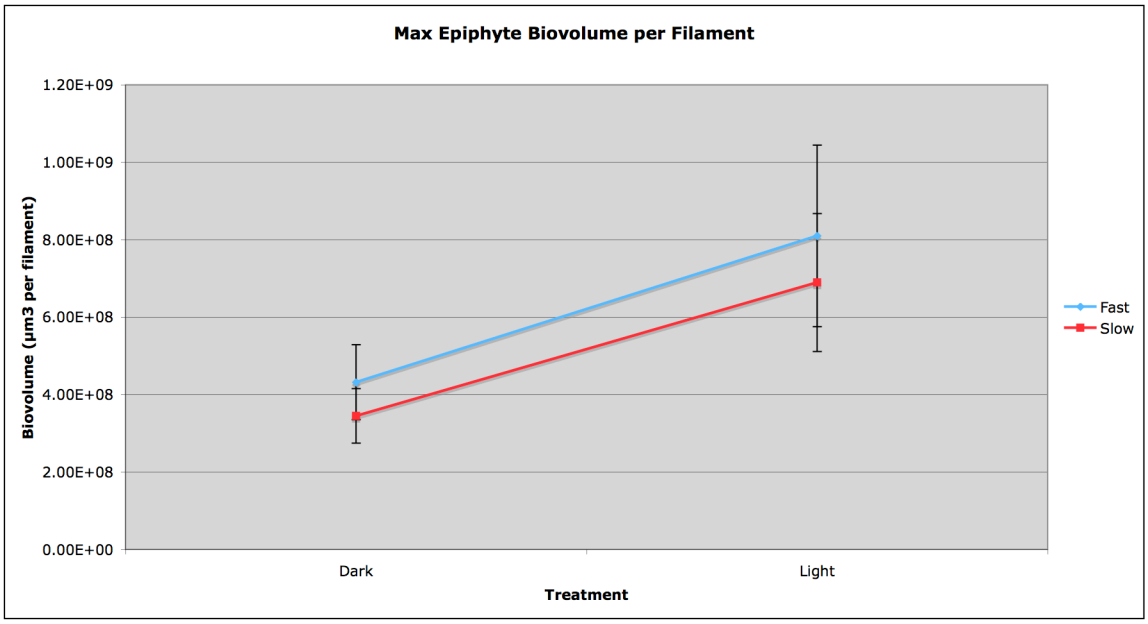

Figure 5f. Maximum total epiphyte biovolume per host filament (μm^3) for replicates of the various treatments, means ± 1 SE. Maximum total epiphyte biovolume per host filament were significantly higher in Light treatments (mean = 7.50 x 10^8 μm^3) than in Dark treatments (mean = 3.88 x 10^8 μm^3) ($F = 5.17$, $P = 0.025$, $df = 1,79$).

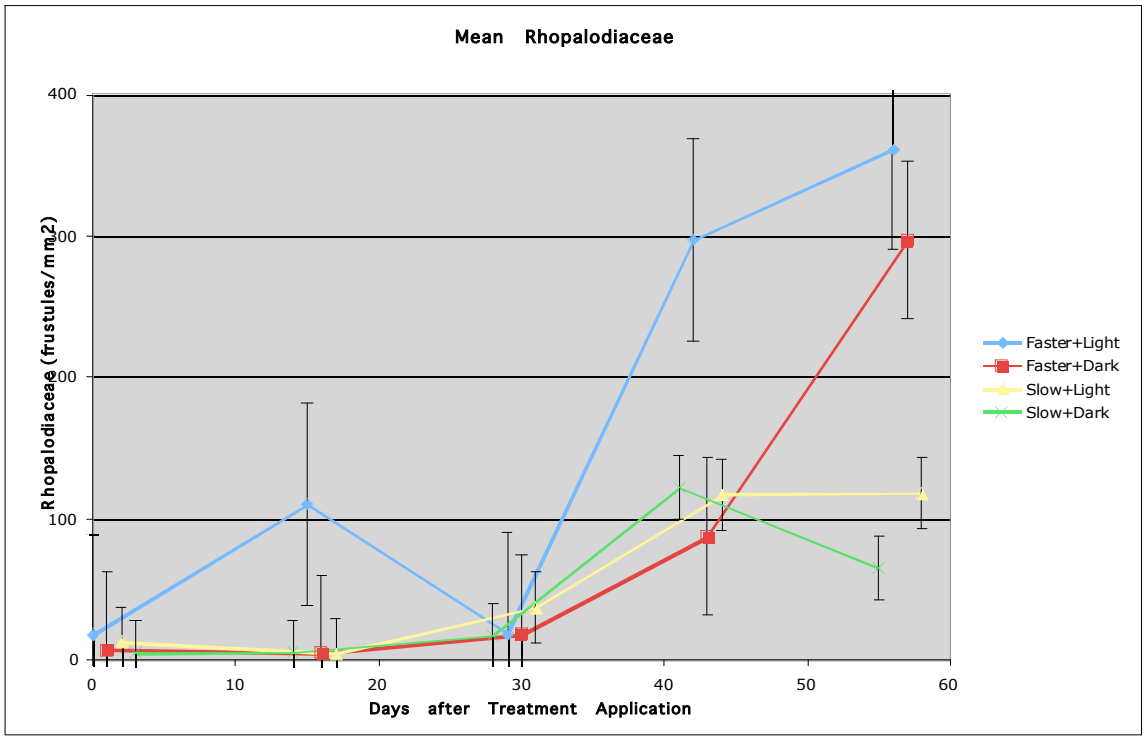

Figure 6a. Mean Rhopalodiaceae epiphytes counted on randomly selected cobbles from each treatment at time periods T_1 through T_4, values averaged over each channel and then averaged by treatment, means ± 1 SE. Mean abundances were significantly higher by T_4 in Fast treatments (mean frustules = 122±31) vs. Slow (mean frustules = 50±11), ($F = 4.71$, $P = 0.03$, $df = 1,79$).

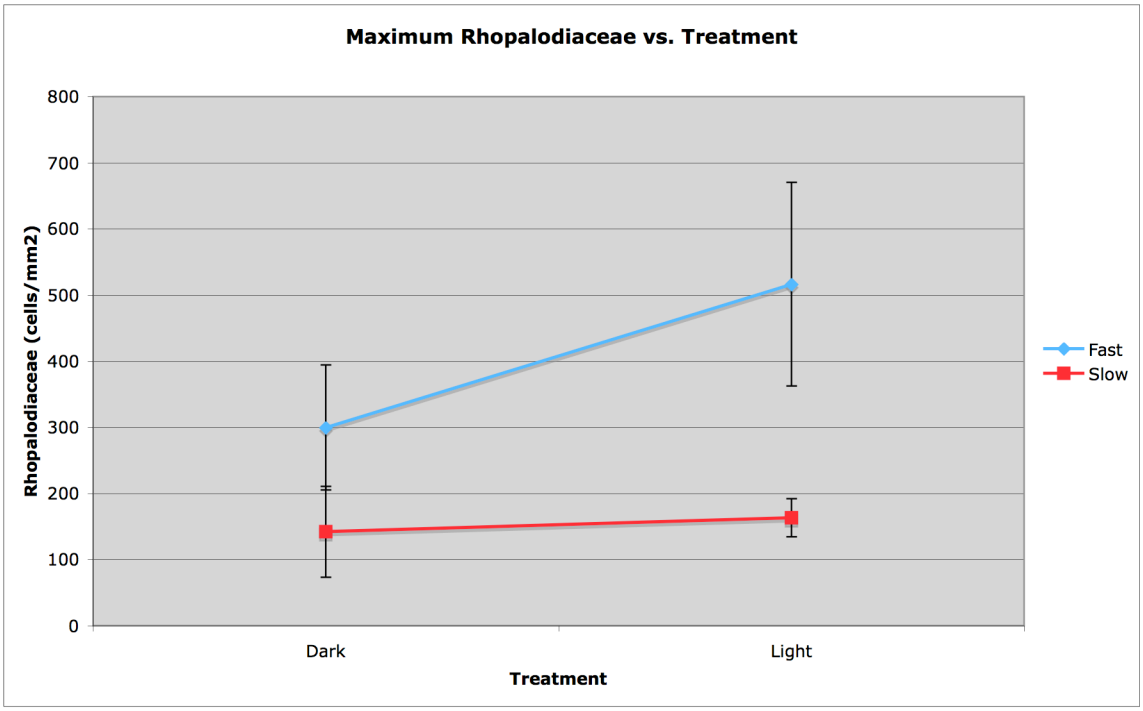

Figure 6b. Maximum Rhopalodiaceae frustules attained in each treatment class. Maximum abundances were higher in Fast treatments (408±93 frustules) vs. Slow treatments (153±35 frustules) ($F = 6.82$, $P = 0.02$, $df = 1,15$). Maxima were reached at T_3 in all Slow treatments, while all Fast treatments peaked at T_4.

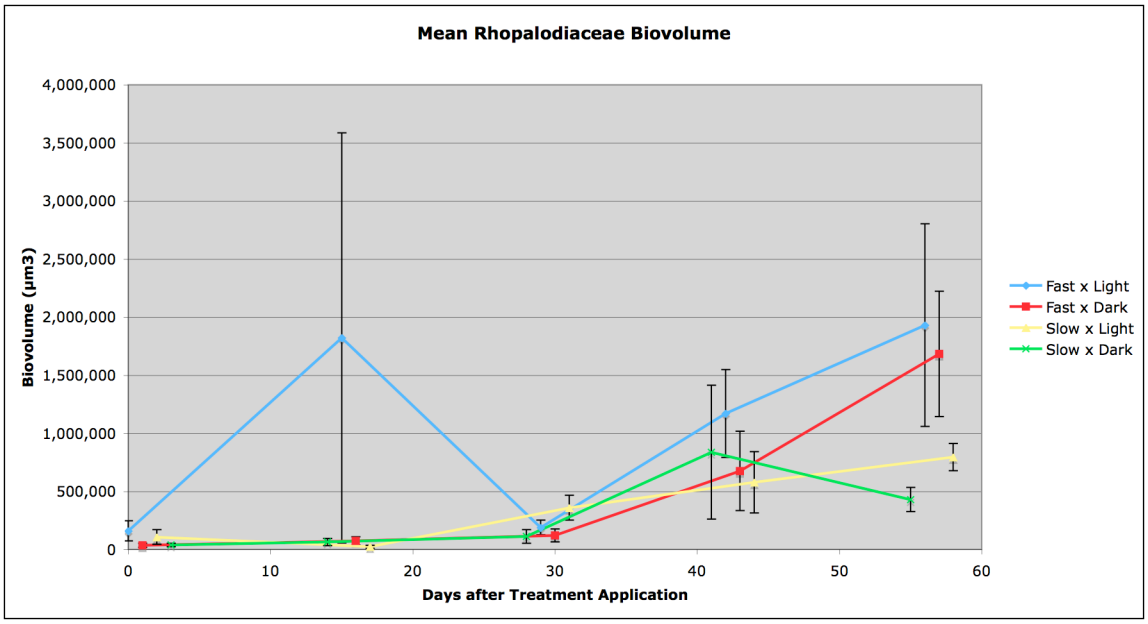

Figure 6c. Total Rhopalodiaceae Biovolume (in cubic microns) from each treatment at time periods T_1 through T_4, values averaged over each channel and then averaged by treatment, means ± 1 SE. Mean total Rhopalodiaceae biovolume was significantly higher in Fast treatments (mean = 957,488 μm^3) than in Slow treatments (mean = 399,645 μm^3) ($F = 3.94$, $P = 0.05$, $df = 1,63$).

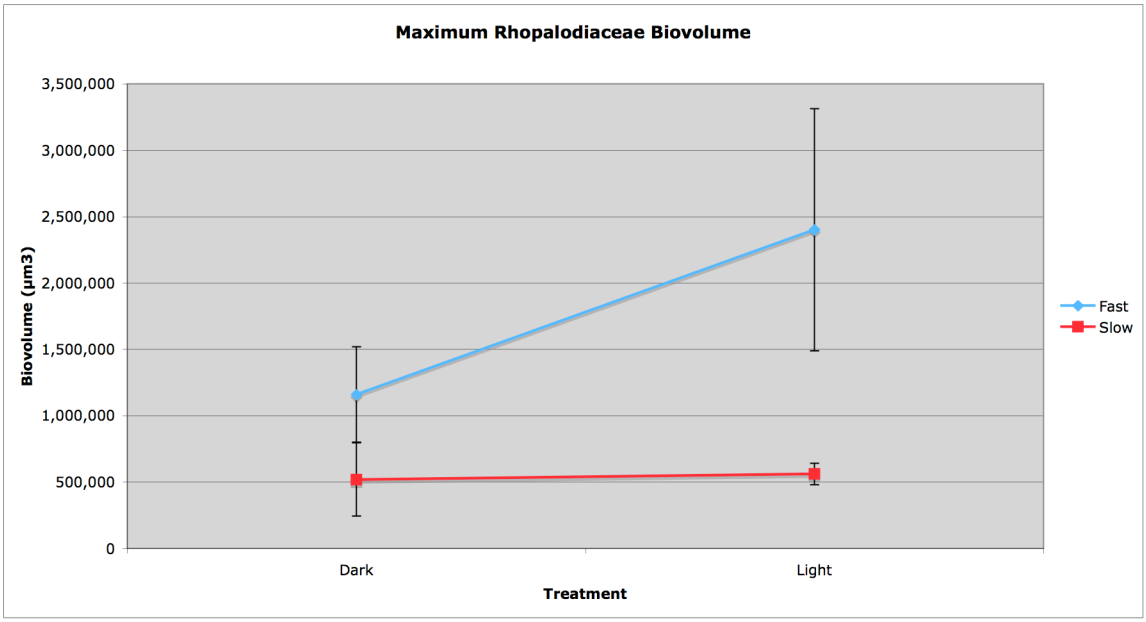

Figure 6d. Maximum Rhopalodiaceae biovolume (μm^3 per mm^2 host) for replicates of the various treatments, means ± 1 SE. Maximum Rhopalodiaceae biovolumes were significantly higher in Fast treatments (mean = 1,780,494) than in Slow treatments (mean = 539,971) ($F = 5.9$, $P = 0.03$, $df = 1,15$).

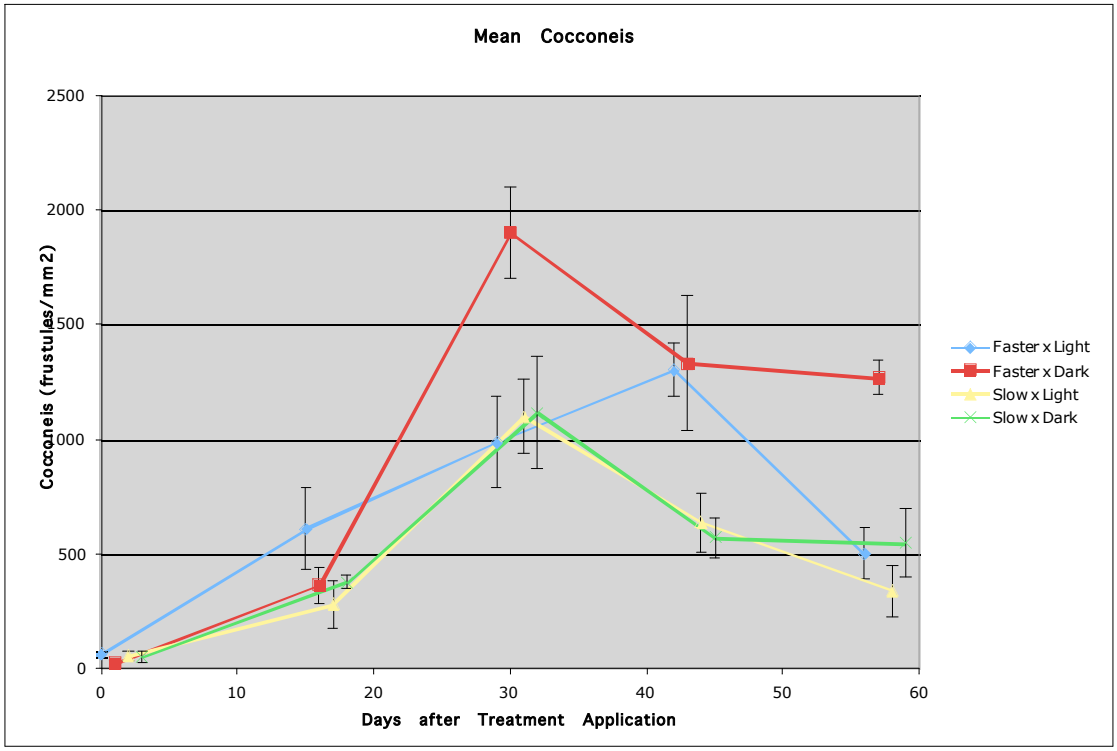

Figure 7a. *Cocconeis* spp. frustule counts over time for each treatment class. Mean counts were higher averaged over all time periods for Fast treatments (mean =837±103 frustules) compared to Slow treatments (mean = 508±66 frustules), ($F = 7.24$, $P = 0.009$, $df = 1,79$). Standard errors are shown.

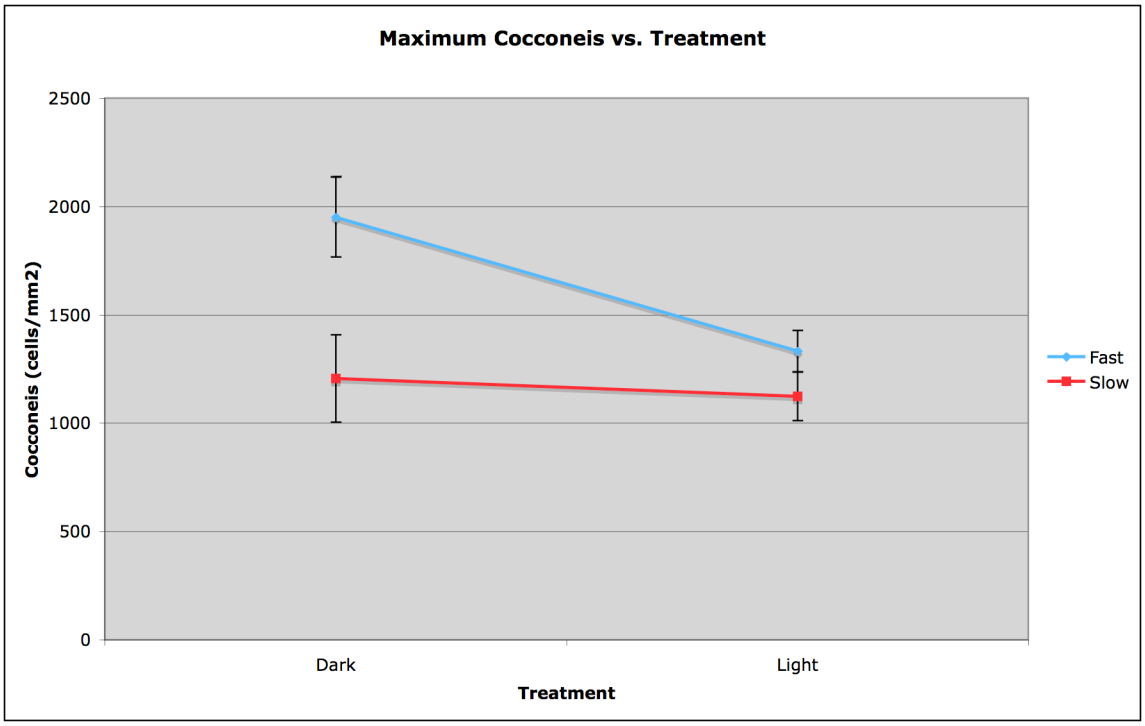

Figure 7b. Maximum *Cocconeis* frustules attained in each treatment class. Maximum counts were higher in Dark treatments (mean = 1578 frustules) than Light treatments (mean = 1229 frustules), (F = 4.58, P = 0.05, df = 1,15), and in Fast treatments (mean = 1642 frustules) compared to Slow treatments (mean = 1165 frustules), (F = 9.43, P = 0.01, df = 1,15).

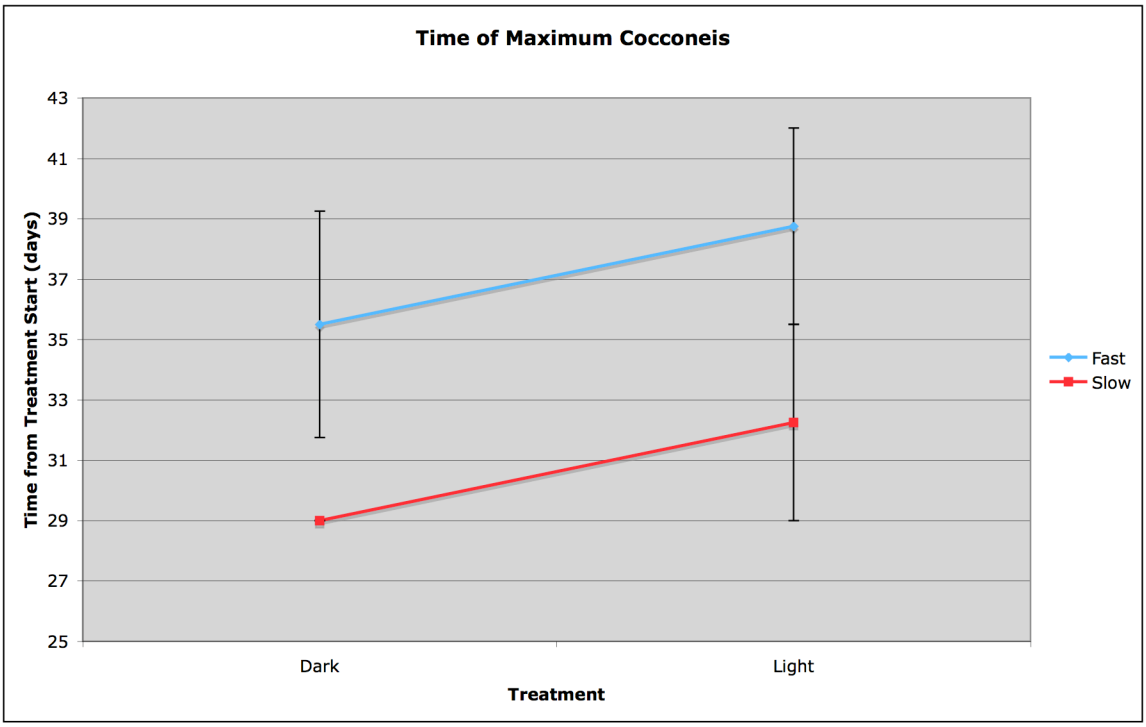

Figure 7c. Time of maximum *Cocconeis* spp. frustules by treatment. *Cladophora* filaments in Fast treatments tended to acquire their maximum loads a week later than in Slow treatments (F = 4.80, P = 0.05, df = 1,15; Two-Way ANOVA).

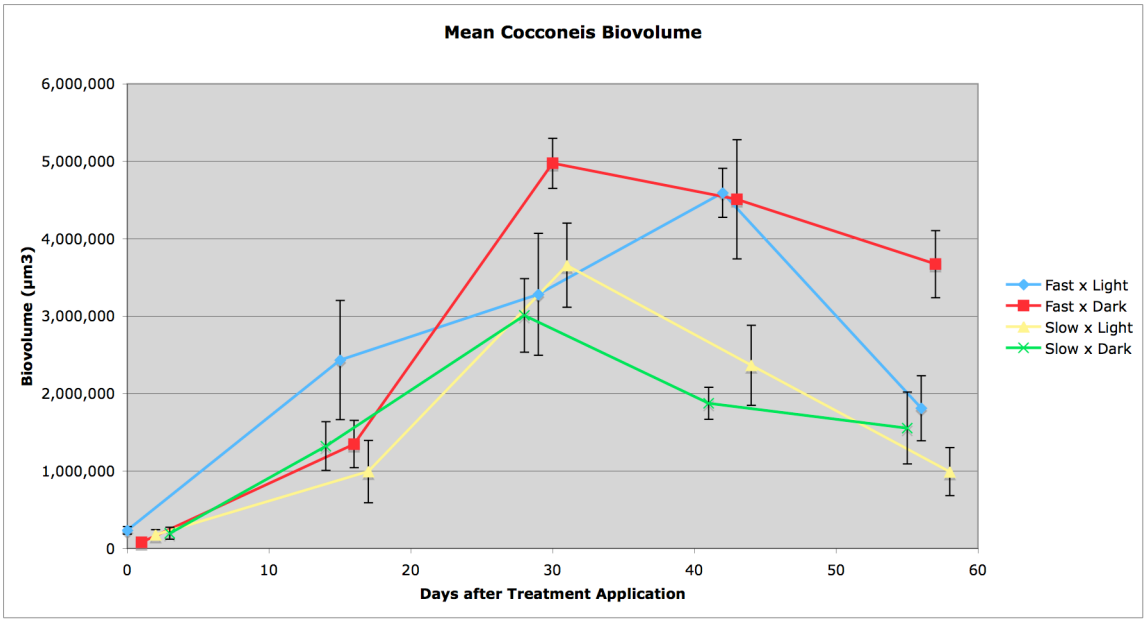

Figure 7d. Mean *Cocconeis* Biovolume (in cubic microns) from each treatment at time periods T_1 through T_4, values averaged over each channel and then averaged by treatment, means ± 1 SE. Mean *Cocconeis* biovolume was significantly higher in Fast treatments (mean = 3,327,406 µm^3) than in Slow treatments (mean = 1,970,648 µm^3) ($F = 14.56$, $P = 0.0003$, df = 1,63).

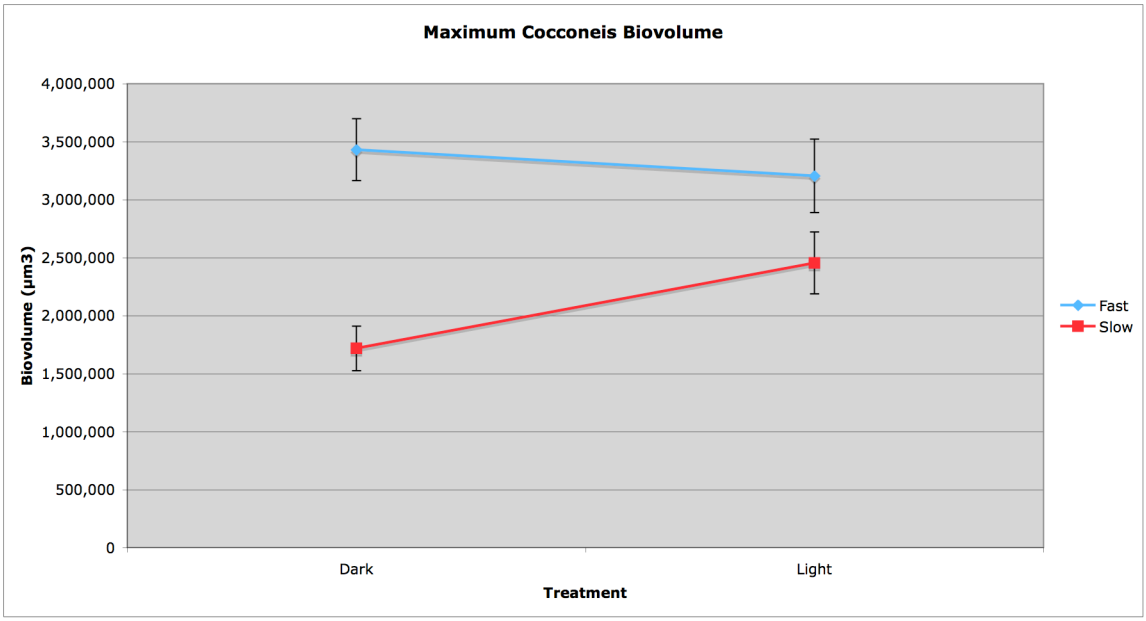

Figure 7e. Maximum *Cocconeis* biovolume (µm^3 per mm^2 host) for replicates of the various treatments, means ± 1 SE. Maximum *Cocconeis* biovolumes were significantly higher in Fast treatments (mean = 3,317,892) than in Slow treatments (mean = 2,086,261) ($F = 21.69$, $P = 0.0005$, df = 1,15).

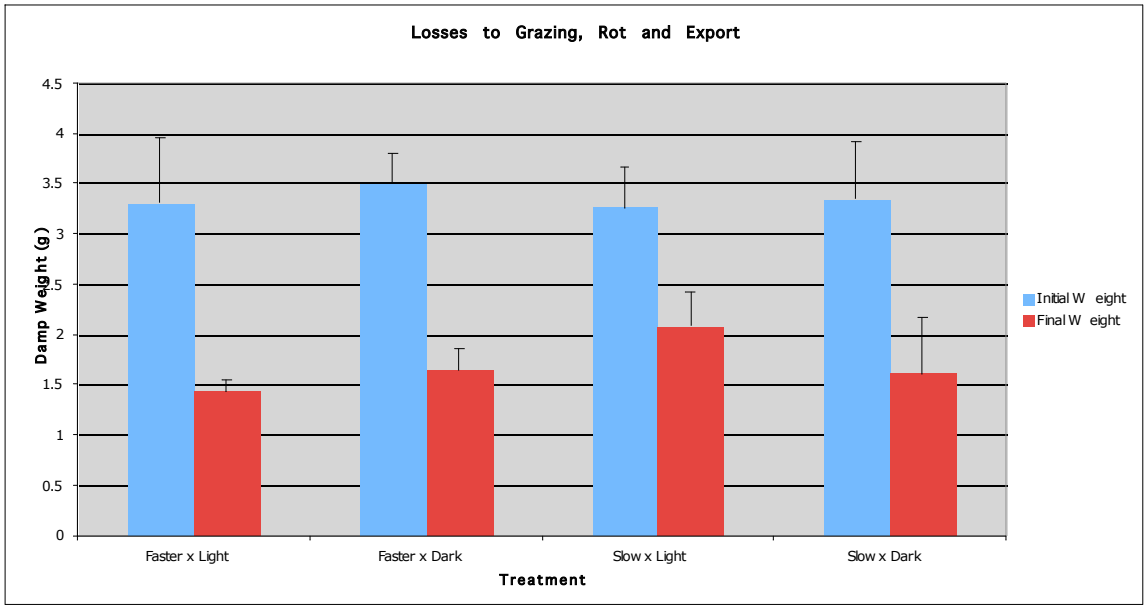

Figure 8. Results from study of detached clumps of algae secured to tiles with rubber bands to evaluate losses from rotting, sloughing and grazing. Values for algae losses due to grazing, rot and export are the difference between initial and final damp weights in grams. Results are grouped by treatment, not stream channel. There were no significant differences in mean algae lost between treatments, suggesting that differences in the filament and epiphyte results above are due to treatments ($F = 1.57$, $P = 0.23$, $df = 1,19$).

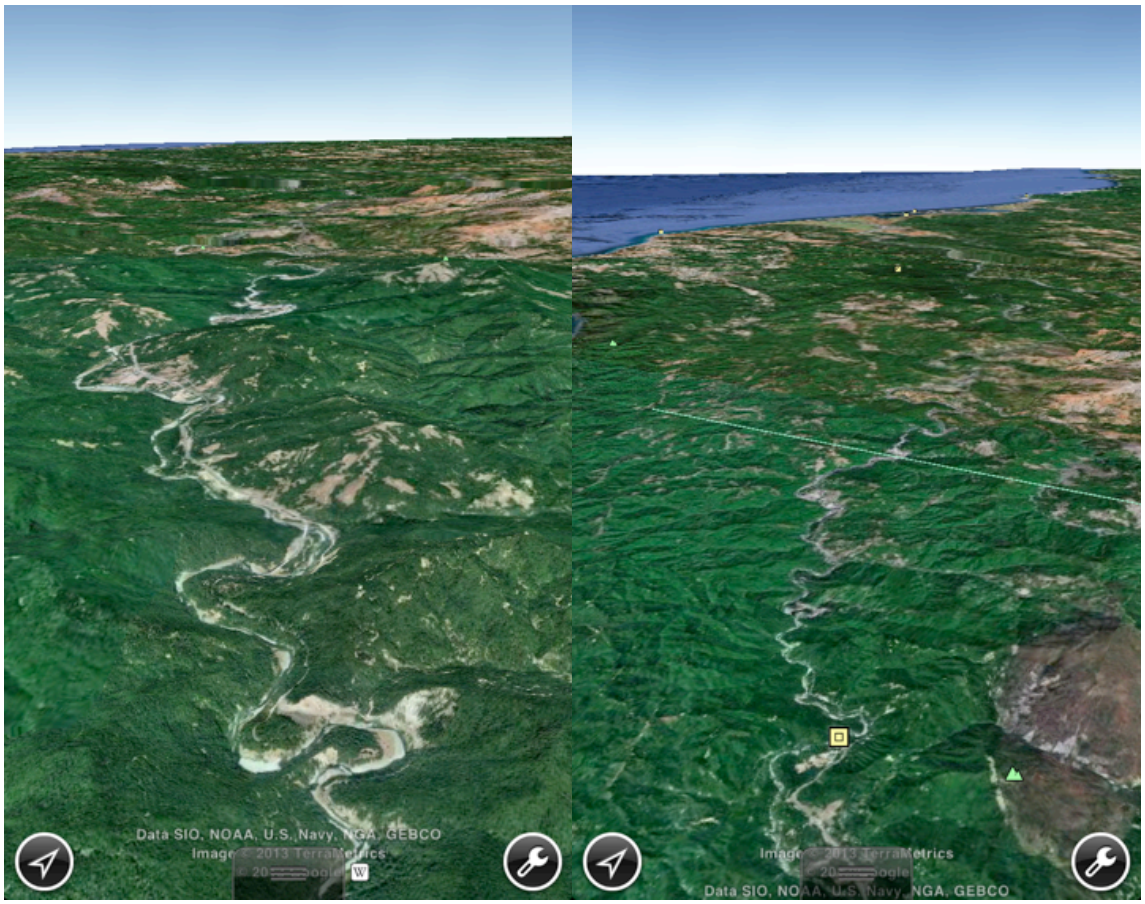

Figure 1. The canyon-bound, bedrock-based Eel has very few depositional environments. Bedrock and boulder substrate in the headwaters grades to cobbles, pebbles and gravel in the delta. Even at Fernbridge, a few kilometers from the mouth, the riverbed is gravel, and deposition is limited to a narrow estuarine zone before crossing the bar into the Pacific. (Graphics courtesy Google Earth).

Figure 2. Scanning electron micrograph of heavily epiphytized strand of *Cladophora glomerata.* Almost all of the attached epiphytes are *Epithemia* spp. Photo credit Rex Lowe.

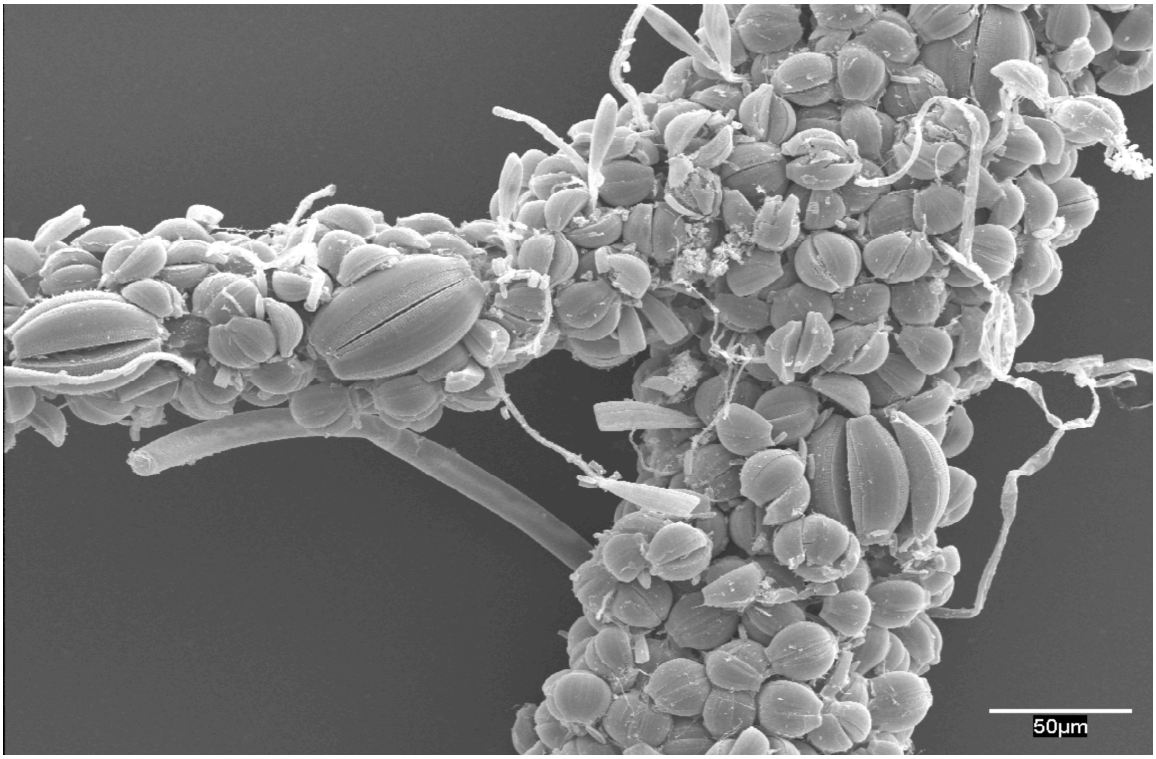

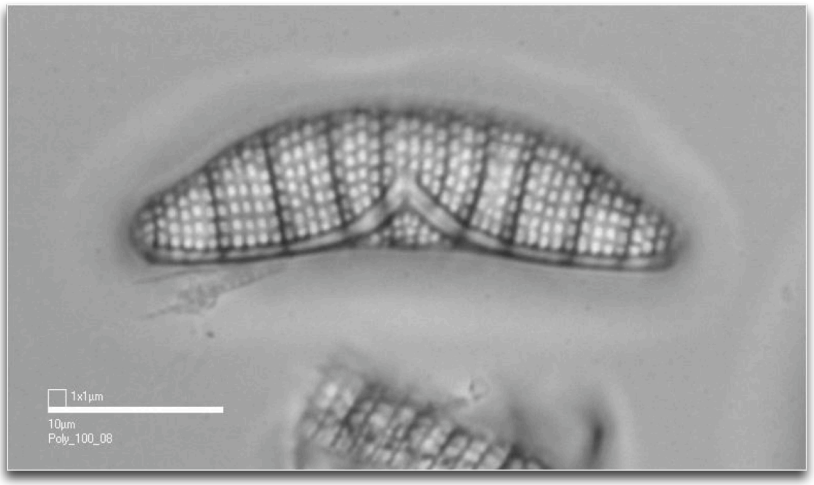

Figure 3. The genus *Epithemia* is in many ways highly suitable as a productivity marker or proxy because it is exclusively freshwater, it closely tracks its host *Cladophora*'s bloom size, it has a robust frustule that resists breaking and dissolution, and it is very recognizable (the "mustache" raphe seen above is diagnostic). Further, *Cladophora* is a dominant macroalga in temperate streams worldwide (Whitton 1970, Dodds 1991a, Guiry and Guiry 2012), and *Epithemia* appears to be a dominant late-successional epiphyte on *Cladophora* in nitrogen-limited freshwaters (Floener and Bothe 1980, Peterson and Grimm 1992, Power et al. 2009). Photo credit Rex Lowe.

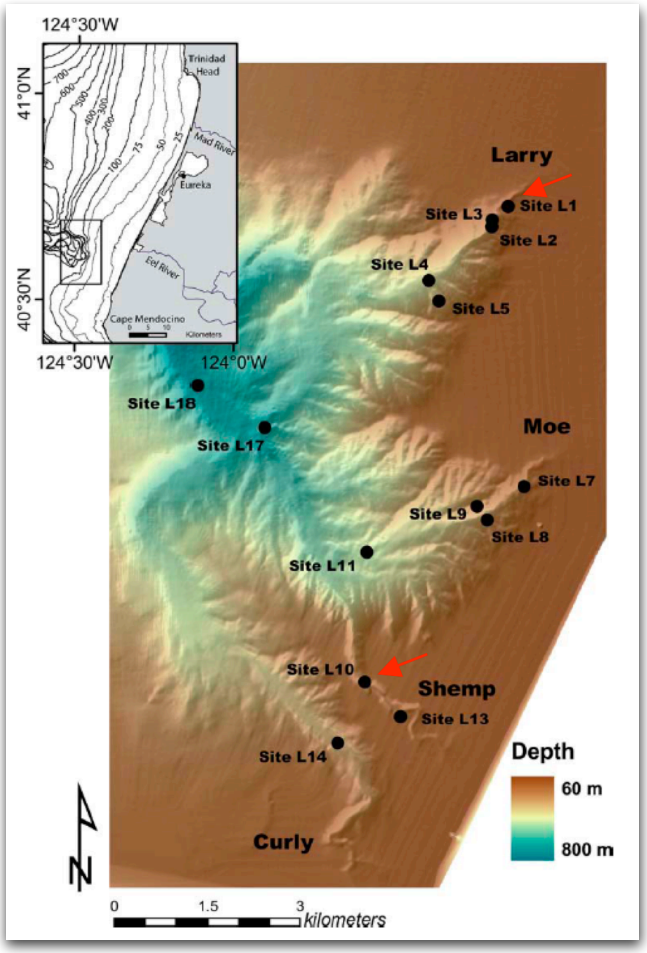

Figure 4. A topographic view of the submarine Eel Canyon. Cores used in this study were obtained from Site L1 and Site L10 (marked with red arrows). Site L1 is a thalweg at the head of the Larry canyon entrance at a depth of 138 m. Larry is the northernmost entrant channel (sites L1–L5), just south of the Eel River mouth, and exhibits a dendritic configuration of side gullies, and an overall width of 4 km by 6 km length. Wall gradients vary in the channels from common gentle slopes (<5%) to vertical walls exhibiting exposed strata. Site L10 is a thalweg halfway down the Shemp canyon entrance. Shemp (sites L10, L13) is a very narrow, meandering entrant with steep walls, and joins Moe at ~300 m water depth. Shemp has thick beds of shell hash and wood debris in cores at several locations. Inset shows the location of the canyon about 15 km offshore of the Eel River mouth (Figure modified from Drexler *et al.* 2006, © Society for Sedimentary Geology).

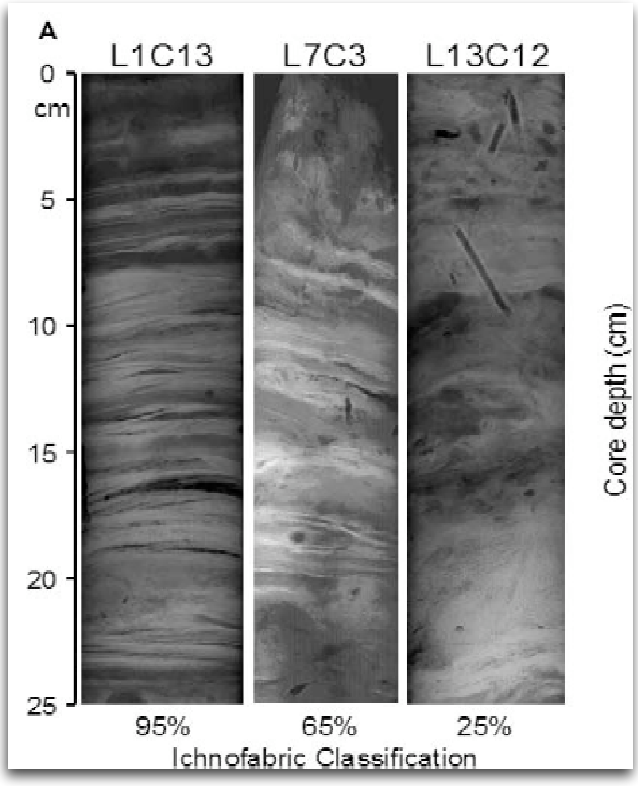

Figure 5. Representative cores showing differential sedimentary layer preservation: an "Ichnofabric classification" value is assigned to each core to indicate its level of preservation: thalweg cores range from 80-95%, and wall cores from 40-85%. On the left core L1C13 shows a high degree of bed preservation, while on the right core L13C12 shows extensive burrows and bioturbation. Isotopic analyses constrain accumulation rates, more precisely for wall cores. There is thus a tradeoff between dating accuracy and preservation for all but a few cores (Figure from Drexler *et al.* 2006, © Society for Sedimentary Geology).
.

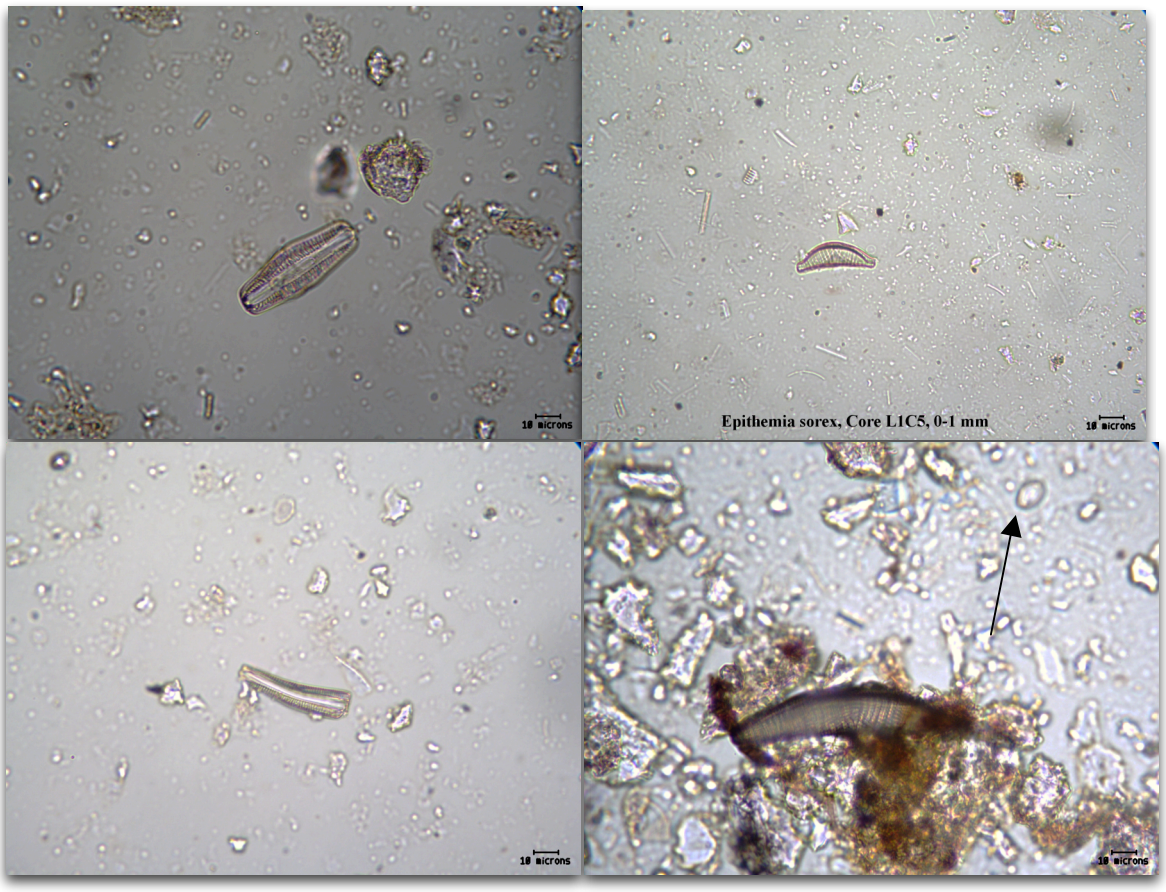

Figure 6a. This core (L1C5) contained a few valves of *Rhopalodia gibba*, which is a late successional freshwater species like *Epithemia* and also like *Epithemia* has nitrogen-fixing endosymbionts. Thousands of centric marine diatom frustules were present for every valve of *Rhopalodia*.	Figure 6b. This is a photograph taken at 400x magnification of an *Epithemia sorex* valve, which is the smallest of the three *Epithemia* species found in the Eel River. Its quite distinctive shape (we call it a Captain Crunch or Bonaparte hat) aids in its identification. This diatom traveled all the way from its host algae in a channel in the Eel watershed all the way down to the ocean floor 15 km offshore and 140 meters deep.
Figure 6c. *Rhoicosphenia* spp. is a mid-successional epiphytic diatom that often supplants *Cocconeis* and is supplanted by *Epithemia* as the growing season progresses. Note its distinctive "bent rectangle" shape.	Figure 6d. A view of *Epithemia turgida,* which is the larger of the two epiphytic *Epithemia* species found in the Eel River. To some eyes it resembles a banana slug, and is unlike any marine diatoms found in these cores. and an early successional dominant diatom, *Cocconeis pediculus* (arrow). 400x magnification.

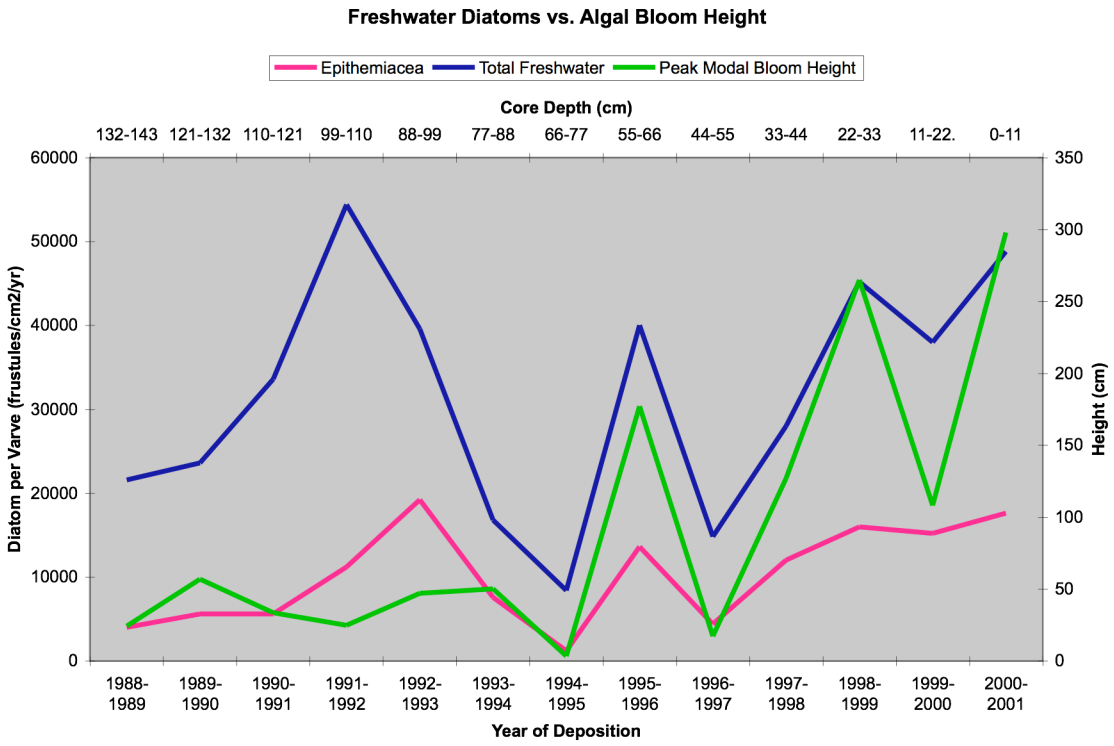

Figure 7. Results from comprehensive diatom survey of core L10C3 from the Shemp canyon entrance, showing the twelve years of overlap with the algal survey record. Frustule counts are summed over the entire year of deposition in a given varve.

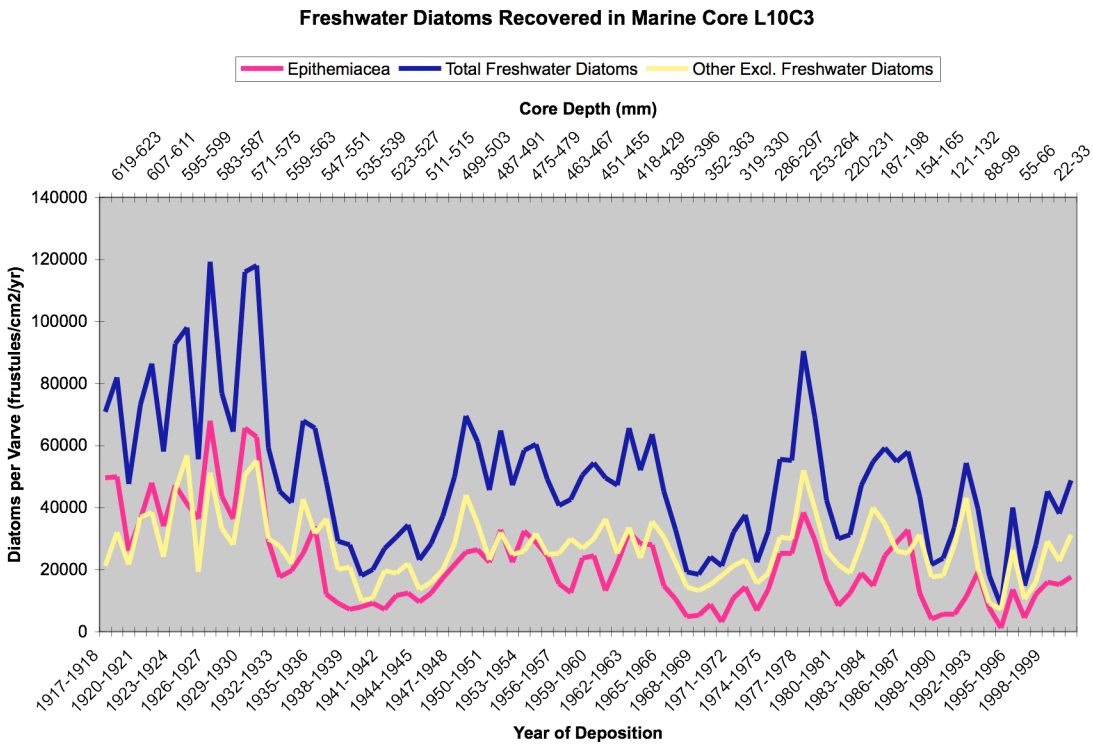

Figure 8. Results from comprehensive diatom survey of core L10C3 from the Shemp canyon entrance, showing the entire record from core base to core top for Rhopalodiaceae, other freshwater diatoms and total freshwater diatoms. Frustule counts are summed over the entire year of deposition in a given varve.

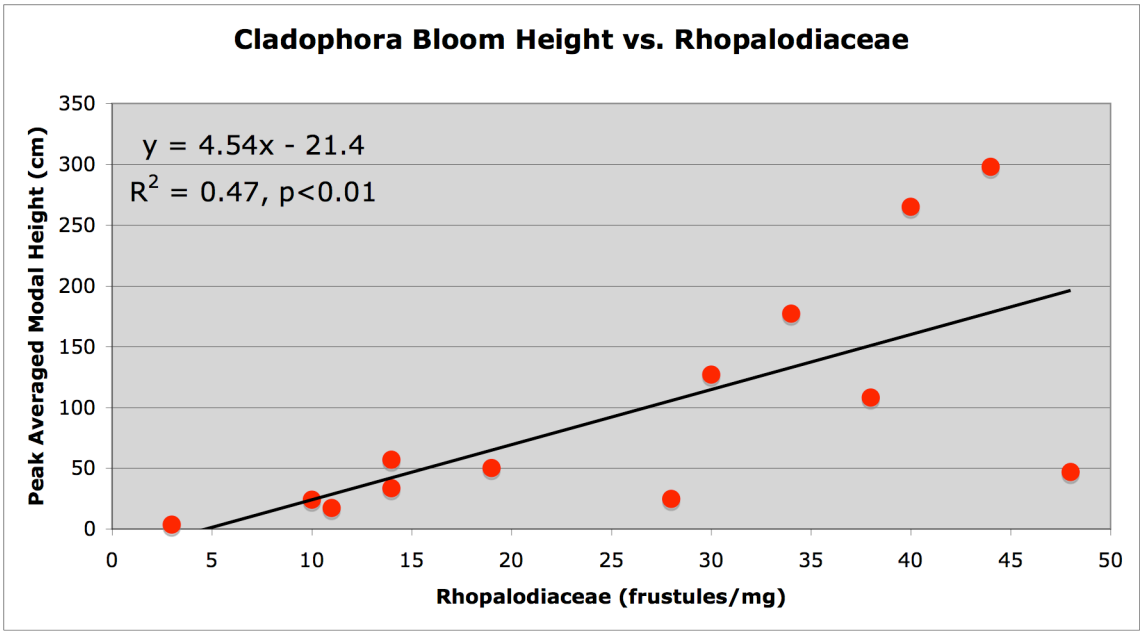

Figure 9. Results from a linear regression analysis of Rhopalodiaceae frustules from core L10C3 against Peak Modal Bloom Height of *Cladophora glomerata* streamers measured in annual algal surveys from 1988-2000. Annual varves in all cores are dated from August to August ending at August 2001. Therefore the algal growing season reflected in the last varve is most likely 2000, and not 2001, as under the low flow conditions that predominate in the growing season very few *Epithemia* diatoms would have reached the canyon in the few weeks between when they likely appeared in July 2001 and the last deposited sediment in August 2001.

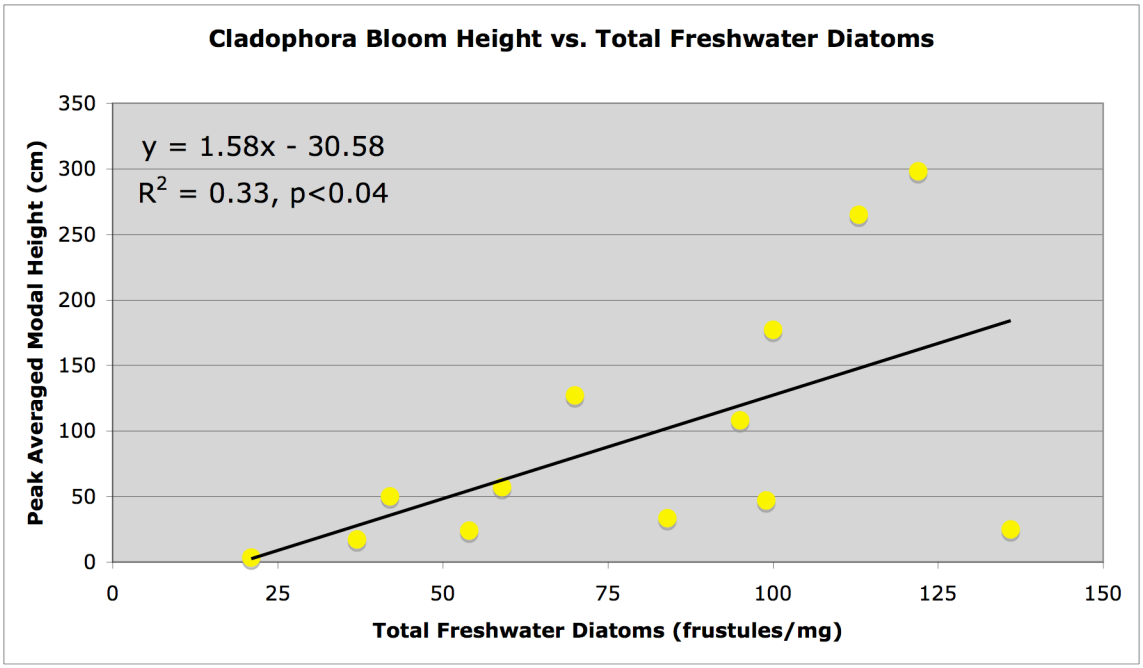

Figure 10. Results from a linear regression analysis of *total* freshwater diatom frustules from core L10C3 against Peak Modal Bloom Height of *Cladophora glomerata* streamers measured in annual algal surveys from 1988-2000.

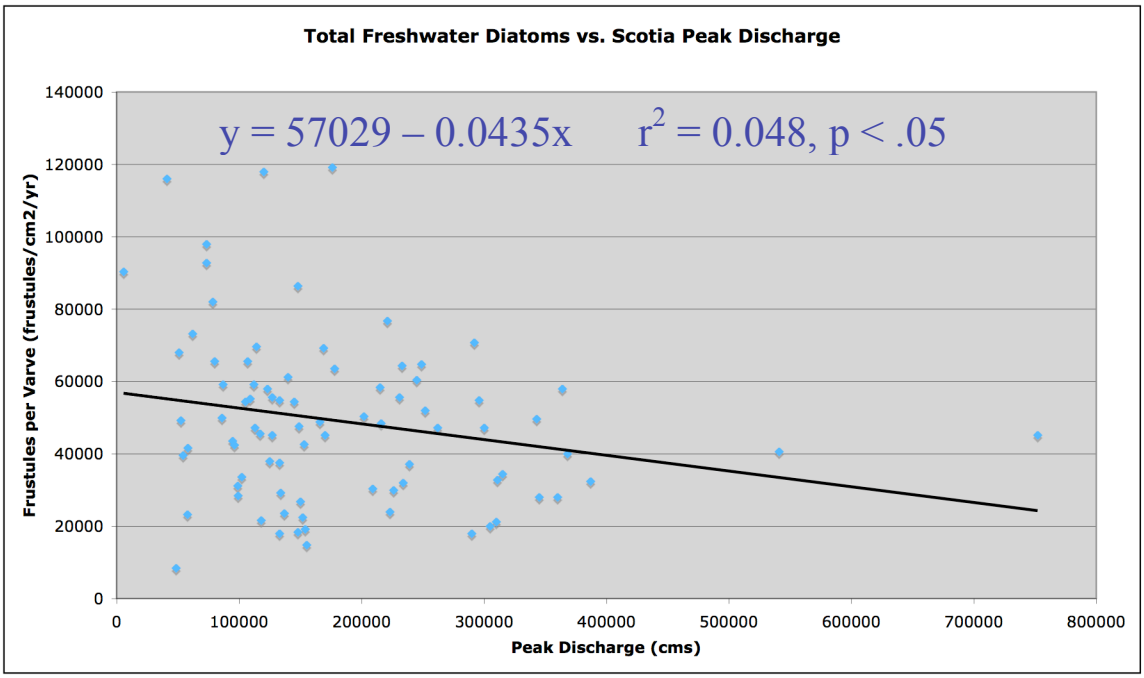

Figure 11. Results from a linear regression analysis of Total Freshwater diatom frustules per year from core L10C3 against peak annual discharge measured at Scotia, California (USGS Station 11477000) from 1918-2001.

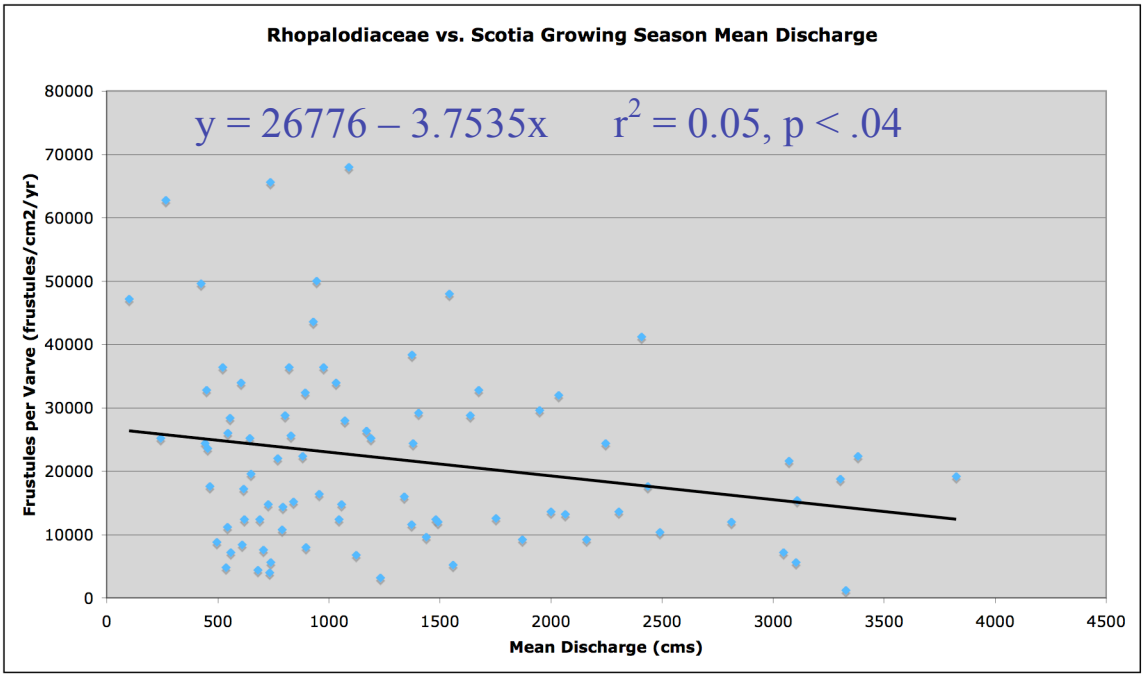

Figure 12. Results from a linear regression analysis of Rhopalodiaceae diatom frustules per year from core L10C3 against mean growing season discharge measured at Scotia, California (USGS Station 11477000) from 1918-2001.

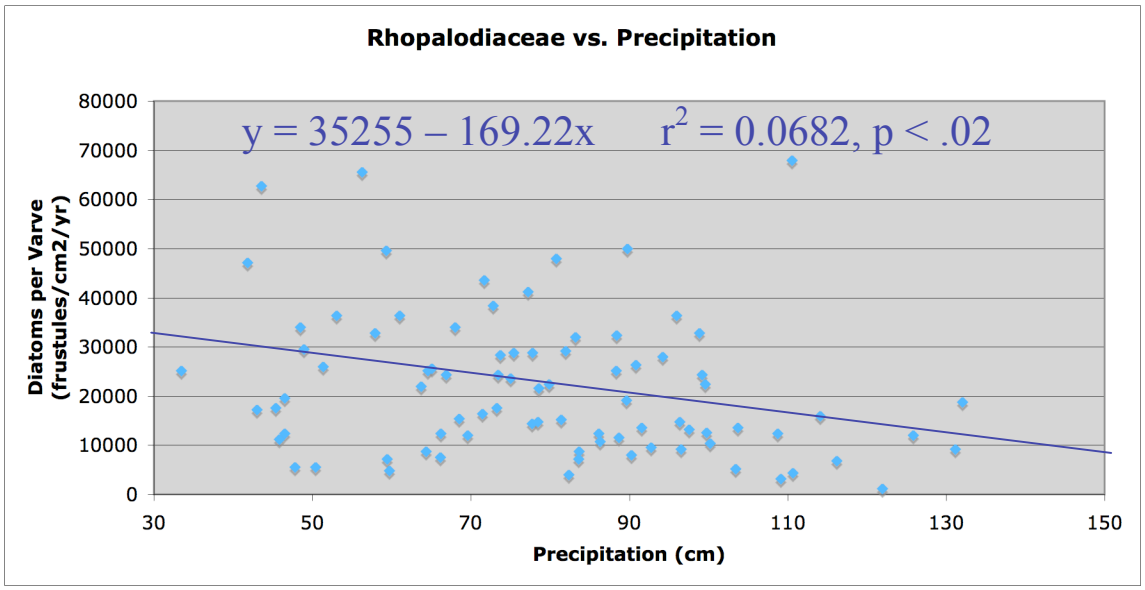

Figure 13. Results from a linear regression analysis of Rhopalodiaceae diatom frustules per year from core L10C3 against annual total precipitation measured at Eureka, California (NWS Station 42910) from 1918-2001.

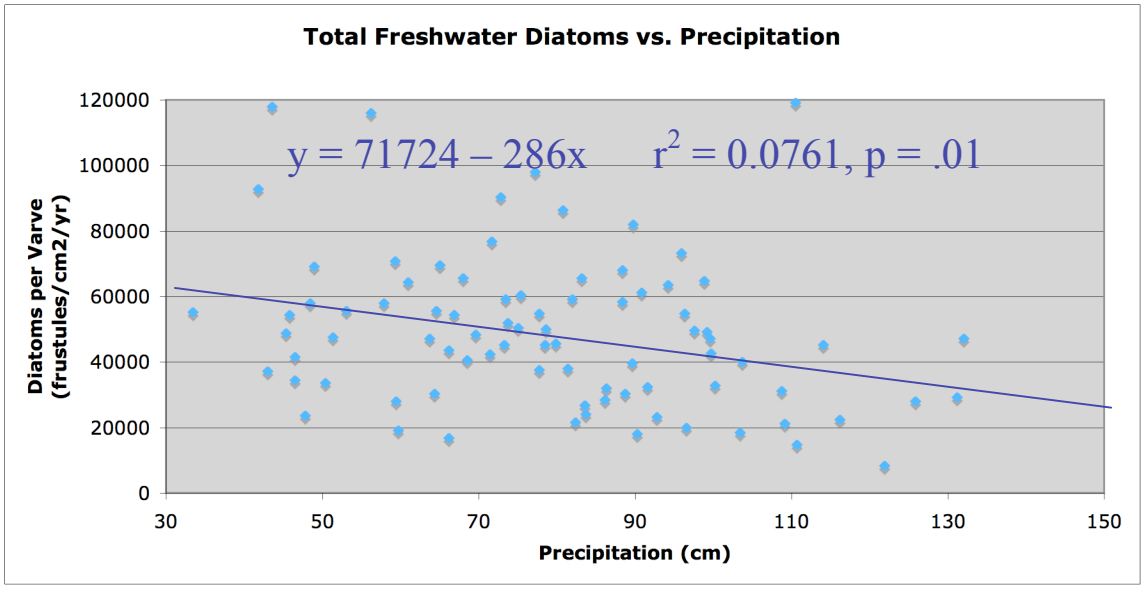

Figure 14. Results from a linear regression analysis of *total* freshwater diatom frustules per year from core L10C3 against annual total precipitation measured at Eureka, California (NWS Station 42910) from 1918-2001.

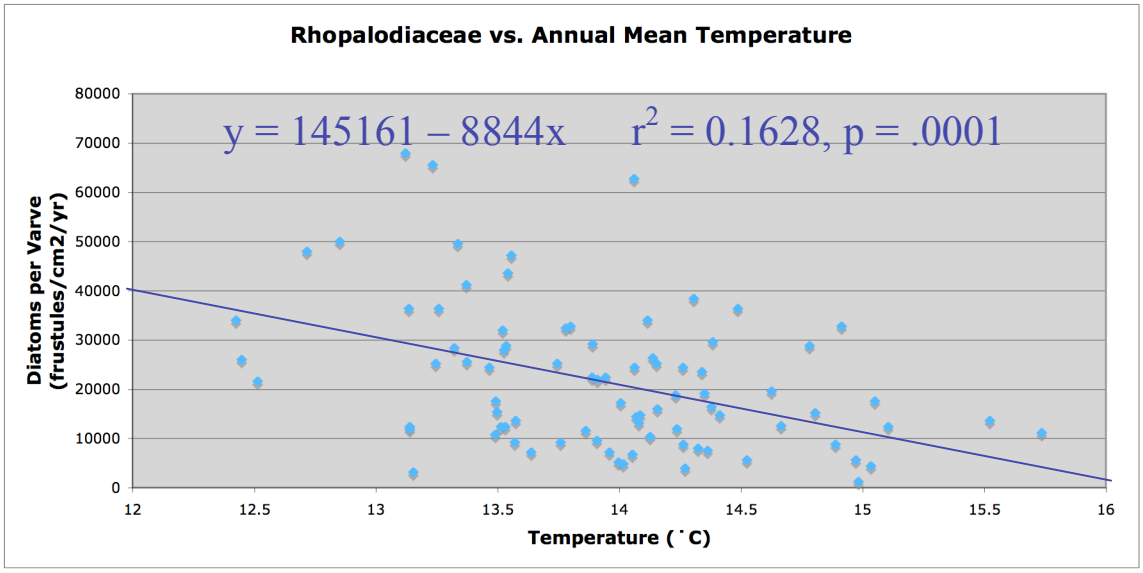

Figure 15. Results from a linear regression analysis of Rhopalodiaceae diatom frustules from core L10C3 against mean annual temperature measured at Ukiah, California (NWS Station 49122) from 1918-2001.

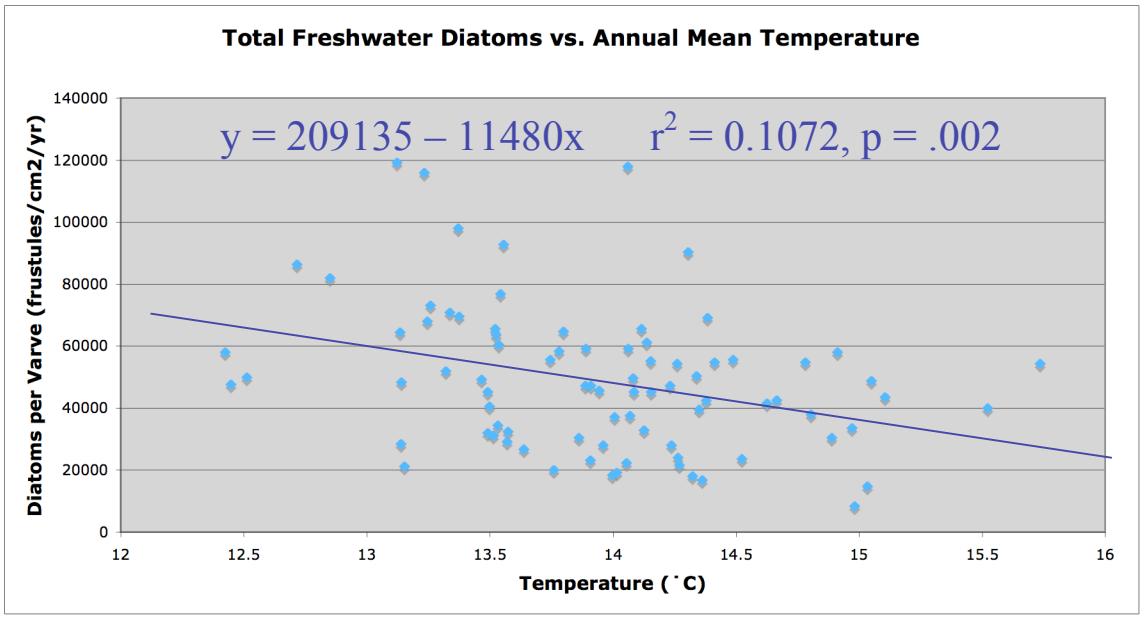

Figure 16. Results from a linear regression analysis of *total* freshwater diatom frustules per year from core L10C3 against mean annual temperature measured at Ukiah, California (NWS Station 49122) from 1918-2001.

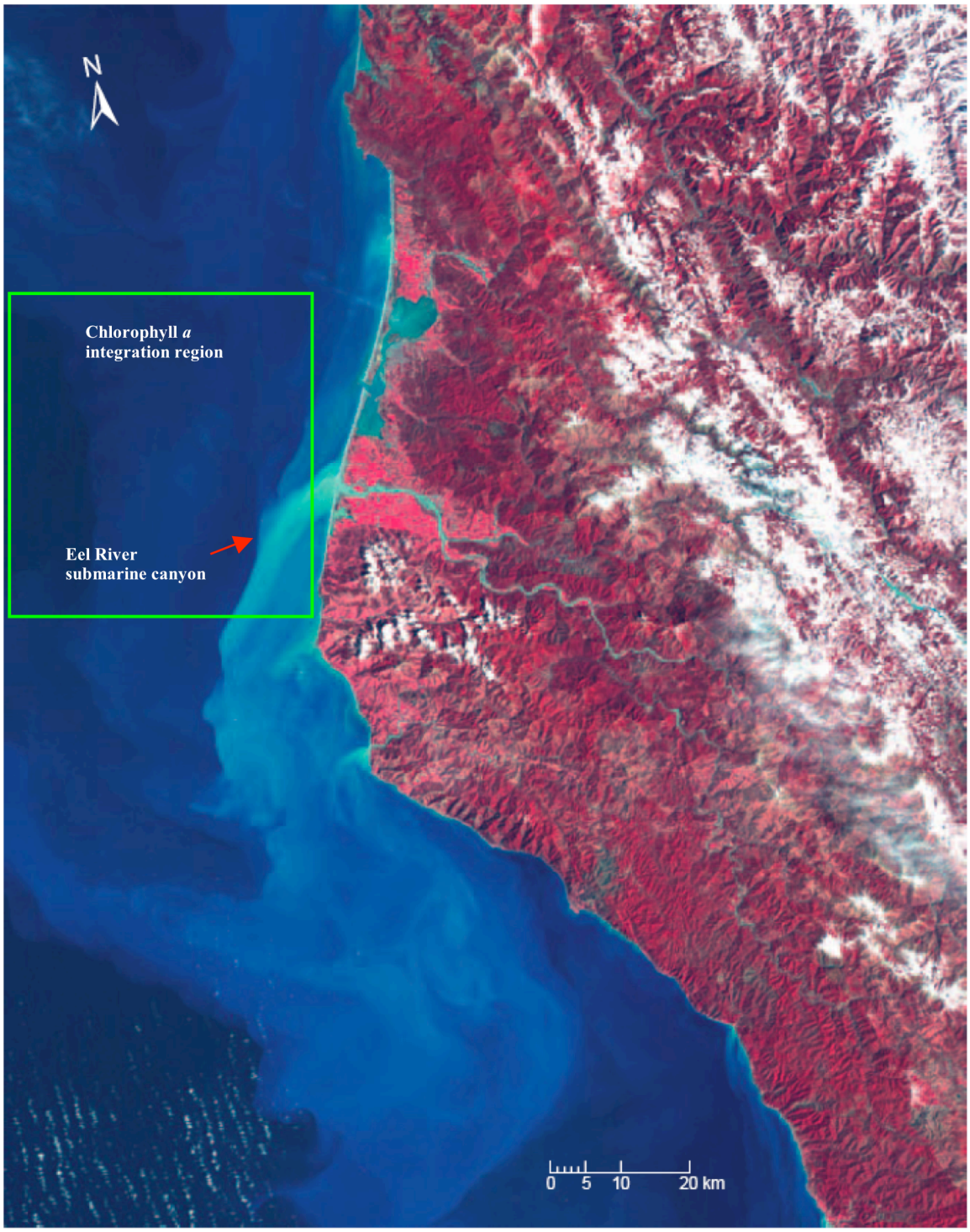

Figure 1. A Landsat image of the Eel River plume under north to south prevailing winds. Much of the sediment is deposited in the submarine Eel canyon (marked with a red arrow), with the remainder settling on the inner shelf before being exported to deeper waters. The ½ degree x ½ degree region used to integrate satellite measurements of chlorophyll *a* is marked with a green square (image courtesy of NSSDC).

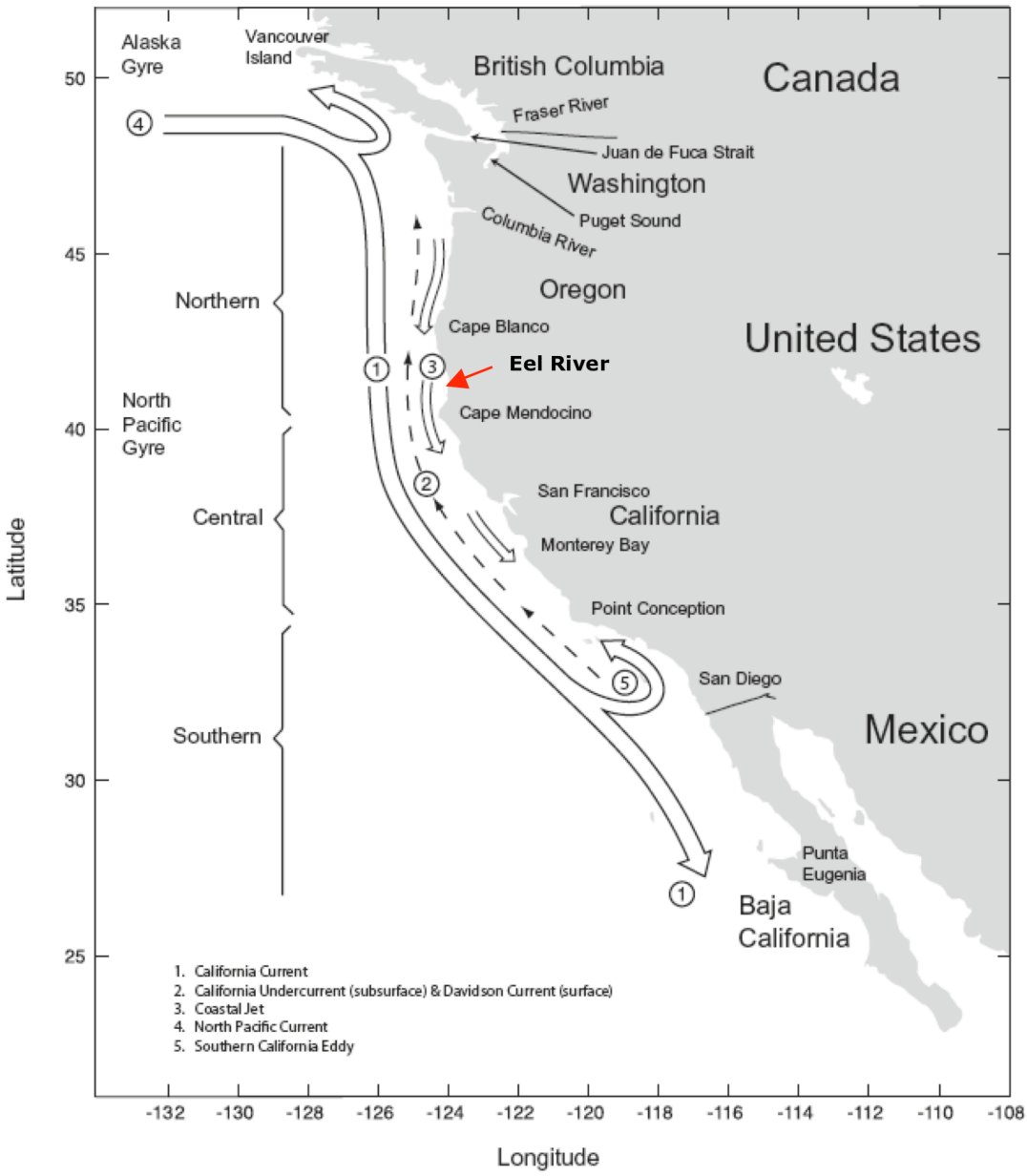

Figure 2. A schematic of the California Current System, adapted from Checkley and Barth (2009), showing the major features relevant to this study. The Eel River mouth is identified with a red arrow. Flow divergence from Cape Blanco creates a retention zone for marine organisms, and nutrient availability is enhanced by topographic upwelling effects on the coastal jet as well as river inputs from the Eel and Mad Rivers.

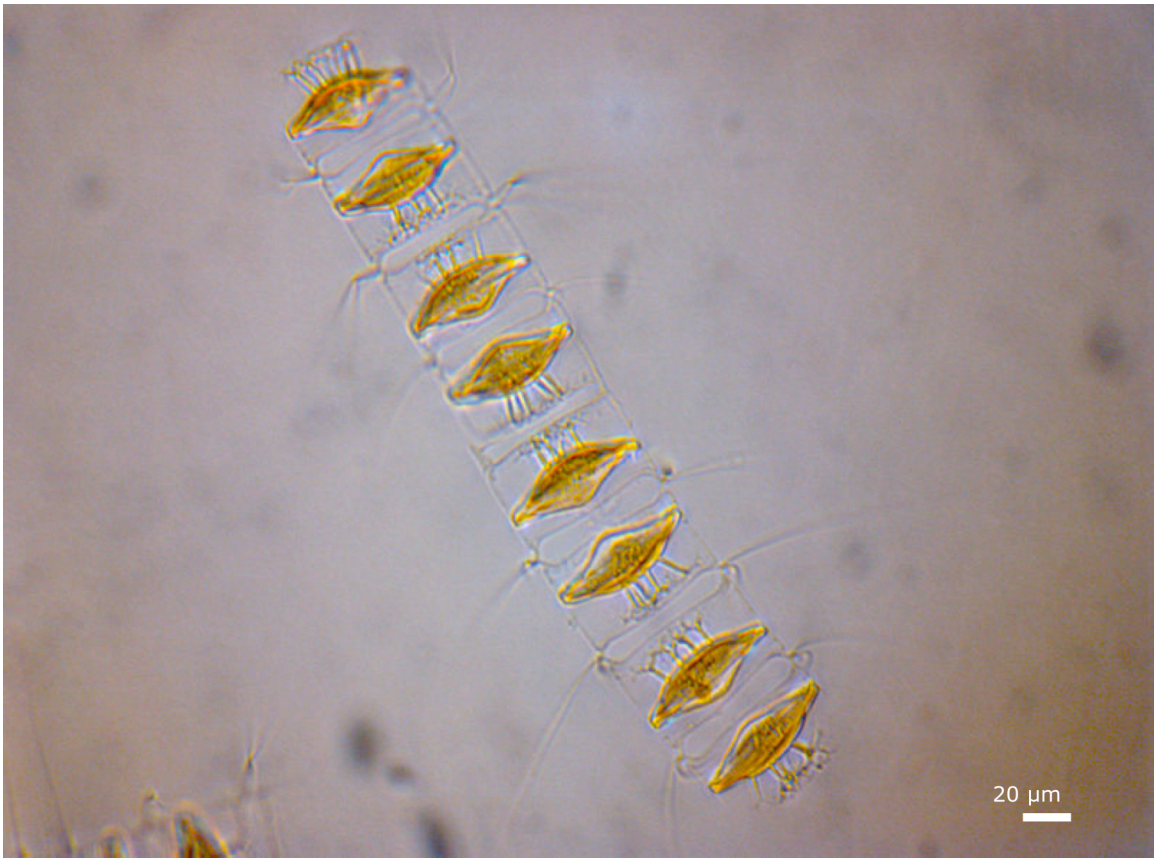

Figure 3. A micrograph of *Chaetoceros diadema* (Ehrenberg) resting spores at 400X magnification. The long translucent appendages jutting out from either side of the chain are used to entrain long chains of this diatom in vertical upwelling currents (Guiry and Guiry 2012).

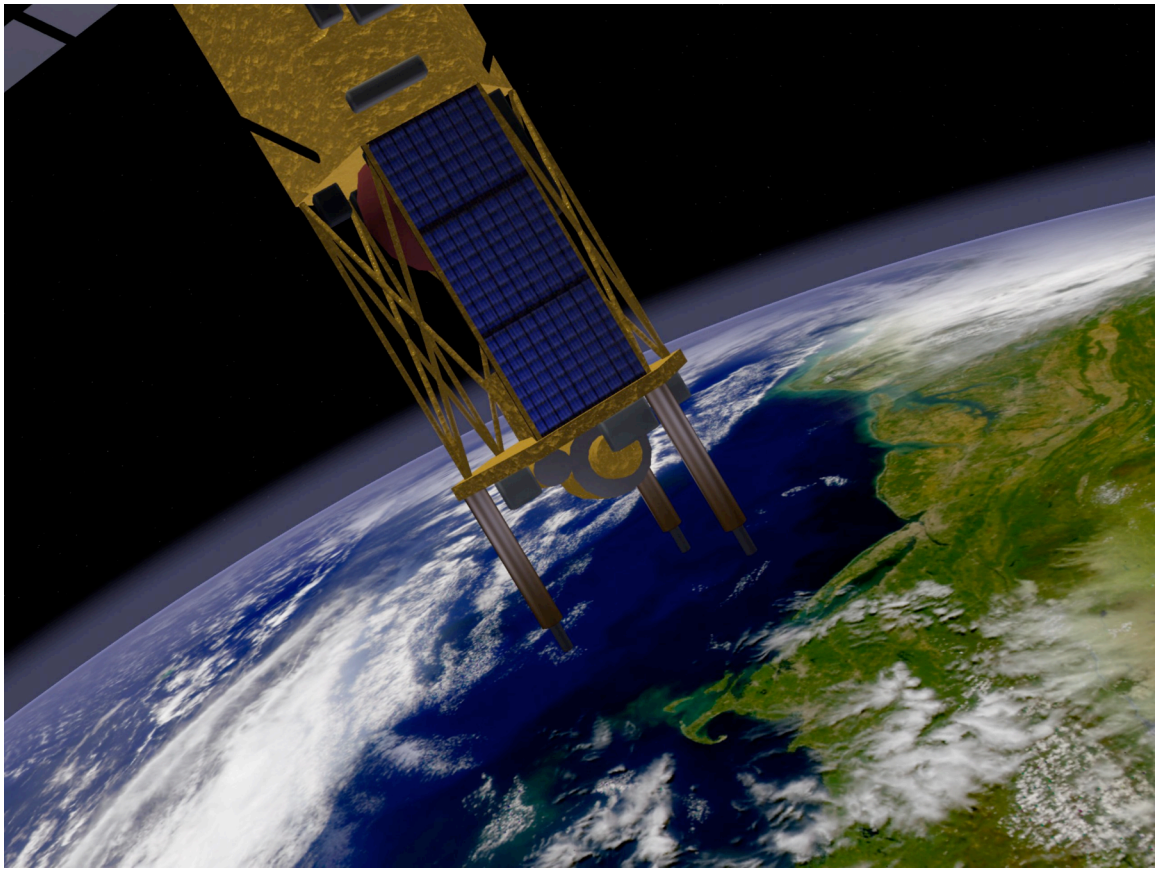

Figure 4. A composite image of the SeaStar spacecraft during its third orbit. The SeaWiFS instrument is visible in-between the three support pylons. The SeaWiFS mission launched in September 1997, and followed the successful Coastal Zone Color Scanner, launched in 1978, and was succeeded by the Aqua MODIS mission in 2002. Each mission increased the resolution, sensitivity and global coverage of ocean color data (image courtesy of NASA).

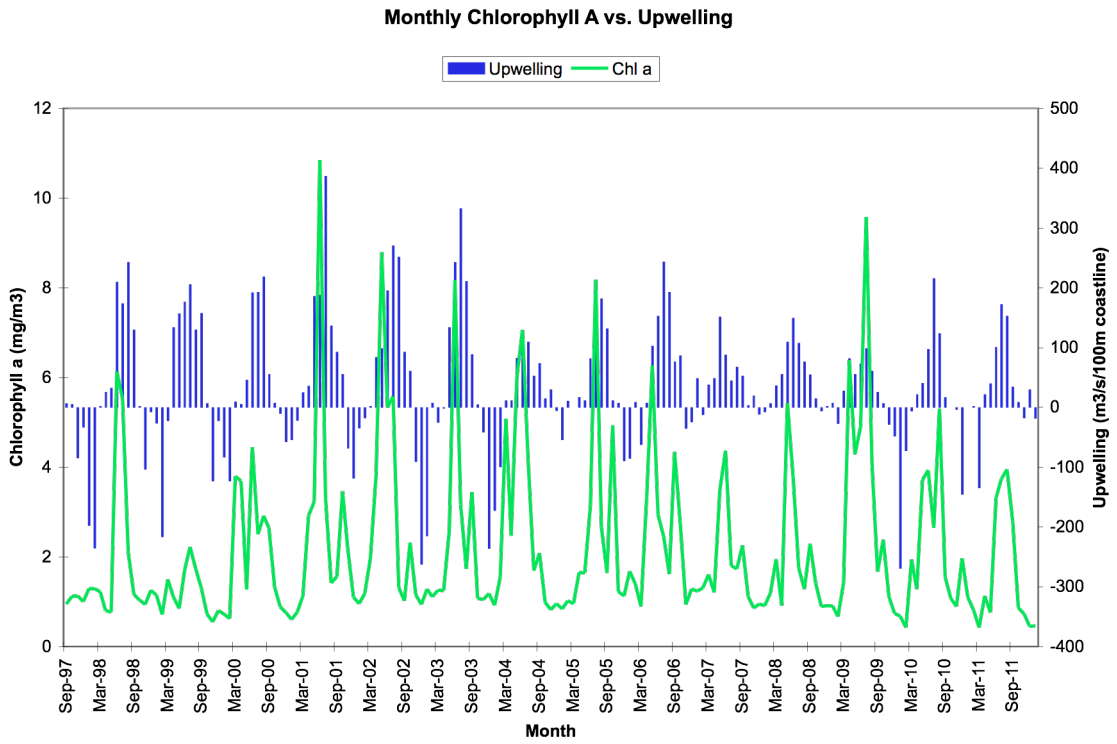

Figure 5. SeaWiFS chlorophyll *a* and upwelling data plotted over the past fifteen years. SeaWiFS chlorophyll data was averaged on a monthly basis across a ½ x ½ degree latitude ~2400 km^2 square (124.41 to 124.91°W, 40.75 to 41.25°N) offshore of the Eel River mouth. Upwelling data was calculated from monthly mean pressure fields using data obtained from the National Oceanographic and Atmospheric Administration's Pacific Fisheries Environmental Laboratory. Winter/spring peaks are present in 10 out of 15 years in my data, defined as between December 1 and April 30 and being at least 33% of the summer peak, and of these at least 9 are in or directly following distinctly downwelling periods with substantial river input. Fall peaks, defined as between September 1 and November 30, are evident during downwelling phases in 5 out of 15 years, with substantial river input.

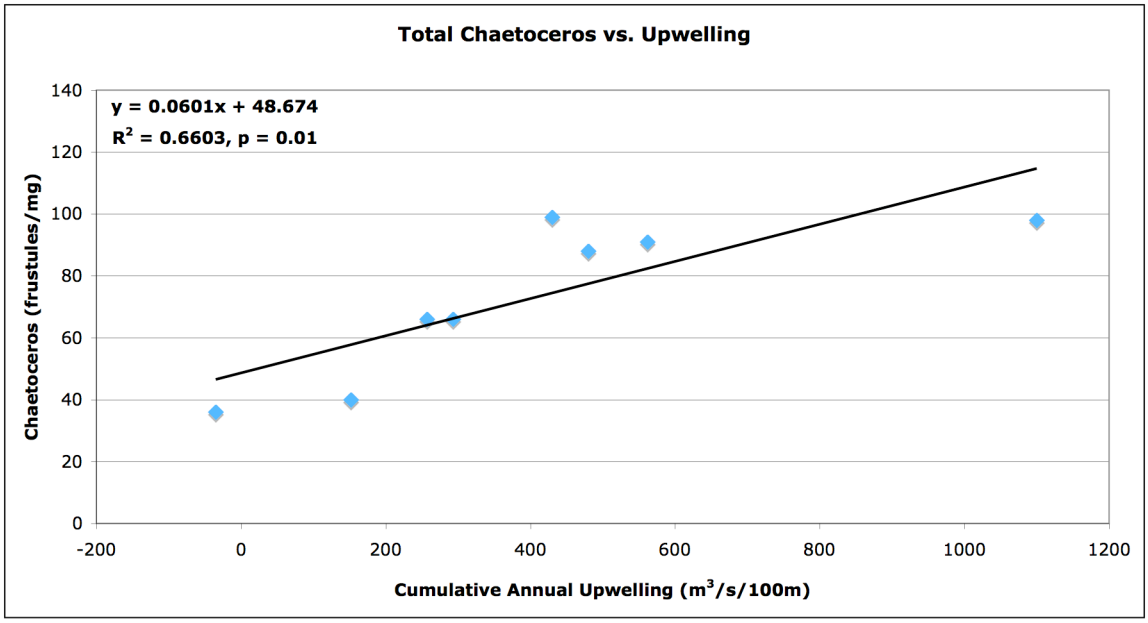

Figure 6. Results from a linear regression of *Chaetoceros* spp. frustules recovered from STRATAFORM core L10C3 and cumulative annual upwelling calculated from data downloaded from the Pacific Fisheries Environmental Laboratory for a location just north of my study region (42°N, 125°W) in the coastal zone near the Eel River mouth between Cape Mendocino and Cape Blanco. *Chaetoceros* spp. frustules were not correlated to peak upwelling intensity.

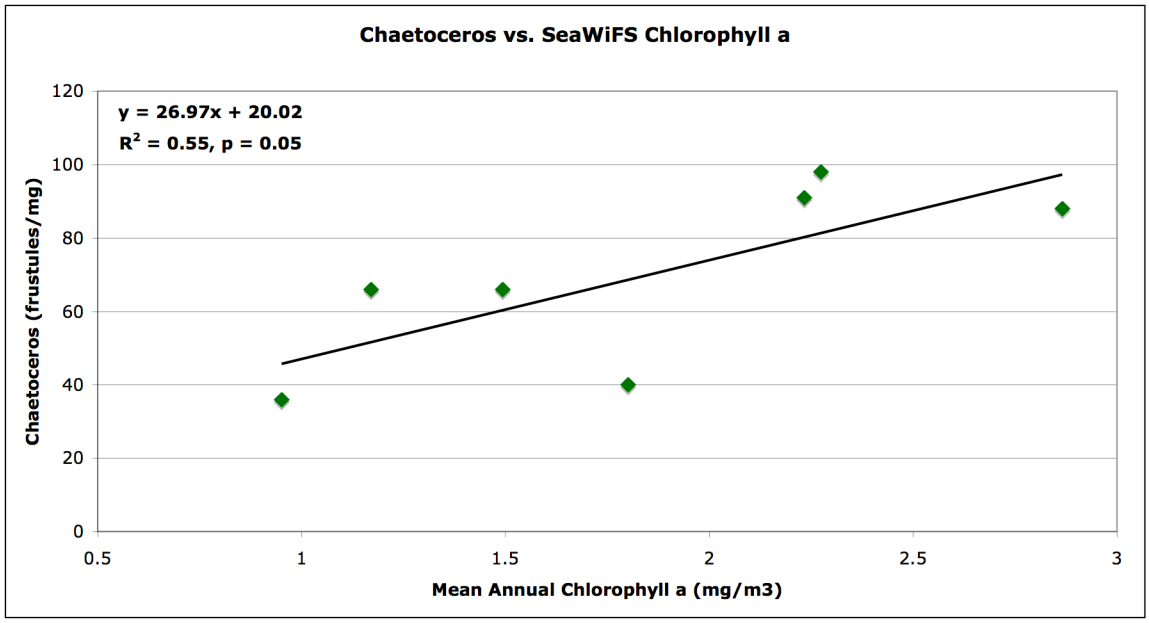

Figure 7. Results from a linear regression of *Chaetoceros* spp. frustules recovered from STRATAFORM core L10C3 and mean annual chlorophyll integrated over a ½ x ½ degree latitude square (124.41 to 124.91°W, 40.75 to 41.25°N) offshore of the Eel River mouth from 1997 to 2001, the period of overlap between this satellite mission and the STRATAFORM core data.

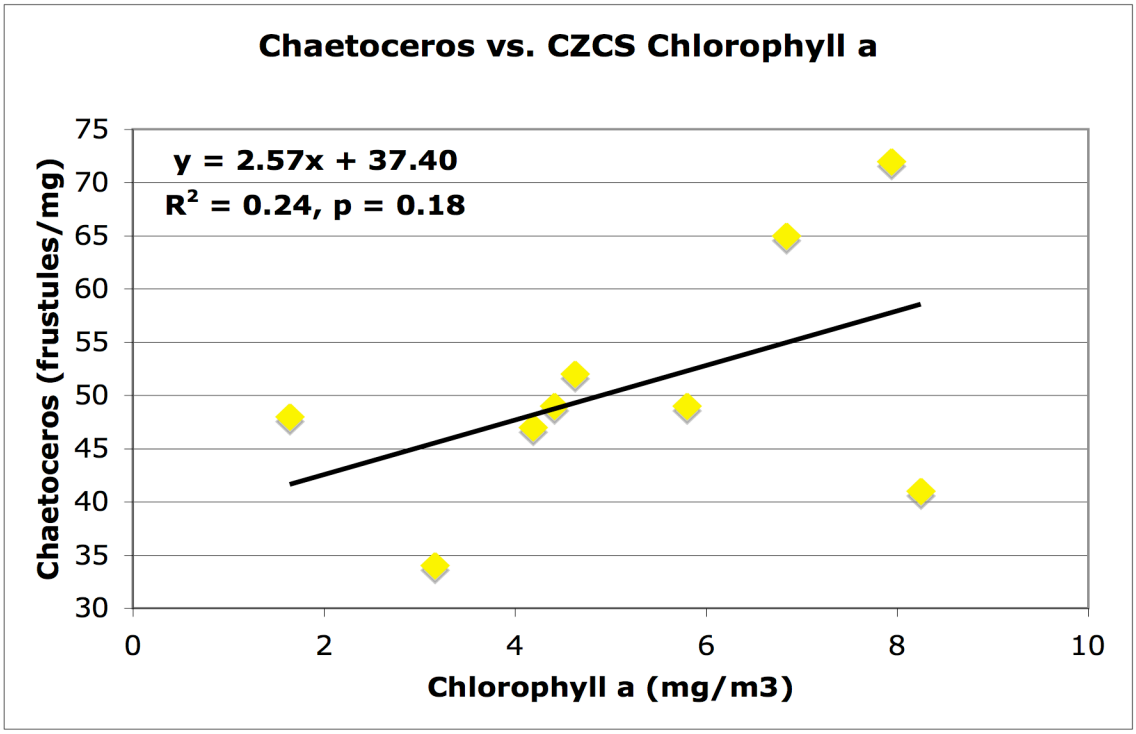

Figure 8. Results from a linear regression of *Chaetoceros* spp. frustules recovered from STRATAFORM core L10C3 and mean annual chlorophyll retrieved from the Coastal Zone Color Scanner (CZCS) dataset and integrated over a ½ x ½ degree latitude square (124.41 to 124.91°W, 40.75 to 41.25°N) offshore of the Eel River mouth from 1978 to 1986, the entire duration of this satellite mission.

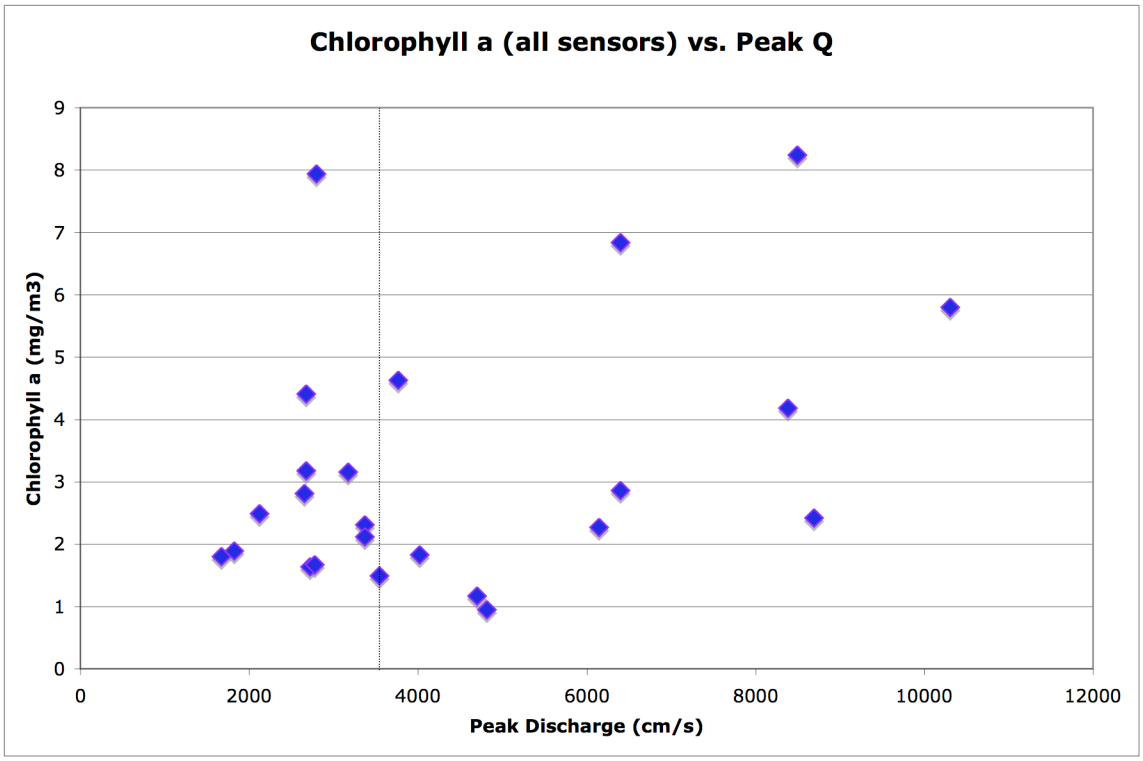

Figure 9. Mean annual marine chlorophyll *a* (from CZCS: 1978-1986, SeaWiFS: 1997-2002 and MODIS: 2002-2012) plotted against peak annual discharge in the preceding calendar year. Dotted vertical line marks the threshold between drought years (to the left of the line) and flood years (to the right of the line).

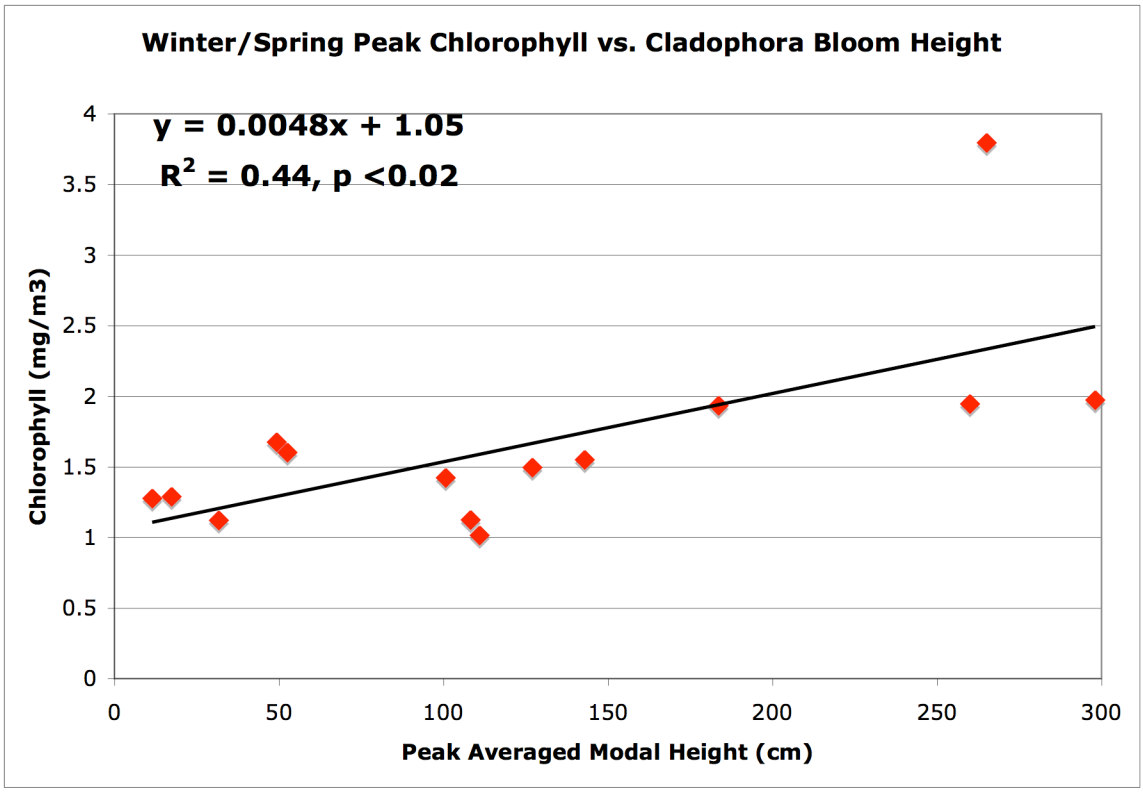

Figure 10. Results from a linear regression of Winter/Spring "non-upwelling" marine chlorophyll *a* peaks against Peak averaged modal height of *Cladophora* blooms as measured in annual upstream surveys at the Angelo Coast Range Reserve (Power et al. 2008 and unpublished data). SeaWiFS chlorophyll data was averaged on a monthly basis across a ½ x ½ degree latitude square (124.41 to 124.91°W, 40.75 to 41.25°N) offshore of the Eel River mouth (r^2=0.44, p<0.02, n=14).

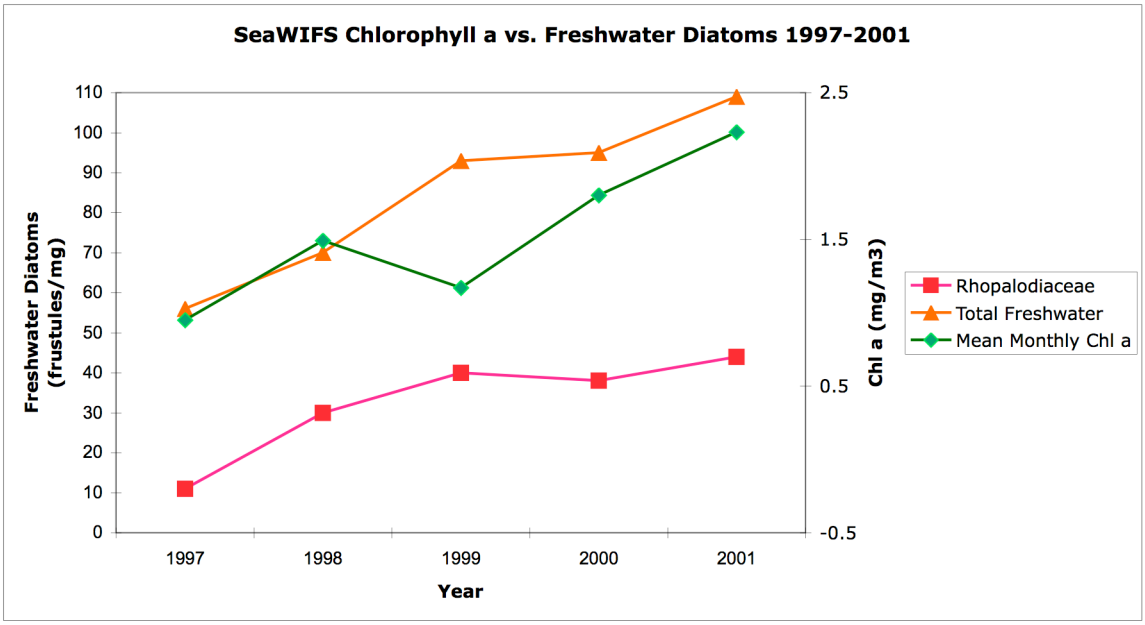

Figure 11. SeaWiFS mean monthly chlorophyll *a* plotted with total sampled freshwater diatom and Rhopalodiaceae frustules from STRATAFORM marine sediment core L10C3 for the period 1997-2001.

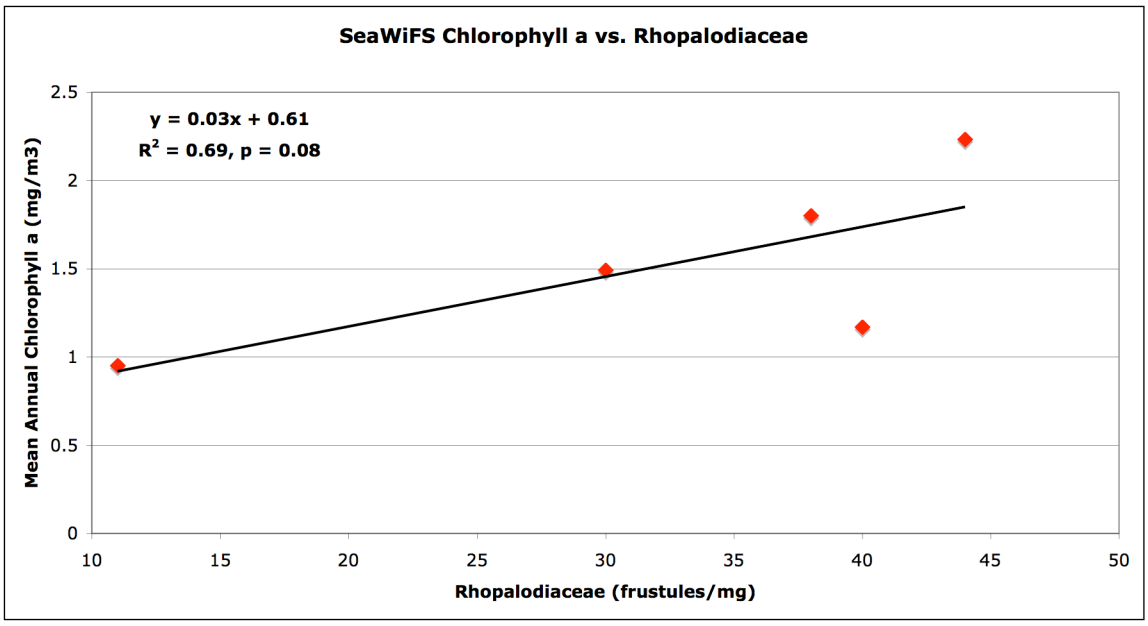

Figure 12. Results from a linear regression of SeaWiFS mean monthly chlorophyll *a* against freshwater Rhopalodiaceae frustules recovered from STRATAFORM marine core L10C3 for the complete period of overlap between the two records of 1997-2003. SeaWiFS chlorophyll data was averaged on a monthly basis across a ½ x ½ degree latitude square (124.41 to 124.91°W, 40.75 to 41.25°N) offshore of the Eel River mouth (r^2=0.69, p=0.08, n=5).

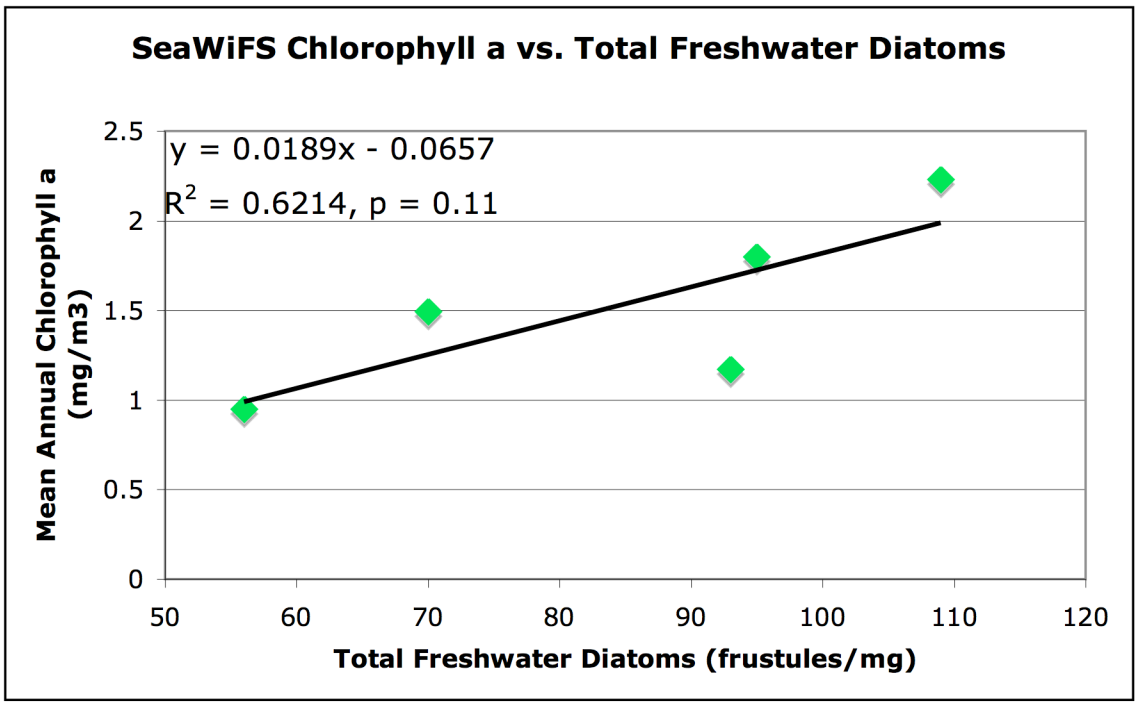

Figure 13. Results from a linear regression of SeaWiFS mean monthly chlorophyll *a* against total freshwater frustules recovered from STRATAFORM marine core L10C3 for the period of overlap between the two records of 1997-2001. SeaWiFS chlorophyll data was averaged on a monthly basis across a ½ x ½ degree latitude square (124.41 to 124.91°W, 40.75 to 41.25°N) offshore of the Eel River mouth (r^2=0.62, p=0.11, n=5).

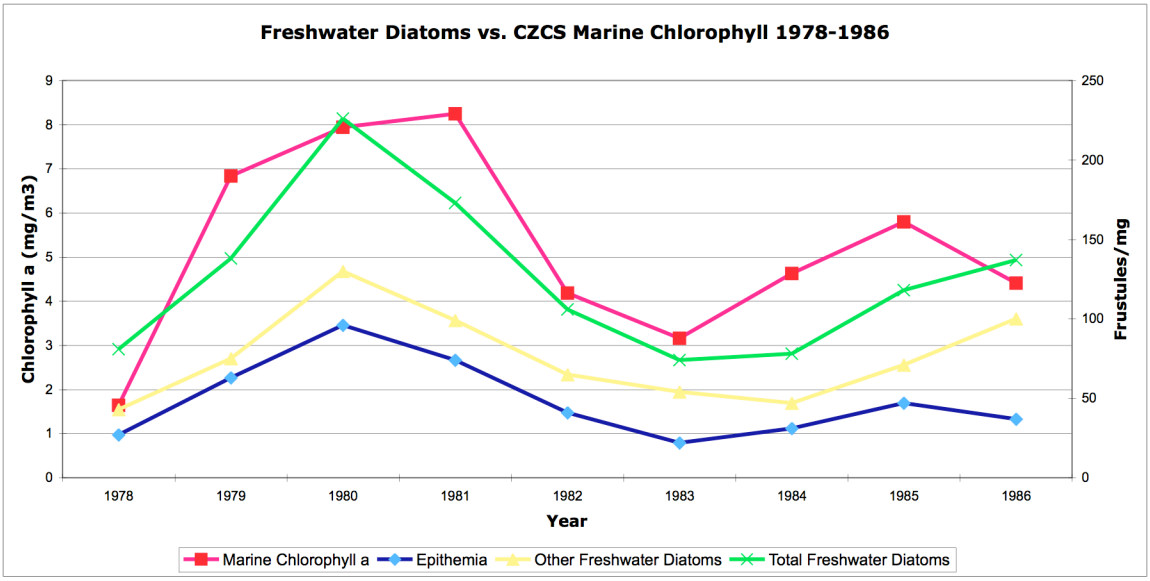

Figure 14. CZCS mean monthly chlorophyll *a* plotted with total sampled freshwater diatom and Rhopalodiaceae frustules from STRATAFORM marine sediment core L10C3 for the period 1978-1986. CZCS chlorophyll data was averaged on a monthly basis across a ½ x ½ degree latitude (~2400 km^2) square (124.41 to 124.91°W, 40.75 to 41.25°N) offshore of the Eel River mouth.

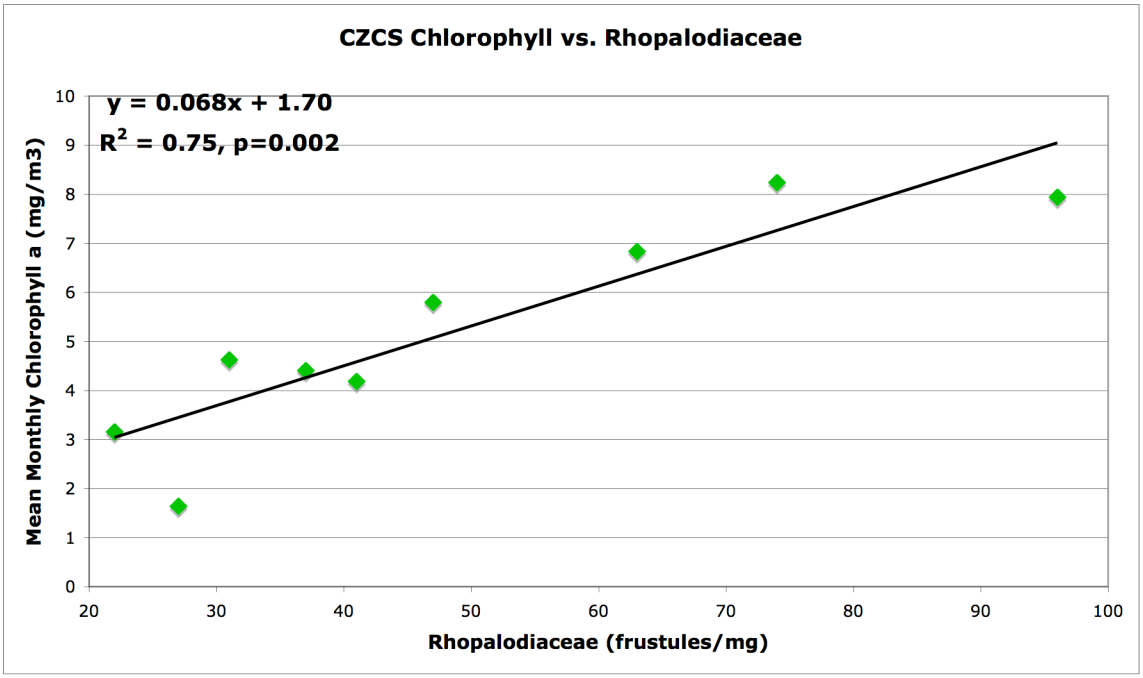

Figure 15. Results from a linear regression of CZCS mean monthly chlorophyll *a* against freshwater Rhopalodiaceae frustules recovered from STRATAFORM marine core L10C3 for the complete period of overlap between the two records of 1978-1986. CZCS chlorophyll data was averaged on a monthly basis across a ½ x ½ degree latitude square (124.41 to 124.91°W, 40.75 to 41.25°N) offshore of the Eel River mouth (r^2=0.75, p=0.002, n=9).

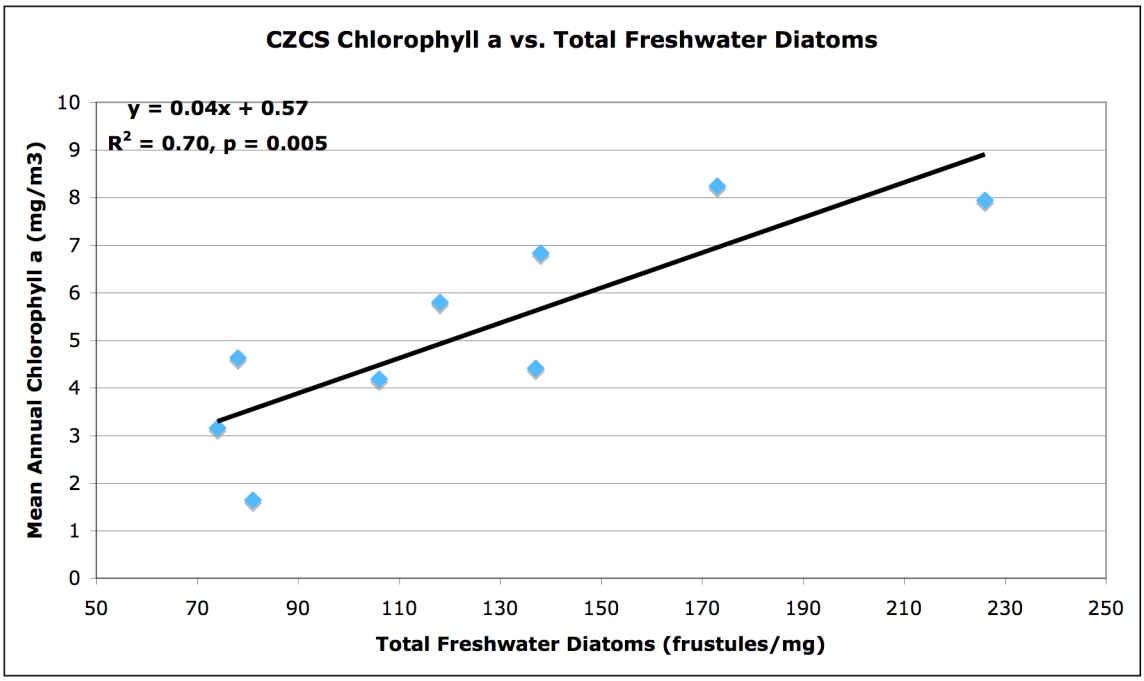

Figure 16. Results from a linear regression of CZCS mean monthly chlorophyll *a* against total freshwater diatom frustules recovered from STRATAFORM marine core L10C3 for the complete period of overlap between the two records of 1978-1986. CZCS chlorophyll data was averaged on a monthly basis across a ½ x ½ degree latitude square (124.41 to 124.91°W, 40.75 to 41.25°N) offshore of the Eel River mouth (r^2=0.70, p=0.005, n=9).